

**Thesis**

**Conservation of  $\beta$ 2-adrenergic signaling in rat and  
human cardiomyocytes during heart failure**

submitted by

**Claudia Fernandes Hollnagel**

in partial fulfillment of the requirements for the degree of

**Doktorin der gesamten Heilkunde**

**(Dr.<sup>in</sup> med. univ.)**

at the

**Medical University of Graz**

executed at the **University Department of Internal Medicine**

**Division of Cardiology**

under the supervision of

**Senka Holzer, Ass. Prof. Priv.-Doz. PhD**

**Peter Rainer, Assoz. Prof. Priv.-Doz. Dr.med.univ. Dr.scient.med.**

Graz, Date 05.04.2024

*Eidesstattliche Erklärung*

*Ich erkläre ehrenwörtlich, dass ich die vorliegende Arbeit selbstständig und ohne fremde Hilfe verfasst habe, andere als die angegebenen Quellen nicht verwendet habe und die den benutzten Quellen wörtlich oder inhaltlich entnommenen Stellen als solche kenntlich gemacht habe.*

*Graz, am 05.04.2024*

*Claudia Fernandes Hollnagel eh.*

## **Acknowledgments**

I would like to express my sincere gratitude to my mentor and supervisor, Dr. Senka Holzer, for consistently believing in me and dedicating time to provide constructive feedback throughout my thesis. Special thanks to Rainer Peter for initiating the project idea, supplying essential literature, and offering incentives at the commencement of my experiments.

I am indebted to the Cardio Group, particularly Ingrid Matzer, Julia Voglhuber, and Natasa Djalinać, for introducing me to lab work, offering assistance whenever I had questions, and providing valuable data for my thesis.

Heartfelt appreciation goes to my friends, especially Anna Ammer, Thomas Brauchert (for showing me the BioRender: Scientific Image and Illustration Software program), and Esther Tuffour, for standing by me during times of frustration. Furthermore, I extend special thanks to Korax and Craig P. Teller for sharing insightful information and providing constructive feedback on my writing.

I want to acknowledge the support of my family, including my aunt Heloisa Hollnagel and grandparents Bruno and Neusa Hollnagel, for their interest, shared experiences, and valuable perspectives on my project. Finally, none of my achievements would have been possible without the unwavering support of my parents, Carlos and Rose Hollnagel, who not only allowed me to pursue my studies but also provided steadfast financial and moral support throughout my years of education.

## **Zusammenfassung in Deutsch (maximal 5000 Zeichen)**

**Einführung:** Die Rolle der beta-2-adrenergen Rezeptoren ( $\beta$ 2AR) in der Herzinsuffizienz ist nach wie vor ein aktives Forschungsgebiet. Das duale Verhalten der  $\beta$ 2AR-Signaltransduktion, mit sowohl kardioprotektiven als auch kardiotoxischen Effekten, ist noch nicht vollständig verstanden. Darüber hinaus ist die Relevanz von Tiermodellen für die Übertragung auf den Menschen noch nicht ausreichend geklärt.

**Material und Methoden:** In dieser Arbeit wird die Aufrechterhaltung des  $\beta$ 2AR in männlichen Rattenherzen und in männlichen und weiblichen menschlichen Herzen während der Herzinsuffizienz untersucht. Wir verwendeten ein hypertensives Dahl salt-sensitive Rattenmodell mit einer salzangereicherten Diät (HSD, 8% NaCl), um das Verhalten des  $\beta$ 2AR genauer zu verstehen. Männliche Dahl salt-sensitive Ratten, die mit einer salzarmen Diät (LSD, 0,3% NaCl) gefüttert wurden, dienten als Kontrollgruppe für das Rattenmodell. Die Rattenherzen wurden sowohl zu einem frühen Zeitpunkt von 12 Wochen als auch zu einem späten Zeitpunkt von 17 oder 19 Wochen gesammelt. Das menschliche Herzzellgewebe wurde von Transplantat Spendern erworben, die verschiedene Ausprägungen der Herzinsuffizienz aufwiesen. Die Charakterisierung der Ratten als Herzinsuffizienz mit erhaltener Ejektionsfraktion (HFpEF) erfolgte mittels Gravimetrie und Echokardiographie. Menschliche Probanden wurden anhand der echokardiographischen Daten in die Gruppen HFpEF und Herzinsuffizienz mit reduzierter Ejektionsfraktion (HFrEF) eingeteilt. Die Kardiomyozyten wurden nach der Langendorff-Isolationsmethode gewonnen. Zur Quantifizierung von  $\beta$ 2AR wurden Immunzytochemie (ICC), Immunoblotting und Microarray eingesetzt. ICC-Zellen wurden zusätzlich mit dem  $\beta$ -adrenergen Agonisten Isoprenalin stimuliert.

**Ergebnisse:** (1)  $\beta$ 2AR war in den Microarray- und ICC-Analysen des Dahl salt-sensitive Rattenmodells signifikant herunterreguliert, insbesondere am späten Zeitpunkt von 17 Wochen; (2) Ratten-Immunoblots konnten diese Beobachtung nicht reproduzieren; (3)  $\beta$ 1AR und  $\beta$ 2AR waren in vergleichbarem Ausmaß in 17 Wochen alten Ratten in ICC herunterreguliert; (4) Die ISO-induzierte schnelle Herunterregulation war in HSD Dahl salt-sensitive Ratten beeinträchtigt; (5) Die

Herunterregulation von  $\beta$ 2AR wurde in humanen Immunoblots bei diastolischer Dysfunktion, aber nicht bei dilatativer Kardiomyopathie beobachtet.

**Diskussion:** Wir kommen zum Schluss, dass  $\beta$ 2AR, bei Ratten mit hypertonieinduzierter Herzinsuffizienz während des späten kardialen Remodelings, in vergleichbarem Ausmaß wie  $\beta$ 1AR herunterreguliert wird. Bei Patient\*innen mit diastolischer Dysfunktion war die  $\beta$ 2AR-Konzentration im Vergleich zu Patient\*innen mit dilatativer Kardiomyopathie und normaler Herzfunktion reduziert. Diese Ergebnisse deuten auf ein spezifisches adrenerges Expressionsmuster hin, das von der Art, dem Stadium und der Ätiologie der Herzinsuffizienz abhängt. Zukünftige Experimente, einschließlich der Übertragung von Experimenten auf menschliches Gewebe und der Analyse nachgeschalteter  $\beta$ 2AR-Signalmoleküle, versprechen weitere molekulare Einblicke in den  $\beta$ 2AR-Signalweg beim Menschen während der Herzinsuffizienz. Diese Erkenntnisse könnten zu neuen Behandlungsstrategien führen, die auf bestimmte Typen, Stadien und Ätiologie der Herzinsuffizienz zugeschnitten sind und damit zum Paradigma der personalisierten Medizin beitragen würden.

**Schlagwörter:**  $\beta$ 2AR, beta-2-adrenerge Rezeptoren, Herzinsuffizienz, HFpEF, Hypertension, Dahl salt-sensitive Ratten Modell, Immunocytochemie, Immunoblot, Langendorff-Isolationsmethode, Cardiomyocyten, Microarray

## **Abstract in English (maximal 5000 Zeichen)**

**Introduction:** Beta-2 adrenergic ( $\beta$ 2AR) signaling in heart failure remains an area of active investigation, presenting diverse insights. The dual nature of  $\beta$ 2AR signaling, exhibiting both cardioprotective and cardiotoxic effects, remains incompletely understood. Moreover, the translational relevance of animal models to human data is yet to be fully established.

**Material and Methods:** This thesis investigates the preservation of  $\beta$ 2AR signaling in male rat and male and female human hearts during heart failure. To discern the intricacies of  $\beta$ 2AR behavior, we utilized a hypertensive Dahl salt-sensitive rat model fed a high-salt-diet starting at 7 weeks (HSD, 8% NaCl) for 5 (early remodeling) and 10 to 12 (late remodeling) weeks. The control group comprised male Dahl salt-sensitive rats on a low-salt-diet (LSD, 0.3% NaCl). In addition, we had valuable access to donor and explanted human heart tissue with various degrees of cardiac remodeling. Phenotyping of rats as heart failure with Preserved Ejection Fraction (HFpEF) occurred through gravimetric analyses and echocardiography. Human subjects were categorized into HFpEF and heart failure with Reduced Ejection Fraction (HFrEF) groups based on echocardiography data provided by the Department of Cardiology. Cardiomyocytes were obtained through Langendorff isolation methods. Quantification of  $\beta$ 2AR involved Immunocytochemistry (ICC), immunoblotting, and microarray techniques. Cells used for ICC were additionally stimulated with  $\beta$ -adrenergic agonist isoprenaline.

**Results:** (1) Significant  $\beta$ 2AR downregulation, particularly at a late remodeling time point, in the microarray and ICC analyses of the Dahl salt-sensitive rat model; (2) Conversely, rat immunoblots failed to reproduce this observation; (3) Comparable rates of  $\beta$ 1AR and  $\beta$ 2AR downregulation in rats in the ICC at a late remodeling timepoint; (4) Impaired rapid-ISO-induced  $\beta$ 2AR downregulation in HSD Dahl salt-sensitive rats; (5)  $\beta$ 2AR downregulation observed in human immunoblot for diastolic dysfunction, but not for dilated cardiomyopathy.

**Discussion:** We conclude that  $\beta$ 2AR downregulation occurs at a comparable rate to  $\beta$ 1AR during late-stage cardiac remodeling in rats with systemic hypertension heart failure. In humans, superior downregulation was evident in patients with

diastolic dysfunction compared to dilated cardiomyopathy. These insights suggest a specific adrenergic expression pattern depending on heart failure type, stage, and etiology. Future experiments, including translation to human tissue and analysis of  $\beta$ 2AR downstream targets, promise additional molecular insights into  $\beta$ 2AR signaling in humans during the development and progression of heart failure. Such insights may inform novel treatment strategies tailored to specific heart failure types, stages, and etiologies, contributing to the paradigm of personalized medicine.

**Topic Tags:**  $\beta$ 2AR, beta-2-adrenergic receptor, heart failure, HFpEF, hypertension, Dahl salt-sensitive rat, Immunocytochemistry, immunoblot, Langendorff-isolation method, cardiomyocytes, Microarray

## Information on previous publications

A part of this Thesis has been published in:

Matzer, I. (2021) 'Role of  $\beta$ 1-adrenergic signalling in early- and late-stage hypertensive cardiac remodelling, Master thesis submitted at the Master Degree Course Mass Spectrometry and Molecular Analytics for the degree Master of Science in Engineering (MSc)'.

Matzer, I. *et al.* (2022) 'beta-Adrenergic Receptor Stimulation Maintains NCX-CaMKII Axis and Prevents Overactivation of IL6R-Signaling in Cardiomyocytes upon Increased Workload', *Biomedicines*, 10(7), p. 1648. Available at:

<https://doi.org/10.3390/biomedicines10071648>

**Both publications are open access and fall under the terms and conditions of the Creative Commons Attribution (CC BY 4.0) license. This license allows the unrestricted use and adaption of materials, providing appropriate credit is given and made changes are indicated.**

<https://creativecommons.org/licenses/by/4.0>

# Table of contents

Acknowledgments .....	II
Zusammenfassung in Deutsch (maximal 5000 Zeichen).....	III
Abstract in English (maximal 5000 Zeichen) .....	V
Information on previous publications .....	VII
Table of contents.....	VIII
Abbreviations.....	XI
List of figures .....	XIV
List of tables .....	XVI
1. Introduction .....	1
1.1 Clinical insights .....	1
1.1.1 Definition and epidemiology of heart failure .....	1
1.1.2 Types of heart failure, etiology, risk factors .....	2
1.1.3 Symptoms of heart failure .....	3
1.1.4 Clinical classification and diagnosis of heart failure .....	3
1.1.5 Treatment of heart failure .....	5
1.1.6 Pathophysiology of heart failure.....	7
1.1.7 Heart failure due to hypertension.....	8
1.2 Cellular and molecular insights .....	11
1.2.1 Hypertensive cardiac remodeling.....	11
1.2.2 Adrenergic signaling in the heart .....	15
1.3 Objectives and description of the thesis project .....	32
2. Material and Methods.....	33
2.1 Overview .....	33
2.2 Dahl salt-sensitive rat model .....	34
2.3 Human tissue collection .....	36
2.4 Ventricular cardiomyocyte rat isolation via Langendorff perfusion .....	37
2.4.1 Solutions for rat ventricular cardiomyocyte isolation .....	39
2.5 Hypertrophy measurements .....	41
2.6 Immunocytochemistry (ICC).....	42
2.6.1 Drug treatments and fixing isolated Cardiomyocytes.....	42
2.6.2 ICC staining .....	42
2.7 Immunoblotting.....	43
2.7.1 Tissue homogenization.....	44

2.7.2	Pierce BCA assay .....	45
2.7.3	Sodium dodecyl sulfate polyacrylamide gel electrophoresis (SDS-PAGE) and immunoblotting .....	45
2.7.4	Membrane stripping .....	46
2.7.5	Analysis .....	47
2.8	Microarray .....	47
2.9	Statistical Analysis.....	47
3.	Results .....	49
3.1	Dahl salt-sensitive rats .....	49
3.1.1	<i>In vivo</i> and <i>in vitro</i> phenotyping of hypertensive Dahl salt-sensitive rats	49
3.1.2	Echocardiography development of diastolic dysfunction with preserved ejection fraction in Dahl salt-sensitive rats .....	52
3.1.3	$\beta$ 2AR expression decreases in the whole cell in hypertensive Dahl salt-sensitive rats .....	53
3.1.4	$\beta$ AR stimulation decreases $\beta$ 2AR expression in ICC of the LSD Dahl salt-sensitive rat group .....	54
3.1.5	$\beta$ 2AR expression in relation to $\beta$ 1AR expression in Dahl salt-sensitive rats	55
3.1.6	$\beta$ 2AR expression in the left ventricular tissue at early- and late-stage cardiac remodeling .....	56
3.1.7	$\beta$ 2AR gene expression is downregulated in the late cardiac remodeling stage.....	57
3.2	Human data.....	58
3.2.1	Human cohort characteristics .....	58
3.2.2	$\beta$ 2AR is decreased in humans during diastolic dysfunction .....	59
4.	Discussion.....	60
4.1	HSD-fed Dahl salt-sensitive rats develop a hypertensive phenotype with hypertrophy, preserved ejection fraction, and diastolic dysfunction .....	60
4.2	$\beta$ 2AR expression decreases in rats that develop hypertension in late-stage remodeling .....	62
4.3	$\beta$ 2AR receptor is downregulated when stimulated with ISO in LSD rats .	63
4.4	$\beta$ 2AR is downregulated in humans with diastolic dysfunction .....	64
4.5	Comparing $\beta$ 2AR with $\beta$ 1AR expression behavior .....	65

5. Conclusion .....	68
6. Future perspectives.....	69
7. References.....	70

## Abbreviations

AC	Adenylyl cyclase
ACE-I	Angiotensin-converting enzyme inhibitor
ADH	Antidiuretic hormone
ARB	Angiotensin II receptor blocker
ARNI	Angiotensin receptor-neprilysin inhibitor
ATP	Adenosine triphosphate
BCA	Bicinchoninic acid
BDM	Butanedione monoxime
BMI	Body Mass Index
BNP	Brain natriuretic peptide
BP	Blood pressure
BSA	Bovine serum albumin
BW	Body weight
Ca <sup>2+</sup>	Calcium <sup>2+</sup> ions
CamKII	Calmodulin-dependent kinase II
cAMP	Cyclic adenosine monophosphate
CCB	Calcium channel blockers
CRP	C-reactive protein
DAGK	Diacylglycerol kinase
DCM	Dilated cardiomyopathy
E/e'	Mitral velocity/septal velocity
ECG	Echocardiography
EF	Ejection fraction
EGFR	Epidermal growth factor receptor
eNOS	Endothelial nitric oxide synthase
EPac1	Exchange protein directly activated by cAMP 1
ERK1/2	Extracellular signal-regulated kinase 1/2
ESC	European society of cardiology
GDP	Guanosine diphosphate
GPCR	G-protein-coupled receptors
GRK	G-protein-coupled receptor kinases
GRK2	G-protein-coupled receptor kinase 2

GTP .....	<i>Guanosine triphosphate</i>
HDAC5 .....	<i>Histone deacetylase 5</i>
HFmrEF .....	<i>Heart failure with moderately reduced ejection fraction</i>
HFpEF .....	<i>Heart failure with preserved ejection fraction</i>
HFrEF .....	<i>Heart failure with reduced ejection fraction</i>
HSD .....	<i>High-salt-diet</i>
ICC .....	<i>Immunocytochemistry</i>
IL6R .....	<i>Interleukine-6-receptor</i>
IP2 .....	<i>Inositol-4,5 bisphosphate</i>
IP3 .....	<i>Inositol 1,4,5-triphosphate</i>
ISO .....	<i>Isoprenaline</i>
LCC .....	<i>L-type calcium channels</i>
LSD .....	<i>Low-salt-diet</i>
LVEF .....	<i>Left ventricular ejection fraction</i>
MRA .....	<i>Mineralocorticoid receptor antagonist</i>
NCX .....	<i>Sodium/calcium exchanger</i>
NF .....	<i>Not failing</i>
NHERF .....	<i>Na<sup>+</sup>/H<sup>+</sup> exchange regulation factor</i>
NT-ProBNP .....	<i>N-terminal prohormone of brain natriuretic peptide</i>
NYHA .....	<i>New York Heart Association</i>
p38 MAPK .....	<i>Mitogen-activated protein kinase</i>
PDEs .....	<i>Phosphodiesterases</i>
PI3K-Akt .....	<i>Phosphoinositide 3-Kinase- serine/threonine kinase</i>
PI4P .....	<i>Phosphatidylinositol-4-phosphate</i>
PIP2 .....	<i>Phosphatidylinositol 4,5-bisphosphate</i>
PKA .....	<i>cAMP dependent protein kinase</i>
PKC .....	<i>Protein kinase C</i>
PKD .....	<i>Protein kinase D</i>
PLB .....	<i>Phospholamban</i>
PLC .....	<i>Phospholipase C<math>\beta</math></i>
RAAS .....	<i>Renin-angiotensin-aldosterone-system</i>
RyR .....	<i>Ryanodine receptors</i>
SERCA .....	<i>Sarco/Endoplasmatic reticulum calcium ATPase</i>
SGLT2i .....	<i>Sodium-glucose cotransporter 2 inhibitors</i>

SR .....	<i>Sarcoplasmic reticulum</i>
TBST .....	<i>Tris-buffered saline with Tween 20</i>
VEGF .....	<i>Vascular endothelial growth factor</i>
$\beta$ 1AR .....	<i>Beta 1 adrenergic receptor</i>
$\beta$ 2AR .....	<i>Beta 2 adrenergic receptor</i>
$\beta$ 3AR.....	<i>Beta 3 adrenergic receptor</i>
$\beta$ AR .....	<i>Beta adrenergic receptors</i>

## List of figures

Figure 1: Heart failure diagnostic algorithm .....	4
Figure 2: Heart failure therapy for patients with HFrEF .....	6
Figure 3: Development of hypertensive cardiomyopathy .....	10
Figure 4: Mechanisms of Cardiac Remodeling .....	11
Figure 5: G-protein-coupled receptor (GPCR) with an N- and C-terminus and G-protein in its subunits.....	17
Figure 6: Overview of G-protein subsets and effects.....	18
Figure 7: Deactivation of GPCR signals .....	19
Figure 8: Mechanisms of $\beta$ 1AR signaling in heart failure .....	22
Figure 9: Physiological signaling of $\beta$ 2AR: .....	24
Figure 10: Overview of the experiments .....	33
Figure 11: Experimental timeline and parameters for the high-salt-diet induced hypertension study .....	35
Figure 12: Langendorff perfusion setup.....	37
Figure 13: Cardiomyocyte ADRB2 fluorescence analysis using Image J software	43
Figure 14: Phenotypical characterization and <i>in vivo</i> measurements of Dahl salt-sensitive rats on low-salt-diet (LSD) and high-salt-diet (HSD).....	50
Figure 15: <i>In vitro</i> cell hypertrophy of Dahl salt-sensitive rat cardiomyocytes divided into low-salt-diet (LSD) and high-salt-diet (HSD) groups.....	51
Figure 16: Echocardiography measurements of Dahl salt-sensitive rats on low-salt-diet (LSD) and high-salt-diet (HSD):.....	52
Figure 17: Expression of $\beta$ 2AR in isolated cardiomyocytes from the low-salt-diet (LSD) and high-salt-diet (HSD) Dahl salt-sensitive rats.....	53
Figure 18: Expression of $\beta$ 2AR in isolated cardiomyocytes from the low-salt-diet (LSD) and high-salt-diet (HSD) Dahl salt-sensitive rats upon $\beta$ -adrenergic stimulation with 100 nM isoprenaline (ISO) for 1h.....	53
Figure 19: Expression of $\beta$ 2AR in isolated cardiomyocytes from the low-salt-diet (LSD) and high-salt-diet (HSD) Dahl salt-sensitive rats upon $\beta$ -adrenergic stimulation with 100 nM isoprenaline (ISO) for 1h compared to normal tyrode (NT). .....	54
Figure 20: $\beta$ 2AR immunoassay of the left ventricle of Dahl salt-sensitive rats in early (12 weeks) and late (19 weeks)-stage remodeling. ....	56

Figure 21 Expression of  $\beta$ 2AR mRNA in left ventricular tissue from low-salt-diet (LSD) and high-salt diet (HSD) Dahl salt-sensitive rats in early (12 weeks) and late (17 weeks) timepoints. .... 57

Figure 22:  $\beta$ 2AR immunoblot of the left ventricle in humans with not failing (NF) hearts, hearts with diastolic dysfunction (DD), or dilated cardiomyopathy (DCM). 59

## List of tables

Table 1: Overview of $\beta$ 2AR signaling effects .....	29
Table 2: Rat perfusion solution, pH =7.4 .....	39
Table 3: Rat perfusion buffer .....	39
Table 4: Rat cannulation solution .....	39
Table 5: Rat calcium solutions.....	39
Table 6: Rat myocyte digestion solution .....	40
Table 7: Rat myocyte stopping solution 1 .....	40
Table 8: Rat myocyte stopping solution 2.....	40
Table 9: Rat calcium series. ....	40
Table 10: Rat normal tyrode solution (NT).....	41
Table 11: Homogenisation buffer .....	44
Table 12: Human cohort characteristics for the immunoblot experiment.....	58

# 1. Introduction

For heart failure, understanding the intricacies of beta 2 adrenergic receptor ( $\beta$ 2AR) signaling is critical to fully understand its pathophysiology. This signaling pathway presents a complex duality, with both protective and detrimental effects on cardiac function. Yet, despite extensive research efforts, gaps persist in comprehending its role. Against this backdrop, this thesis delves into the conservation of  $\beta$ 2AR signaling in rat and human cardiomyocytes during heart failure, aiming to unravel its behavior across species and disease states. In the following clinical, cellular, and molecular aspects of heart failure will be explored, elucidating the rationale behind our investigation, and delineating the objectives of our study.

## 1.1 *Clinical insights*

### 1.1.1 Definition and epidemiology of heart failure

The European Society of Cardiology defines heart failure as a syndrome characterized by various symptoms such as shortness of breath, edema, and fatigue that can be attributed to structural changes in the heart (McDonagh *et al.*, 2021). This condition is progressive, initially presenting symptoms only under stress, but advancing to the point where symptoms occur at rest (Silbernagl *et al.*, 2020).

Heart failure is a prevalent condition, affecting 1-3% of the global adult population. It is associated with a substantial mortality rate, ranging from 50-75% within 5 years (Savarese *et al.*, 2023). In 2010 in Germany, 61.4% of treated heart failure patients were female most likely because of their higher life expectancy (Klauber *et al.*, 2014). It is notably widespread among older individuals; the Spanish PRICE study conducted in 2004/2005 revealed that 16.1% of individuals aged >74 years screened positive for heart failure (Anguita Sánchez *et al.*, 2008). As the population ages, healthcare costs related to heart failure are escalating, reaching up to 25,500€ per patient per year in Germany (Savarese *et al.*, 2023). Due to demographic changes and improved survival rates in acute myocardial infarction, valvular heart diseases, cardiomyopathies, or secondary myocardial conditions, the number of patients with heart failure is expected to continue rising (Arzneimittelkommission Der Deutschen Apotheker *et al.*, 2023).

### **1.1.2 Types of heart failure, etiology, risk factors**

Heart failure can manifest as an acute incident, for example, through acute ischemia or arrhythmias (Severino *et al.*, 2020), (McDonagh *et al.*, 2021) or as a chronic disorder. The affected part of the heart can be described as left, right, or global. Furthermore, it can be categorized based on functional disorders, such as systolic dysfunction with compromised contraction that leads to reduced ejection fraction, diastolic dysfunction with reduced filling capacity and impaired relaxation, or a combination of both (McDonagh *et al.*, 2021).

The etiologies for this clinical syndrome are highly diverse. In the Western hemisphere, predominant causes of heart failure include coronary heart disease and hypertension, along with their comorbidities. The remaining cases develop through various rarer conditions, such as non-ischemic cardiomyopathies, valve disorders, arrhythmias, or diseases of the pericardium. Additionally, toxins such as alcohol or chemotherapies play a role in the development of heart failure (McDonagh *et al.*, 2021), (Arzneimittelkommission Der Deutschen Apotheker *et al.*, 2023).

Heart failure is often associated with various comorbidities, including cardiovascular conditions like atrial fibrillation, coronary heart disease, valve disorders, hypertension, and stroke. It is also linked to other diseases such as diabetes, electrolyte disorders, depression, arthritis, renal disorders, and erectile dysfunction. Considering and treating these comorbidities is essential (McDonagh *et al.*, 2021), (Arzneimittelkommission Der Deutschen Apotheker *et al.*, 2023).

As heart failure is not a distinct disease entity but rather a consequence of one or multiple underlying diseases, risk factors for heart failure are closely linked to their causes. These risk factors include hypertension, coronary heart disease, smoking, alcohol abuse, physical inactivity, obesity, as well as genetic predispositions. Patients with multiple risk factors and nonspecific symptoms, such as weakness that may be attributed to heart failure, should be screened for the condition. (Arzneimittelkommission Der Deutschen Apotheker *et al.*, 2023), (McDonagh *et al.*, 2021).

### **1.1.3 Symptoms of heart failure**

Symptoms of heart failure vary depending on which side of the heart is affected. Left heart failure can cause fatigue and shortness of breath as pulmonary venous pressure increases and cardiac output decreases. This condition may progress to pulmonary edema, leading to dyspnea and respiratory alkalosis (Silbernagl *et al.*, 2020). Right heart failure results in increased systemic venous pressure and peripheral edema, commonly seen as ankle swelling and nocturia. Hepatic hypertrophy and malabsorption are also one of the many consequences of increased fluid in the systemic circulation (Silbernagl *et al.*, 2020).

Symptoms are classified according to the New York Heart Association (NYHA) Classification, where NYHA I denotes mild symptoms, and NYHA IV represents the highest severity of symptoms (Arzneimittelkommission Der Deutschen Apotheker *et al.*, 2023).

### **1.1.4 Clinical classification and diagnosis of heart failure**

To diagnose heart failure, clinical evaluation is essential, including the cardinal symptoms of heart failure, such as dyspnea, ankle edemas, and weakness, along with signs observed during clinical examination and objective evidence of heart dysfunction. Screening involves laboratory parameters involving the hormones brain natriuretic peptide (BNP) and N-terminal prohormone of brain natriuretic peptide (NT-ProBNP), which rise significantly under cardiac stress. Electrocardiography (ECG) may reveal signs of hypertrophy, high filling pressures, disorders in repolarization, or may even appear normal. Figure 1 describes the diagnostic algorithm used by the European Society of Cardiology (ESC) Guidelines of 2021.

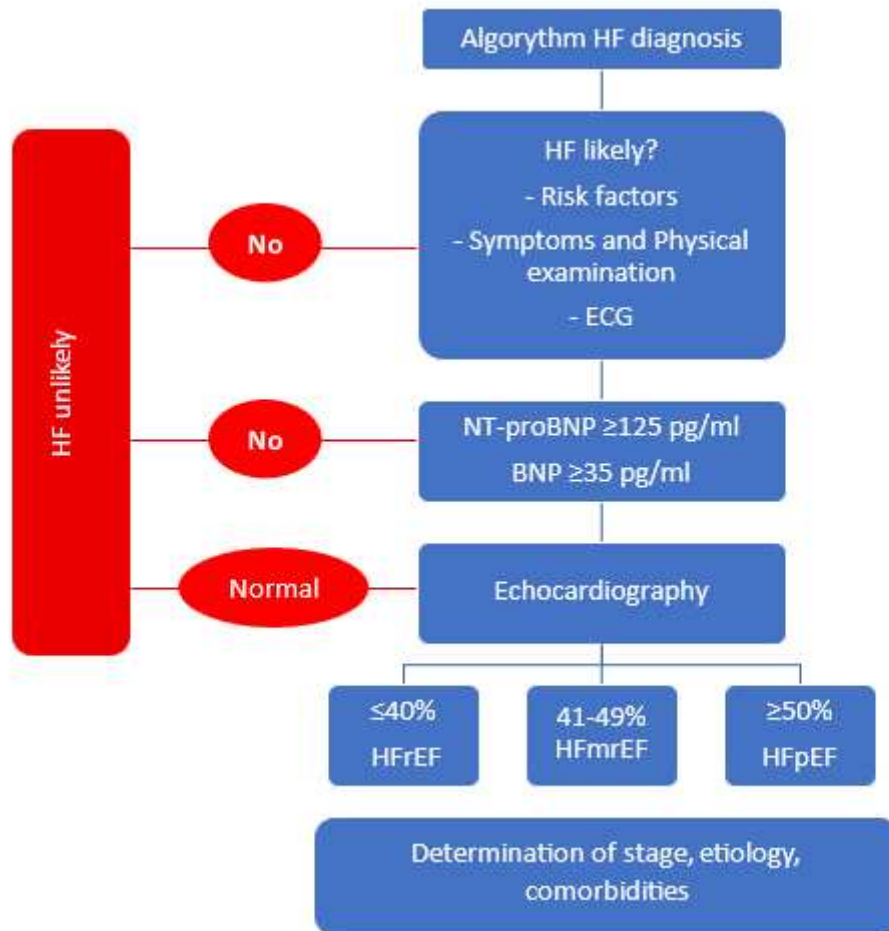


**Figure 1: Heart failure diagnostic algorithm**

To diagnose heart failure, commence with an anamnesis of risk factors and symptoms, along with a clinical examination. If available, perform an electrocardiogram (ECG). If the gathered information suggests heart failure, conduct screening using NT-proBNP or BNP, markers detecting heart stress. A normal result makes heart failure unlikely, while a positive result necessitates an echocardiography. This diagnostic tool categorizes heart failure into three groups: HFrEF (heart failure with reduced ejection fraction), HFmrEF (heart failure with moderately reduced ejection fraction), and HFpEF (heart failure with preserved ejection fraction). Subsequent therapy and prognosis rely on this categorization. Following the diagnosis, proceed to define the patient's stage, etiology, and comorbidities for optimal care and treatment. The scheme has been adapted and translated from the ESC 2021 Guidelines for acute and chronic heart failure (McDonagh *et al.*, 2021).

If these parameters suggest heart failure, further evaluation can be conducted using echocardiography. Heart failure is classified by measuring the left ventricular ejection fraction (LVEF), indicating the volume the left ventricle ejects per contraction in percent (McDonagh *et al.*, 2021). With this parameter, heart failure is divided into three groups: Preserved ejection fraction (HFpEF) LVEF  $\geq 50\%$ , moderately reduced ejection fraction (HFmrEF) LVEF 41-49%, and reduced ejection

fraction (HFrEF) LVEF  $\leq 40\%$  (McDonagh *et al.*, 2021). About 50% of patients with heart failure have a HFpEF (Zile *et al.*, 2015).

Additionally, diastolic dysfunction (DD) can be quantified through echocardiographic measurements (Pieske *et al.*, 2019). DD refers to a condition marked by irregularities in the relaxation and filling of the heart during the diastolic phase of the cardiac cycle. In essence, diastole denotes the interval when the myocardium loses its capacity to generate force and contract, returning to an unstressed length and force. Diastolic dysfunction manifests when these processes become prolonged, slowed, or incomplete. (Zile and Brutsaert, 2002). Following parameters such as the size of the left atrium (left atrial volume index  $> 32 \text{ ml/m}^2$ ), mitral velocity E  $> 90 \text{ cm/s}$ , septal velocity  $e' < 9 \text{ cm/s}$ , and E/ $e'$  ratio  $> 9$  have been identified as relevant threshold values for diastolic dysfunction. Exceeding these thresholds is associated with an increased risk of cardiovascular mortality (McDonagh *et al.*, 2021).

#### **1.1.5 Treatment of heart failure**

The following treatment regimen is adopted from the 2021 ESC Guidelines for the diagnosis and treatment of acute and chronic heart failure (McDonagh *et al.*, 2021).

Heart failure is treated with lifestyle interventions such as rehabilitation, medications, and, as a last resort, device therapy, which encompasses pacemakers and defibrillators, as heart failure is often associated with arrhythmias and cardiac assist devices. Drug therapy plays a central role in heart failure treatment and in the following section, the currently available and most commonly used medications for HFrEF and HFpEF will be elaborated.

HFrEF drug therapy, being the most studied entity, is constituted of four pillars (Figure 2) Modulation of the Renin-angiotensin-aldosterone-system (RAAS) and the sympathetic nervous system through an Angiotensin-converting-Enzyme Inhibitor (ACE-I) or an Angiotensin Receptor-Nepriylsin Inhibitor (ARNI). A beta-blocker further inhibits the sympathetic nervous system. Thirdly, a Mineralocorticoid Receptor Antagonist (MRA) blocks aldosterone from binding to the mineralocorticoid receptor in the kidneys, inhibiting further water and sodium retention and promoting potassium excretion. Lastly, sodium-glucose co-transporter 2 Inhibitors (SGLT2I) have shown a positive impact on morbidity and mortality in

patients with HFrEF and constitute the final pillar. Loop diuretics are used for symptomatic relief of volume overload, such as peripheral or pulmonary edemas, but are not shown to reduce mortality. If the therapy above proves to be insufficient drugs like Ivabradin or Digitoxin can be given.

### Heart failure Drug Therapy for patients with HFrEF

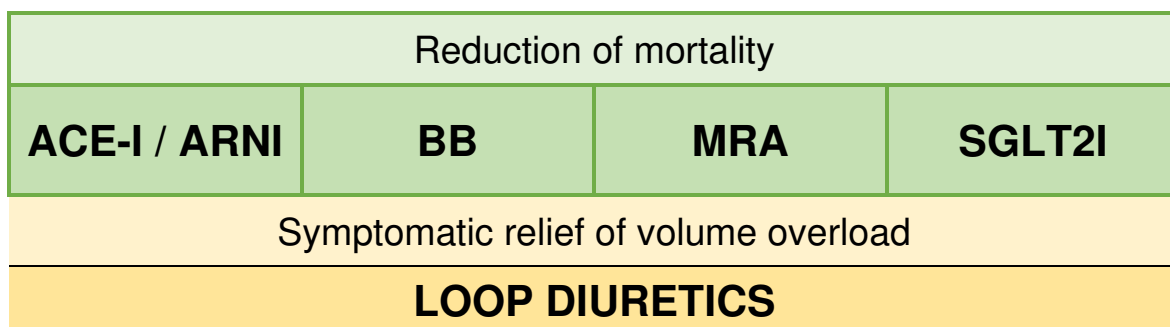


**Figure 2: Heart failure therapy for patients with HFrEF**

This figure illustrates the primary drug pillars of heart failure therapy for patients with HFrEF. A combination of ACE-I/ARNI, BB, MRA, and SGLT2I has been proven to reduce mortality. Loop diuretics are administered to alleviate symptoms of volume overload, such as dyspnea or swelling, but do not reduce mortality rates. ACE-I = Angiotensin-converting-Enzyme Inhibitor, ARNI = Angiotensin Receptor-Nepriylsin Inhibitor, BB = Betablocker, MRA = Mineralocorticoid Receptor Antagonist, SGLT2I = sodium-glucose co-transporter 2 Inhibitor. This figure was adapted and translated from the 2021 ESC Guidelines for the diagnosis and treatment of acute and chronic heart failure (McDonagh *et al.*, 2021).

Data is scarcer in patients with HFpEF. Consequently, the guidelines are not as elaborated. It is suggested that risk factors, comorbidities, and the cause of heart failure should be the main focus of therapy. Many patients are treated with an ACE-I or an Angiotensin II receptor blocker (ARB), beta-blocker, or MRA because most of them have either coronary heart disease or hypertension. The ARB is also a RAAS inhibitor like ACE-I and is given against hypertension. There is a possibility of SGLT2I becoming a new pillar in the therapy of HFpEF. Dapagliflozin and Empagliflozin are active substances of this group. The “DELIVER” trial demonstrated that Dapagliflozin reduces cardiovascular death and hospitalization in HFmrEF and HFpEF (Solomon *et al.*, 2021). Additionally, the “Emperor Preserved” trial showed that Empagliflozin has a reduction in hospitalization and mortality in patients with HFpEF (Zinman *et al.*, 2015). Symptomatic therapy with loop diuretics is indicated for the same reasons as in HFrEF. These therapeutic

approaches have been implemented in the German heart failure guidelines (Arzneimittelkommission Der Deutschen Apotheker *et al.*, 2023).

There are many new subcellular mechanisms we are finding that counteract the development of cardiac failure. Enhanced comprehension of the molecular biology and pathophysiology underlying heart failure presents an avenue for developing more effective pharmaceuticals and improved disease management.

#### **1.1.6 Pathophysiology of heart failure**

The pathophysiology of heart failure starts with cardiac stress, for example through volume and/or pressure overload, or tissue loss. This increases ventricular wall tension, initially leading to alterations in systolic function. The calculation of ventricular wall tension, guided by Laplace's law, involves the interplay between radius, wall thickness, transmural pressure, and tension. In response, the body initiates signals promoting concentric hypertrophy of the ventricles, enhancing systolic function but impairing diastolic function due to reduced end-diastolic volume (Silbernagl *et al.*, 2020).

Additional countermeasures involve neurohumoral responses triggered by a decline in blood pressure. This results in the release of antidiuretic hormone (ADH) and activation of the sympathetic nervous system (Silbernagl *et al.*, 2020). These responses lead to water retention, vasoconstriction, increased heart rate and contractility, and centralization of blood volume. Kidney underperfusion and the sympathetic nervous system activate the RAAS, further promoting water retention (Silbernagl *et al.*, 2020). While these compensatory mechanisms counteract the heart's increased workload for an extended period, in the long run, they prove non-beneficial and accelerate cardiac remodeling by increasing preload and afterload.

Atrial natriuretic peptide and BNP are released in response to elevated atrial and ventricular pressures, increasing water excretion to compensate for volume overload (Silbernagl *et al.*, 2020). These hormones are commonly used to diagnose heart failure (McDonagh *et al.*, 2021).

Mechanical and neurohumoral stressors induce myocardial remodeling through various signaling molecules and growth factors, leading to myocardial hypertrophy

and decreased sympathetic sensitivity. Furthermore, this remodeling results in a weak cardiomyocyte action potential and a reduction in resting potential elevating the risk of arrhythmias (Silbernagl *et al.*, 2020).

### **1.1.7 Heart failure due to hypertension**

#### **1.1.7.1 Epidemiology and etiology**

This thesis specifically focuses on myocardial disease and heart failure resulting from hypertension, so an emphasis will be put on this topic. Hypertension stands out as a primary cause of heart failure and myocardial infarction in the western world. The global prevalence of hypertension is anticipated to surpass 1.5 billion people by 2025 (Slivnick and Lampert, 2019), (Kearney *et al.*, 2005). The development of hypertension is a complex phenomenon unique to each patient, encompassing factors such as increased sympathetic nervous system activity, long-term high sodium intake, overproduction of sodium-retaining hormones and vasoconstrictors, diabetes, inappropriate renin secretion, vasodilator deficiencies, vessel abnormalities, and alterations in the kallikrein-kinin system (Elliott, 2007).

#### **1.1.7.2 Pathophysiology**

Hypertensive cardiomyopathy emerges as a significant end-organ damage triggered by hypertension, manifested as ventricular hypertrophy that, over time, leads to diastolic dysfunction and, in the end phase, systolic dysfunction (Phillips and Diamond, 2001), (Nadruz, 2015). This cardiomyopathy affects 20% of patients with mild hypertension and nearly 100% of patients with severe hypertension, imposing a substantial socio-economic burden on healthcare (Ruilope and Schmieder, 2008). Additionally, the Framingham study, spanning over 14 years and following more than 5000 patients, reveals that 91% of patients with newly developed heart failure had underlying hypertension (Levy *et al.*, 1996).

Furthermore, hypertension is intricately linked to other cardiovascular diseases such as coronary heart disease, stroke, atrial fibrillation, and peripheral vascular diseases (Slivnick and Lampert, 2019). These connections negatively impact the development of heart failure. For instance, hypertension induces endothelial dysfunction, exacerbating the atherosclerotic process in coronary heart disease. Left ventricular hypertrophy in hypertensive cardiomyopathy reduces coronary

reserve and increases myocardial oxygen demand, both contributing to myocardial ischemia that further worsens heart failure (Escobar, 2002).

Although several stages have been consistently observed, understanding how hypertension leads to hypertensive cardiomyopathy and subsequently heart failure remains incomplete (Figure 3). In the early stages, hypertensive patients may develop left ventricular hypertrophy, either concentric or eccentric, without symptoms but with elevated filling pressures. However, only 23-48% of hypertensive patients reach this stage (Devereux *et al.*, 1987). Later symptoms may progress to HFpEF and, in a subset of patients, a reduced ejection fraction may develop. The reasons why only a subset of hypertensive patients develop HFrEF are not fully understood. The clinical study by Salas-Pacheco *et al.* suggests that the extent of hypertrophy determines the development of systolic dysfunction, and LVEF is an insensitive method to determine systolic dysfunction in hypertensive patients (Salas-Pacheco *et al.*, 2022). Patients with an eccentric hypertrophy phenotype have a higher probability of developing HFrEF presenting with dilated cardiomyopathy (Velagaleti *et al.*, 2014). In their review article, Borlaug and Redfield propose that a second hit, such as an infarction, cardiotoxic substances like drugs or medication, infection, or inflammation, damages the heart and leads it from HFpEF to HFrEF (Borlaug and Redfield, 2011). When patients reach HFrEF, the mortality rate is significantly higher (Frazier *et al.*, 2007). The variability in disease progression may be caused by differences in pressure and volume loads, neurohormonal status, genetic basis, and cardiovascular risk factors such as diabetes, obesity, and smoking (Palmiero *et al.*, 2014).

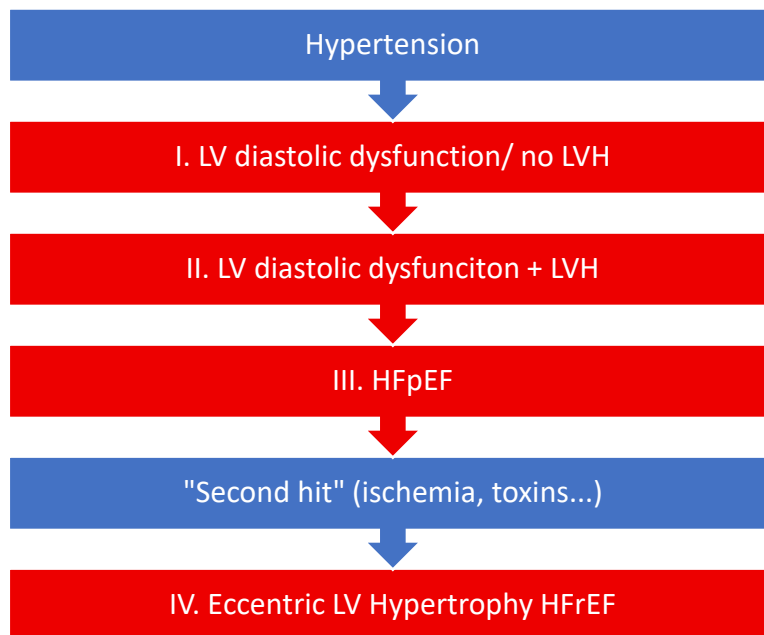


**Figure 3: Development of hypertensive cardiomyopathy**

Flow chart illustrating the potential development of heart failure due to hypertension. Patients with hypertension may progress through various stages of cardiac remodeling, potentially leading to heart failure, although this progression is not obligatory. The reasons behind why some patients undergo these stages while others do not are still under research. Slivnick and Lampert propose a second hit, such as ischemia, inflammation, or exposure to cardiotoxic substances, which may contribute to hypertensive patients with HFpEF transitioning to HFrEF. LV = Left ventricular, LVH = Left ventricular hypertrophy, HFrEF = heart failure with reduced ejection fraction. This figure was adapted from the Review “Hypertension and Heart Failure” (Slivnick and Lampert, 2019).

### 1.1.7.3 Treatment

Effectively treating hypertensive cardiomyopathy involves the prevention and treatment of hypertension before the onset of cardiac remodeling (Slivnick and Lampert, 2019). This can be achieved through ACE-I, ARB, dihydropyridine calcium channel blockers (CCB), and thiazide diuretics (Whelton and Carey, 2017). During left ventricular hypertrophy, antihypertensive medications are—at least in part—able to reverse the phenotype (Slivnick and Lampert, 2019). In cases where heart failure manifests, the treatment approach should align with established heart failure guidelines (see 1.1.5). A blood pressure target of 130/80 should be attained (Cushman *et al.*, 2016). Furthermore, prioritizing the prevention of coronary heart disease in individuals with hypertension is of utmost importance. This goal can be effectively pursued by initiating a combined regimen involving antiplatelet agents, lipid-lowering medications, and antihypertensive drugs (Slivnick and Lampert, 2019).

## 1.2 Cellular and molecular insights

In the following section, I will explain various mechanisms that occur during the development and presentation of heart failure at the cellular and subcellular levels, that are already within our understanding.

### 1.2.1 Hypertensive cardiac remodeling

Hypertensive heart disease leading to heart failure can be explained by cardiac remodeling—a complex restructuring involving cellular and subcellular alterations in the heart. This encompasses processes such as cardiomyocyte hypertrophy, interstitial inflammation, cardiomyocyte apoptosis, interstitial fibrosis, reorganization of the cellular matrix, changes in receptor expression, and reduced capillarization (Figure 4). These cellular changes lead to ventricular dilation, dysfunctional filling, altered metabolic homeostasis, and reduced contractility (González, Ravassa, *et al.*, 2018), (Martin *et al.*, 2012). Cardiac remodeling already starts in the compensated stage of heart failure where symptoms on the level of the whole organism are not yet present. While  $\beta$ -adrenergic signaling plays a crucial role in the heart's adaptation to external stressors, chronic stimulation of these receptors plays a pivotal role in cardiac remodeling and the development of heart failure.

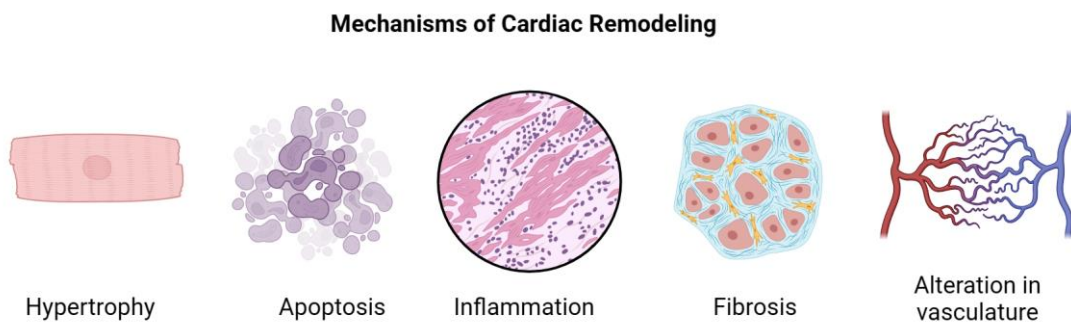


**Figure 4: Mechanisms of Cardiac Remodeling**

This figure provides an overview of mechanisms involved in cardiac remodeling. This process occurs as a response to a cardiac stressor, encompassing cardiac hypertrophy, apoptosis, inflammation, fibrosis, and alterations in vasculature. The figure has been adapted from the paper "Myocardial Remodeling in Hypertension" (González, Ravassa, *et al.*, 2018) and was created using BioRender.com.

### **1.2.1.1 Hypertrophy**

Pressure overload, a stressor for the heart, induces protein synthesis in cardiomyocytes, which enlarges intracellular sarcomeres, leading to cell growth (Sugden and Clerk, 1998). Neurohumorally, pressure overload triggers a response involving angiotensin II (ATII) (Lijnen and Petrov, 1999) and catecholamines through activation of the sympathetic nervous system (Zimmer, 1997). Additionally, this stressor leads to the release of growth factors and cytokines by non-cardiomyocytes such as fibroblasts, vascular cells, and blood cells. These factors contribute to the development of hypertrophy (Kamo, Akazawa, and Komuro, 2015). The exact mechanisms by which the heart senses strain is not fully understood. Hypotheses include stretch-sensitive ion channels and other membrane-bound and internal stretch sensors (McCain and Parker, 2011).

Cardiomyocyte hypertrophy further induces genetic changes that disrupt various cellular processes including metabolism, contraction, cytoskeleton, and membrane properties (González, Ravassa, *et al.*, 2018). Metabolic alterations associated with cardiomyocyte hypertrophy include reduced fatty acid oxidation, increased glucose utilization, dysfunction of the mitochondrial electron transport chain, and reduced adenosine triphosphate (ATP) production, crucial for both systolic and diastolic function (Tuomainen and Tavi, 2017), (Neubauer, 2007), (Facundo *et al.*, 2017).

Furthermore, at myocyte level increased microtubule density initially leads to improved contractility and left ventricular mass (Tagawa *et al.*, 1996). Later on, derangements in calcium handling, microtubule disarray, and hyperphosphorylation of titin protein lead to increased cardiomyocyte stiffness (Shah *et al.*, 2014), (Zile *et al.*, 2015).

### **1.2.1.2 Pressure overload-induced Apoptosis**

As cells hypertrophy, there is a dysregulation of protein synthesis and processing in the endoplasmic reticulum. Such dysregulation results in an accumulation of unfolded proteins that can cause dysfunction and therefore trigger apoptosis—the process of programmed cell death (Dickhout, Carlisle, and Austin, 2011), (Sun *et al.*, 2008). The increase in apoptosis can lead to left ventricular dysfunction, manifested by reduced systolic function and chamber dilation. This outcome can be

attributed, in part, to the reduction in ventricular mass and the activation of various mechanisms during apoptosis. These mechanisms can influence cardiomyocyte function even before their demise, such as the impairment of ATP production (Narula *et al.*, 2001). In addition to apoptosis, other forms of cell death, including necrosis, i.e. unplanned cell death, and excessive autophagy, i.e. intracellular recycling of cellular components, are induced by cardiac injury and hypertension contributing to myocardial remodeling (Wang, Rothermel and Hill, 2010), (Whelan, Kaplinskiy and Kitsis, 2010).

### **1.2.1.3 Inflammation**

There is accumulating evidence that indicates hypertensive cardiac injury may be caused by inflammation (Kvakan, Luft, and Muller, 2009), (McMaster *et al.*, 2015). Animal models suggest that hypertension-induced inflammation is triggered through neurohumoral factors such as ATII (Kvakan, Luft, and Muller, 2009), aldosterone (Yoshida *et al.*, 2005), mineralocorticoids (Ogata *et al.*, 2004) and the sympathetic nervous system (Levick *et al.*, 2010). These models demonstrate increased capillary wall permeability, elevated secretion of cytokines and chemokines, and infiltration of inflammatory cells into the myocardium. Another pathomechanism involves inflammation due to cardiomyocyte injury resulting from pressure overload in hypertension. When cardiomyocytes are damaged, the release of molecules (e.g., DNA fragments, heat shock proteins) prompts healthy cardiomyocytes to produce inflammatory mediators, leading to leukocyte activation and recruitment (Ghigo *et al.*, 2014). In experimental models and clinical trials, an imbalance in T effector and regulatory lymphocyte subsets, key cell components of the immune system, has been observed during hypertension, contributing to low-grade inflammation and end-organ damage (Idris-Khodja *et al.*, 2014). Moreover, hypertensive patients not only experience local inflammation but also manifest an increase in systemic inflammatory markers such as the C-reactive protein (CRP) (Hage, 2014) and CXCR3, triggering T cell homing. This homing mechanism directs T cells to migrate to the required tissue, in this case, the myocardium (Youn *et al.*, 2013).

All of these inflammatory signals, in combination with changes to the extracellular matrix, drive the activation and differentiation of fibroblasts, which then regulate inflammation and promote fibrosis (Shinde and Frangogiannis, 2017). Systemic inflammation induces endothelial oxidative stress, reducing myocardial nitric oxide

availability, resulting in cardiomyocyte stiffness and hypertrophy (Franssen *et al.*, 2016).

#### **1.2.1.4 Fibrosis**

The accumulation of type I and type III collagen fibers in the interstitium and perivascular space is a characteristic feature of cardiac fibrosis (Berk, Fujiwara, and Lehoux, 2007). The pathogenesis of fibrosis involves the differentiation of fibroblasts into myofibroblasts, which synthesize procollagen, various enzymes, cytokines, and growth factors promoting fibrosis (Shinde and Frangogiannis, 2017). This response can be triggered by the stretching of the myocardial wall, the replacement of small areas of necrosis/apoptosis, as well as hormones such as the RAAS, and chemical factors such as reactive oxygen species (González, Schelbert, *et al.*, 2018). Enzymes called membranometalloproteases may play a key factor in increased collagen turnover during fibrotic remodeling (Ahmed *et al.*, 2006). Fibrosis is associated with left ventricular dysfunction as it impairs relaxation and diastolic filling and, in later stages, compromises systolic performance (Brower *et al.*, 2006), (López *et al.*, 2006). Additionally, it may also compromise coronary blood flow by compressing intramural arteries and induce arrhythmias by promoting local re-entry mechanisms through conduction abnormalities and the interaction of cardiomyocytes with myofibroblasts (Schwartzkopff *et al.*, 1993), (Dai *et al.*, 2012), (McLenachan and Dargie, 1990), (Rohr, 2012).

#### **1.2.1.5 Change in Myocardial perfusion and Oxygen supply**

Hypertension is linked to alterations in the macrocirculation, such as coronary artery disease (Tackling and Borhade, 2023). Additionally, it induces changes in the coronary microvasculature, leading to arterial stiffness, reduced diastolic myocardial perfusion pressure, and increased susceptibility to ischemia and end-organ damage (Feihl *et al.*, 2008), (François, Liaudet, and Waeber, 2009).

Furthermore, the arterial medial wall thickness-to-lumen ratio increases. In this context, the sympathetic nervous system plays a role in the hypertrophy of smooth muscle in the vasculature; while  $\alpha$ 1-adrenergic activation leads to growth,  $\beta$ 1-adrenergic stimulation leads to atrophy of these cells (O'Callaghan and Williams, 2002). Furthermore, myocardial vascular density decreases, potentially due to dysfunction in so-called pericytes situated in close proximity to the vasculature.

These pericytes play a crucial role in angiogenesis and fibrosis (Avolio and Madeddu, 2016). One significant factor is the interplay between high pulsatile blood pressure in hypertension combined with relatively low vascular resistance (Feihl *et al.*, 2008). Another point to consider is the increased fibrotic tissue in the perivascular area that extends the oxygen diffusion distance, leading to impaired oxygen delivery to the cardiomyocytes (Frohlich, 2001). Lastly, hypertension can damage the endothelium, a critical regulator of microvascular tone, resulting in compromised coronary vasodilation (Konukoglu and Uzun, 2017). Collectively, these changes contribute to a reduction in coronary flow reserve, which is associated with left ventricular systolic and diastolic dysfunction (Galderisi *et al.*, 2002).

### **1.2.2 Adrenergic signaling in the heart**

Hypertension triggers multiple mechanisms that alter the microstructure of the heart, leading to functional impairments. One key neurohumoral pillar in this process is the sympathetic nervous system, specifically adrenergic signaling. As explained above, chronic overstimulation of adrenergic signaling contributes to cardiac remodeling by promoting hypertrophy, inflammation, apoptosis, fibrosis, and influencing angiogenesis (de Lucia *et al.*, 2014). That is why the blockade of  $\beta$ -adrenergic signaling through  $\beta$ -blockers is one of the main pillars of heart failure therapy (McDonagh *et al.*, 2021).

The upcoming section will provide a more in-depth exploration of adrenergic signaling mechanisms, detailing the various receptors, their role in cardiac function, and the alterations observed in adrenergic signaling during heart failure, placing special emphasis on the beta 2 adrenergic receptor ( $\beta$ 2AR).

Adrenergic receptors are receptors that react to the hormones released by the sympathetic nervous system, such as adrenalin (epinephrin) from the adrenal glands and noradrenalin (norepinephrine) from the postganglionic nerve endings and adrenal glands. These hormones play a crucial role by interacting with diverse cells in various organs, triggering the renowned "fight or flight" reaction (Romero, 2010).

There are different types of adrenergic receptors expressed in the heart, with  $\alpha$  receptors mostly in the vasculature of the heart and  $\beta$  receptors in the myocardium. These are divided into  $\beta_1$ ,  $\beta_2$ ,  $\beta_3$ ,  $\alpha_1A$ , and  $\alpha_1B$  adrenergic receptors (Romero, 2010).

Beta adrenergic receptors ( $\beta$ AR) are the primary receptors in the heart, with beta 1 adrenergic receptors ( $\beta_1$ AR) being the predominant subtype, constituting about 70-80%, followed by  $\beta_2$ ARs at approximately 20-30% in human hearts (Bristow *et al.*, 1986).  $\alpha_1$  receptors account for approximately 20% of the adrenergic receptors in the heart (Woodcock *et al.*, 2008).  $\beta_3$  receptors are nearly non-expressed; however, de Lucia suggests they might have a role in cardiac function, and remodeling, as well as in cardiac diseases (de Lucia, Eguchi and Koch, 2018).

### **1.2.2.1 Molecular mechanisms of GPCR**

$\alpha$  and  $\beta$ ARs are G-protein-coupled receptors (GPCR) located in the cell membrane. GPCRs are involved in most of the heart's physiological processes, including contraction, growth, apoptosis, hypertrophy, and fibrosis. These receptors consist of a perceiving extracellular N-terminus that interacts with the specific hormone and an intracellular C-terminus that mediates the intracellular response.

A contributing unit in the intracellular response is the G-protein subset of the GPCR receptor, the so-called heterotrimeric guanine nucleotide-binding protein, composed of  $\alpha$ ,  $\beta$ , and  $\gamma$  subunits. When bound to the activated GPCR, the  $\alpha$  subunit releases a guanosine diphosphate (GDP) molecule, takes up a guanosine triphosphate (GTP) molecule, and dissociates from the G-protein. The free  $\alpha$  subunit and bound  $\beta\gamma$  subunits then modulate the downstream effectors. The cell recycles the  $\alpha$  subunit by hydrolyzing GTP to GDP, thereby inactivating it, and then the G-protein subunit is bound to the GPCR (Martin *et al.*, 2012) (Figure 5).

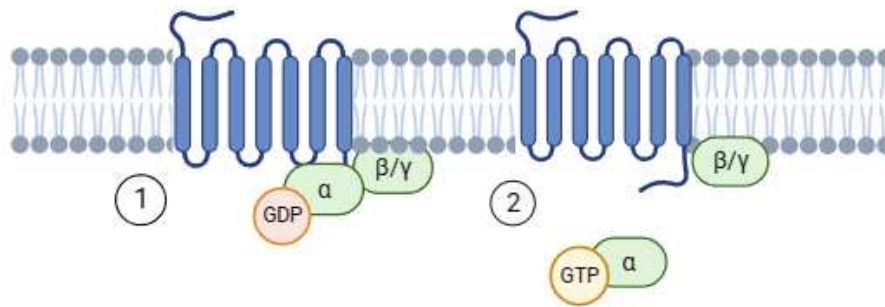


**Figure 5: G-protein-coupled receptor (GPCR) with an N- and C-terminus and G-protein in its subunits**

This figure illustrates the structure of a GPCR receptor embedded in a cell membrane, featuring its extracellular N-terminus for communication with its effector molecule and the intracellular C-terminus interacting with the G-protein subunits. 1) Depicts the GPCR in the inactivated state, where  $\alpha$  and  $\beta\gamma$  subunits are attached to the receptor, and the  $\alpha$  subunit is bound to a GDP molecule. 2) Portrays the GPCR in its activated state, with the  $\alpha$  subunit incorporating a GTP molecule and dissociating from the receptor. Created with BioRender.com and adapted from (Martin *et al.*, 2012).

The response to the sympathetic stimulus varies due to different G-protein types, which can be made up of different  $\alpha$ ,  $\beta$ , and  $\gamma$  subunits. These families of G-proteins are categorized into  $G_{\alpha s}$ ,  $G_{\alpha i}$ ,  $G_{\alpha q}$ , and  $G_{\alpha 12/13}$  (Martin *et al.*, 2012). The  $\beta_1$ AR interacts with  $G_{\alpha s}$  proteins and  $\beta_2$ AR binds with both  $G_{\alpha s}$  and  $G_{\alpha i}$ . The beta 3 adrenergic receptors ( $\beta_3$ AR) interact with  $G_{\alpha i}$  while  $\alpha_1A$  and  $\alpha_1B$  adrenergic receptors interact with  $G_{\alpha q}$  proteins (Martin *et al.*, 2012), (Motiejunaite, Amar and Vidal-Petiot, 2021), (Xiao, Ji and Lakatta, 1995).

$G_{\alpha s}$  proteins activate adenylyl cyclase (AC), which generates the messenger cyclic AMP (cAMP) from ATP.  $G_{\alpha i}$  proteins on the other hand reduce adenylyl cyclase activity. cAMP stimulates cAMP-dependent protein kinase (PKA). This enzyme can phosphorylate and regulate various downstream targets in the cardiomyocyte, including L-type calcium channels (LCC), ryanodine receptors (RyR), phospholamban (PLB), and troponin I. These regulatory actions result in an increased influx of Calcium<sup>2+</sup> ions (Ca<sup>2+</sup>) through LCCs, enhanced Ca<sup>2+</sup> reuptake facilitated by Sarco/Endoplasmic reticulum calcium ATPase (PLB/SERCA) activity, reduced Ca<sup>2+</sup> gating of RyRs, and modulation of myofilament Ca<sup>2+</sup> sensitivity of troponin I. These combined effects lead to heightened contractility and improved cardiac output.

$\alpha$  receptors linked to G $\alpha_q$  activate phospholipase C $\beta$  (PLC). This enzyme cleaves phospholipids, specifically phosphatidylinositol 4,5-bisphosphate (PIP<sub>2</sub>), generating inositol 1,4,5-trisphosphate (IP<sub>3</sub>) and diacylglycerol (DAG). IP<sub>3</sub> leads to Ca<sup>2+</sup> release from the sarcoplasmic or endoplasmic reticulum, and in conjunction with DAG, it activates Protein Kinase C (PKC). In the case of  $\alpha$  receptors, this signaling cascade results in vasoconstriction in vascular cells and the regulation of cardiomyocyte contractility in cardiomyocytes (Martin *et al.*, 2012) (Figure 6).

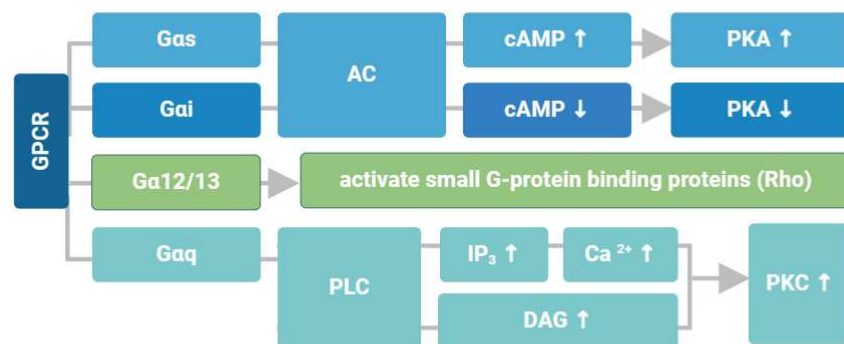


**Figure 6: Overview of G-protein subsets and effects**

This graphic provides an overview of the G-protein-coupled receptor (GPCR) and the potential G-proteins with their respective effects. Gas triggers an increase in Protein Kinase A (PKA) through cyclic adenosine monophosphate (cAMP), generated by the activation of adenylyl cyclase (AC). Conversely, Gai reduces PKA levels by inhibiting AC. G $\alpha_q$  induces a rise in Protein Kinase C (PKC) through a series of steps initiated by phospholipase C $\beta$  (PLC) activation, leading to a cascade effect that elevates calcium, diacylglycerol (DAG), and inositol 1,4,5-trisphosphate (IP<sub>3</sub>). G $\alpha_{12/13}$  activates small G-protein binding proteins. These variations in protein levels within the cell result in diverse effects impacting metabolism, cell growth, and more. Adapted from the book "Muscle: G-Protein-Coupled Receptors in the Heart" (Martin *et al.*, 2012) Created with BioRender.com.

$\beta$ AR can be deactivated through G-protein-coupled receptor kinases (GRK), which phosphorylate agonist-activated GPCRs. This phosphorylation recruits  $\beta$ -arrestins, uncoupling the GPCR from the G-proteins and promoting internalization and downregulation of the receptors (de Lucia *et al.*, 2018). Downstream,  $\beta$ -arrestins can terminate signaling by recruiting phosphodiesterases (PDEs) and diacylglycerol kinase (DAGK), contributing to the breakdown of second messengers such as cAMP (Shenoy and Lefkowitz, 2011) (Figure 7).

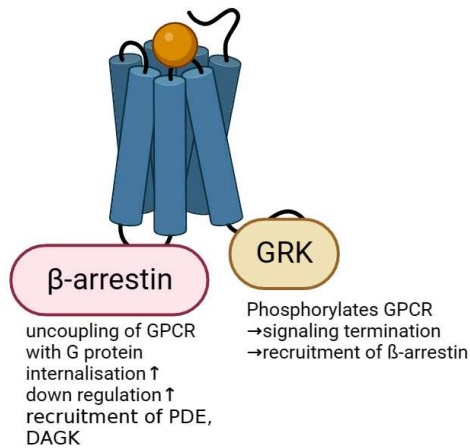


**Figure 7: Deactivation of GPCR signals**

This figure outlines the steps involved in the deactivation of GPCR signals. G-protein-coupled receptor kinase (GRK) and  $\beta$ -arrestin are key players in this process. GRK phosphorylates the GPCR, terminating its signal, and recruits  $\beta$ -arrestin. Subsequently, these proteins decouple the GPCR from its G-protein, internalize the receptor, and promote gene downregulation. Additionally, they recruit phosphodiesterase (PDE) and diacylglycerol kinase (DAGK) to break down second messengers crucial for GPCR signals. Created with BioRender.com.

Another form of downregulation is heterologous desensitization. It desensitizes a GPCR by the activation of another GPCR, without the need for phosphorylation of the former GPCR by GRKs (Woo *et al.*, 2015).

The outcomes of these signaling cascades depend on various factors, including the cellular localization of the receptors (Gorelik *et al.*, 2013), the presence of scaffolding proteins creating subcellular compartments, the types of signaling molecules present, and the extent and duration of receptor stimulation (Tilley, 2011). Additionally, it is essential to consider the high degree of simultaneous signals occurring within a cell at any given moment. The addition of these complex signals and pathways contributes to the ultimate cellular response (Martin *et al.*, 2012).

### 1.2.2.2 $\beta$ 1 physiology

The  $\beta$ 1 receptors are primarily concentrated in the heart, with an additional presence in the kidneys, eyes, and lungs (Khan, 2006). In cardiac tissue, these receptors play a pivotal role as the primary adrenergic receptors expressed in cardiomyocytes (cellxgene, 2024). Their distribution concentrates evenly on the plasma membrane, including the caveolin 3-enriched and other plasma membrane fractions (Rybin *et al.*, 2000), Golgi apparatus (Nash *et al.*, 2019), nuclear envelope (Boivin *et al.*,

2006), and the sarcoplasmic reticulum (Wang *et al.*, 2021). Cardiomyocytes employ the organic cation transporter family of proteins 3 (OCT3 proteins), (Wang *et al.*, 2021) to facilitate the stimulation of intracellular  $\beta$ 1 receptors with norepinephrine.  $\beta$ 1AR demonstrates a binding affinity to norepinephrine that is tenfold higher than that of  $\beta$ 2AR, while having an equivalent affinity to epinephrine (Xu *et al.*, 2021).

Evidence points in the direction that the location of  $\beta$ 1ARs affects the respective response upon stimulation. Plasma membrane-activated  $\beta$ 2ARs produce a global cAMP signal (Yang *et al.*, 2020). On the other hand, Golgi-localized  $\beta$ 1 receptors cAMP signals induce phosphatidylinositol-4-phosphate (PI4P) hydrolysis by phospholipase C (PLC), a response not accessed by cell surface  $\beta$ 1 receptors (Nash *et al.*, 2019). This PI4P hydrolysis in the Golgi further triggers the release of diacylglycerol (DAG) and inactive inositol-4,5-bisphosphate (IP<sub>2</sub>), facilitating nuclear protein kinase D (PKD) and hypertrophic downstream signaling (Zhang *et al.*, 2013).

Physiologically, their activation leads to chronotropic (increase in heart rate), inotropic (increase in contractility), and lusitropic (enhancement of relaxation) effects, contributing to the overall regulation of cardiac function. The chronotropic effect is elucidated through the activation of PKA in pacemaker cells, resulting in PKA-mediated phosphorylation of membrane ion channels and Ca<sup>2+</sup> handling proteins. This process enhances the Ca<sup>2+</sup> cycling rate (Woo and Xiao, 2012). In addition,  $\beta$ 1 receptors play a role in activating the RAAS (Blumenfeld *et al.*, 1999), (van Zwieten and de Jonge, 1986).

### **1.2.2.3 $\beta$ 1 pathophysiology during failure**

During heart failure, the balance between  $\beta$ 1ARs and  $\beta$ 2ARs undergoes a shift from approximately 80:20 to 60:40 due to the downregulation of  $\beta$ 1AR (Bristow *et al.*, 1989). The mechanisms implicated in  $\beta$ ARs signaling are summarized in Figure 8. This alteration in  $\beta$ AR signaling is also characterized by RyR hyperphosphorylation, decreased PLB phosphorylation, and  $\beta$ 1AR desensitization (Hartupée and Mann, 2017). Although the initial desensitization of  $\beta$ 1AR is considered an adaptive response to counteract chronic norepinephrine overstimulation, it subsequently contributes to further cardiac remodeling and the progression of heart failure.

Internalization and desensitization of GPCR, evident in both human and animal models, are mediated by G-protein-coupled receptor kinase 2 (GRK2) (Ungerer *et al.*, 1994). Initially, GRK2 upregulation is triggered by sympathetic nervous system hyperactivity, acting as a countermeasure against excessive catecholaminergic drive. However, prolonged elevated levels of GRK2 ultimately result in dysfunctional  $\beta$ -AR signaling and a decline in contractility and inotropic reserve (Penela *et al.*, 2006), (Ribas *et al.*, 2007), (Giuseppe Rengo, Perrone-Filardi, *et al.*, 2012), (Sato *et al.*, 2015), (Zhai *et al.*, 2022). The pivotal role of GRK in the development of heart failure and cardiac remodeling has been consistently demonstrated across various models, encompassing both human (Montó *et al.*, 2012), (Dzimiri *et al.*, 2004), (Leineweber *et al.*, 2005), (Agüero *et al.*, 2012) and animal studies (Choi *et al.*, 1997), (Shah *et al.*, 2001), (Tevaeearai *et al.*, 2001), (Rengo *et al.*, 2009), (Raake *et al.*, 2008). Additionally, the upregulation of GRK2 emerges as a common event in hypertension (Gros *et al.*, 1997).

The  $\beta$ 1AR downregulation reinforces  $\beta$ 2AR Gai signaling, inhibiting  $\beta$ 1AR-mediated contractile responses. Consequently, there is a reduced ability to initiate  $\text{Ca}^{2+}$  release from the sarcoplasmic reticulum (SR), resulting in a disruption of Excitation-Contraction Coupling (ECC), particularly evident under conditions of intensified workload (W. Zhu *et al.*, 2005). However, this concept has been challenged by Xiao *et al.*, who demonstrated that Gai selectively inhibits the inotropic effect of  $\beta$ 2AR without interfering with  $\beta$ 1AR signaling. (Xiao *et al.*, 2003)

$\beta$ 1AR stimulation through G $\alpha$ s signaling also activates extracellular signal-regulated kinase 1/2 (ERK1/2) via the G $\beta\gamma$  subunit, which can induce hypertrophic remodeling (Vidal *et al.*, 2012).

A study demonstrated that only  $\beta$ 1AR, with the assistance of  $\beta$ -arrestin, can activate  $\text{Ca}^{2+}$ /calmodulin-dependent kinase II (CamKII) with cAMP through a PKA-independent mechanism when chronically stimulated (Zhu *et al.*, 2003). CamKII is known to stimulate apoptosis in cardiomyocytes (Zhu *et al.*, 2007), induce hypertrophy (Ljubojevic-Holzer *et al.*, 2020), and promote arrhythmias (van Oort *et al.*, 2010), (Bengel *et al.*, 2021). It also induces cardiac remodeling (Ling *et al.*, 2009), (Singh and Anderson, 2011) and initiates a fetal gene program in the context of heart failure (Woo and Xiao, 2012). While fetal gene programs are activated in

response to pathological conditions and are meant to initially be adaptive, sustained activation of fetal genes is associated with remodeling.

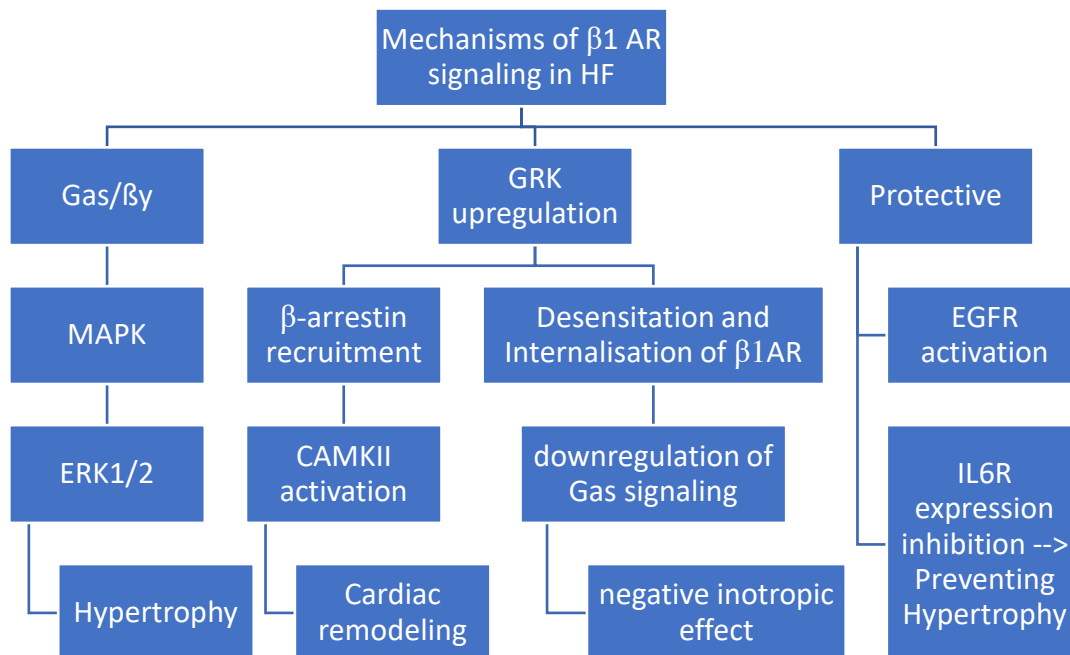


**Figure 8: Mechanisms of  $\beta$ 1AR signaling in heart failure**

The following overview explains the effects of  $\beta$ 1AR in cardiomyocytes. During cardiac stress,  $\beta$ 1AR can induce hypertrophy through the MAPK-ERK 1/2 pathway. Moreover, under cardiac stress conditions, upregulation of GRK proteins results in the desensitization of  $\beta$ 1AR, leading to a reduction in  $\beta$ 1AR-dependent Gas signaling and subsequently, a decrease in contractility. GRK proteins also recruit  $\beta$ -arrestins, activating the  $\beta$ 1AR-dependent CaMKII pathway that promotes cardiac remodeling. Conversely, two cardioprotective mechanisms of  $\beta$ 1ARs have been identified: EGFR activation and a pathway that inhibits IL6R overexpression, preventing hypertrophy.

Interestingly, treatment with a  $\beta$ 1AR-blocker does not affect phospho-CaMKII and CaMKII expression levels in experimental and human heart failure (Dewenter *et al.*, 2017). Consequently, the uncoupling of  $\beta$ 1AR-CaMKII signaling during cardiac remodeling and the initiation of the transition to heart failure remains unclear.

Moreover, a study suggests that  $\beta$ 1-adrenergic signaling may play a protective role in cardiac remodeling by preventing IL6R overactivation and sodium/calcium exchanger (NCX) dysregulation when stimulated in combination with tachycardia, which is associated with hypertrophy (Matzer *et al.*, 2022). Furthermore,  $\beta$ 1ARs have been found to transactivate receptor tyrosine kinases, such as the epidermal growth factor receptor (EGFR). This transactivation, mediated by  $\beta$ -arrestins and

involving GRK5 and GRK6, has shown a cardioprotective role (Noma *et al.*, 2007), (Patel, Tilley and Rockman, 2008).

#### **1.2.2.4 $\beta$ 2AR physiology**

The  $\beta$ 2AR was the first GPCR to be cloned and sequenced in 1986 (Dixon *et al.*, 1986). It is predominantly expressed in the bronchi, vascular smooth muscle, insulin-secreting tissues of the pancreas, gastrointestinal tract, and, to a limited extent, in the heart and coronary arteries (Khan, 2006).

The study by Bristow *et al.* analyzed whole heart tissue, stating about 20% of  $\beta$ ARs are  $\beta$ 2AR (Bristow *et al.*, 1986). A study that examined isolated cardiomyocytes reported a minor fraction (5%) of  $\beta$ 2AR in healthy mice (Myagmar *et al.*, 2017). This aligns with data from the human heart atlas, which explores mRNA patterns of different proteins in the heart. There,  $\beta$ 2AR was primarily expressed in endothelial cells and lymphoid cells, with a small portion in cardiomyocytes and myeloid cells (*cellxgene*, 2023), (Kanemaru *et al.*, 2023). At the organ level, the expression of  $\beta$ AR subtypes varies, and  $\beta$ 2 receptors exhibit a higher concentration in the apex of the heart (Gorelik *et al.*, 2013). Notably, the  $\beta$ 2-subtype is more than 2.5-fold more abundant in the sinoatrial node than in the atrial myocardium in humans. The relatively elevated  $\beta$ 2AR density in the human sinoatrial node aligns with physiological studies implicating this receptor in the regulation of cardiac chronotropism (Rodefeld *et al.*, 1996).

In the cardiomyocyte, research by Marc Bathe-Peters *et al.* and Rybin *et al.* reveal that  $\beta$ 2 receptors are confined to the T-tubular network and caveolae, in contrast to  $\beta$ 1 receptors found on both evenly distributed plasma membranes and T-tubules. This compartmentalization of the cAMP signal likely contributes to signal specificity (Rybin *et al.*, 2000), (Bathe-Peters *et al.*, 2021), (Kuschel *et al.*, 1999). Functional  $\beta$ 2AR-Gas-cAMP signaling occurs almost exclusively on the cell surface sarcolemma of rat ventricular myocytes (Cros and Brette, 2013).

The  $\beta$ 2 receptor exhibits distinct signaling pathways depending on the cell state, efficiently coupling with both Gas and Gai, displaying stronger cAMP coupling than  $\beta$ 1 receptors (Xiao, Ji, and Lakatta, 1995). In the healthy human heart,  $\beta$ 2-adrenoceptors favor coupling to Gas proteins, although coupling to Gai proteins is

also detected (Kilts *et al.*, 2000). In transgenic mice without heart failure, Gai signaling also did not play a role (Nikolaev *et al.*, 2006). The inotropic and lusitropic responses of  $\beta$ 2AR are associated with PKA-mediated phosphorylation of phospholamban at Ser16 (MacDougall *et al.*, 2012), (Molenaar *et al.*, 2007).

In the context of  $\beta$ 2AR signaling downstream, there is considerable discourse. One example is the Mitogen-activated protein kinase (p38 MAPK). This kinase is linked to various outcomes such as hypertrophy, cell death, as well as cardioprotective functions (Zheng *et al.*, 2000). Research indicates activation of p38 MAPK through the Gas PKA pathway in mouse cardiomyocytes (Zheng *et al.*, 2000) while another line of inquiry suggests Gai-protein-driven activation (Communal, Colucci and Singh, 2000). Furthermore,  $\beta$ 2AR operates through G-protein-independent pathways, such as direct inhibition of the  $\text{Na}^+/\text{H}^+$  exchange regulation factor (NHERF), leading to sustained activation and modulation of LCC activity (Hall *et al.*, 1998). Subsequently,  $\beta$ 2AR plays a crucial physiological role in the regulation of  $\beta$ AR signaling and contributes significantly to cardiac function (Figure 9).

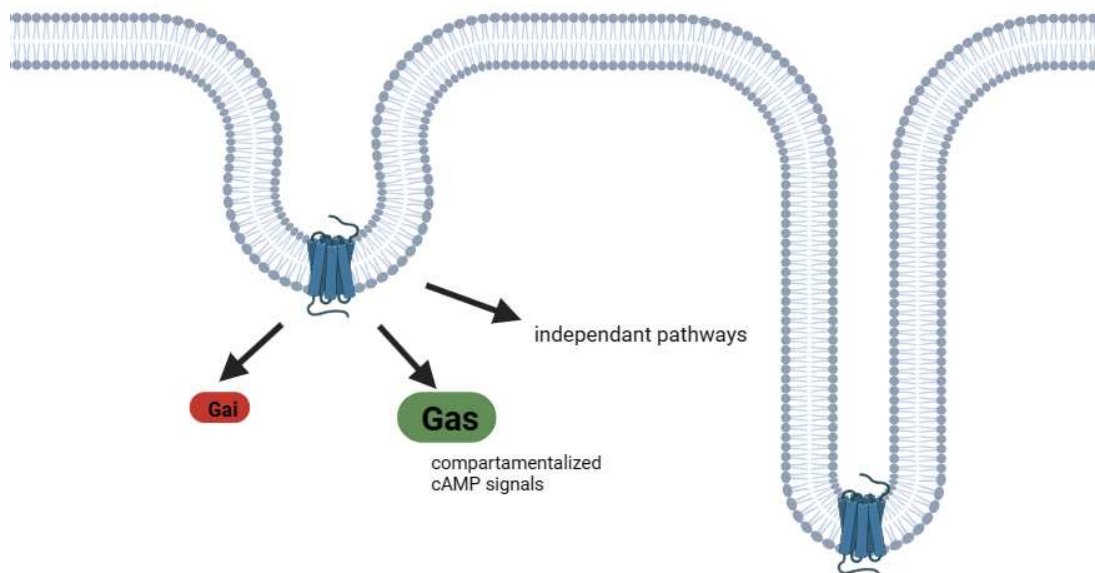


**Figure 9: Physiological signaling of  $\beta$ 2AR:**

The figure illustrates  $\beta$ 2AR in cardiomyocytes under physiological conditions. The receptors are predominantly located in invaginations of the cell membrane, such as caveolae and tubules, with a Gas predominance, resulting in compartmentalized cAMP signals. Signaling pathways mediated by Gai or G-protein-independent pathways play a secondary role. Figure created with BioRender.com.

### 1.2.2.5 $\beta$ 2AR pathophysiology in heart failure

During heart failure, while  $\beta$ 1ARs are chronically downregulated, the expression levels of  $\beta$ 2AR remain relatively unchanged, giving the  $\beta$ 2AR more influence on cardiac function (Bristow *et al.*, 1986).

The following studies examining  $\beta$ 2AR receptor localization in healthy and heart failure rats and humans revealed significant differences. Whereas Gorelik *et al.* found there was a physiologically higher gradient of  $\beta$ 2ARs in the apex of the heart in rat models compared to the base of the heart, Brodde *et al.* found that in humans with end-stage congestive heart failure  $\beta$ 2ARs expression was more prominent in the atria than in the ventricles (Gorelik *et al.*, 2013), (Brodde *et al.*, 1986). In healthy cells,  $\beta$ 2ARs resided within the surface invagination of cell membranes (caveolae) and T-tubules, producing spatially confined cAMP signals. In failing cardiomyocytes,  $\beta$ 2ARs redistributed to other cell surface areas, generating a diffuse cAMP signal, similar to  $\beta$ 1AR signaling (Gorelik *et al.*, 2013), (Nikolaev *et al.*, 2010), (Nikolaev *et al.*, 2006).

Molecular components of the  $\beta$ 2AR signaling also undergo alterations, such as increased GRK-mediated receptor phosphorylation, reduced G $\alpha$ s, and increased G $\alpha$ i-coupling with higher G $\alpha$ i-expression levels (Ceolotto *et al.*, 2008). This minimizes  $\beta$ 1AR-G $\alpha$ s signaling, leading to a negative inotropic response (Woo and Xiao, 2012), (Böhm, Eschenhagen, *et al.*, 1994), (Böhm, Castellano, *et al.*, 1994).

$\beta$ ARs can also form heterodimers, altering ligand binding profiles and enhancing signaling efficiency in regulating myocyte cAMP production and contractility (W.-Z. Zhu *et al.*, 2005). The  $\beta$ 1AR and  $\beta$ 2AR heterodimer inhibits the internalization of  $\beta$ AR, leading to the complete loss of the Gi-ERK1/2 MAPK pathway, which may play a role in the development of cardiac hypertrophy, as shown in HEK293 cells (Lavoie *et al.*, 2002), (Zou *et al.*, 1999). It is plausible to hypothesize that the downregulation of  $\beta$ 1 receptors may result in decreased heterodimerization of  $\beta$ 2AR, thus enhancing G $\alpha$ i signaling and contributing to cardiac remodeling.

### **1.2.2.5.1 Cardioprotective effects of $\beta$ 2AR signaling**

$\beta$ 2ARs are thought to exert cardioprotective effects during heart failure. *In vitro* models demonstrate that  $\beta$ 2 stimulation prevents apoptosis in response to various stimuli, such as hypoxia or chronic norepinephrine stimulation, mediated through G $\alpha$ i-G $\beta$  $\gamma$  induced activation of the PI3K-Akt pathway, a pro-survival kinase (W.-Z. Zhu *et al.*, 2005). These findings were confirmed in various animal models (Zhu *et al.*, 2001), (DeGeorge *et al.*, 2008). Communal *et al.* propose a  $\beta$ 2AR- G $\alpha$ i mediated anti-apoptotic pathway via MAPK p38 (Communal, Colucci, and Singh, 2000), while Hussain and colleagues propose that the G $\alpha$ i pathway plays a role in regulating the basal contractility of failing hearts (Hussain *et al.*, 2013).

Evidence supports the idea that  $\beta$ 2-adrenoceptor-G $\alpha$ i activation is not only beneficial but also life-saving in acute heart failure associated with Takotsubo syndrome (Paur *et al.*, 2012), (Shao *et al.*, 2013). This is likely attributed to the acute nature of catecholamine overstimulation and disease progression, inhibiting the  $\beta$ 1AR cardiotoxic effects, in contrast to the slow, progressive chronic nature of congestive heart failure.

Another cardioprotective role is the positive feedback loop between the growth factor ErbB2 and  $\beta$ 2AR. Inhibition of ErbB2 kinase increases susceptibility to heart injury induced by chronic  $\beta$ -AR stimulation, highlighting the crucial role of ErbB2 kinase in cardioprotection during  $\beta$ -adrenergic stress (Sysa-Shah *et al.*, 2016).

A novel cardioprotective mechanism entails  $\beta$ 2-AR preventing hypertrophy by inhibiting PLC $\epsilon$  signaling at the Golgi apparatus. This mechanism requires the internalization of  $\beta$ 2AR, activation of G $\alpha$ i and G $\beta$  $\gamma$  subunit signaling at endosomes, and ERK activation. The pathway inhibits both angiotensin II and Golgi-b1-AR-mediated stimulation of phosphoinositide hydrolysis at the Golgi apparatus, ultimately leading to decreased PKD and HDAC5 phosphorylation and protection against cardiac hypertrophy (Wei and Smrcka, 2023).

The  $\beta$ 2AR-G $\alpha$ s pathway has shown a positive inotropic effect without activating the CAMKII pathway when chronically stimulated, in contrast to  $\beta$ 1AR. This is because the specific  $\beta$ -arrestin CamKII-EPac1 does not bind to the C-terminus of  $\beta$ 2AR

(Mangmool, Shukla, and Rockman, 2010), (Woo *et al.*, 2015). A rat study model with myocardial infarction showed  $\beta$ 2AR overexpression had an association with pro-angiogenic pathways through activation of the VEGF/PKB/eNOS pathway, which led to a higher capillary density (G. Rengo *et al.*, 2012).

*In vivo* studies have shown enhanced cardiac function with no pathology at high expressions of  $\beta$ 2AR (60-fold). However, grossly overexpressing  $\beta$ 2 in mice (100 and 350-fold) led to heart failure, hypertrophy, fibrosis, increased apoptosis, and ventricular failure of myocytes (Milano *et al.*, 1994), (Liggett *et al.*, 2000), (Dorn *et al.*, 1999), (Zou *et al.*, 1999). Rodent model studies showed that  $\beta$ 2AR stimulation was beneficial against cardiac remodeling (Xydas *et al.*, 2006).

A study using a dog model of heart failure found no expression differences in  $\beta$ 2AR protein during heart failure disease development, but overexpression of  $\beta$ 2AR genes led to improved contraction and function (Gong *et al.*, 2017).

The discovery of these cardioprotective effects has prompted efforts to gain a deeper understanding of  $\beta$ 2 adrenergic signaling, opening up the possibility of exploring it as a novel target for therapies in the realm of heart failure.

#### **1.2.2.5.2 $\beta$ 2AR signaling and the development of heart failure**

The  $\beta$ 2AR has not only cardioprotective functions but is also involved in mechanisms that exacerbate heart failure. One hypothesis is that  $\beta$ 2ARs activation only produces desirable signaling in the failing heart if applied before the structure of the cardiomyocytes changes (Gorelik *et al.*, 2013). The cardioprotective and cardiotoxic effects of  $\beta$ 2AR signaling are comprehensively summarized in Table 1.

G $\alpha$ i signaling was also attributed to weakening cardiomyocyte contraction through negative regulation of Ca<sup>2+</sup> dynamics, leading to HF exacerbation (El-Armouche *et al.*, 2003), (Fajardo *et al.*, 2013). Both  $\beta$ 1 and  $\beta$ 2ARs are found to be involved in pathways that promote hypertrophy (Zhao *et al.*, 2011).  $\beta$ 2ARs stimulation through G $\alpha$ i signaling also activates ERK1/2 via the G $\beta$  $\gamma$  subunit, which can induce hypertrophic remodeling (Zou *et al.*, 1999).

As explained in the  $\beta$ 1ARs passage, GRK2 plays an important role in  $\beta$ 1ARs desensitization and internalization. Additionally, GRK2 exhibits cardiotoxic effects such as the promotion of adrenal sympathetic activity (Lymperopoulos, Rengo, and Koch, 2012), and an increased incidence of myocyte death in ischemic models (Sato *et al.*, 2018). Recent findings suggest that  $\beta$ 2-adrenoceptor Gai-biased signaling is the link between GRK2 up-regulation and the progression to decompensated heart failure (Zhu *et al.*, 2012).

Additionally,  $\beta$ 2ARs expressed in other cells in the heart, other than cardiomyocytes, may play a role in heart failure and cardiac remodeling. For example, immune cell  $\beta$ 2ARs are important for proinflammatory macrophage infiltration to the heart. Macrophage infiltration leads to cardiac injury, cardiomyocyte death, fibrosis, and hypertrophy (Tanner, Maitz, and Grisanti, 2021). Furthermore, both  $\beta$ ARs seem to play a role in the development of fibrosis in cardiac remodeling (Brouri *et al.*, 2004).

A topic of significant debate is the reason behind the superiority of the non-selective  $\beta$ -blocker Carvedilol over its  $\beta$ 1-selective counterparts in heart failure mortality (Rain and Rada, 2015). The central question is: Is this superiority attributed to its blockade of  $\beta$ 2AR signals, which promote heart failure? Various hypotheses attempted to elucidate why Carvedilol may exhibit enhanced efficacy in the treatment of heart failure. In their review, Talan *et al.* proposed that therapies involving a  $\beta$ 1AR blocker +  $\beta$ 2AR agonist,  $\beta$ 1AR blocker + ACE inhibitors, and Carvedilol, all coincide with vasodilation, potentially contributing to superior outcomes compared to  $\beta$ 1AR-selective blockers (Talan *et al.*, 2011). Another theory involves  $\beta$ -arrestin-dependent signaling that activates ERK through  $\beta$ 2AR (Wisler *et al.*, 2007), and the EGFR via  $\beta$ -arrestin-biased signaling at  $\beta$ 1AR (Kim *et al.*, 2008) conferring cardioprotection in animal models (Noma *et al.*, 2007).

**Table 1: Overview of  $\beta$ 2AR signaling effects**

The table provides an overview of  $\beta$ 2AR signaling effects categorized as either cardiotoxic or cardioprotective, along with corresponding references. Numbers added in the "Cardiotoxic" or "Cardioprotective" column correspond to the number in the references provided.

<b>Effects of <math>\beta</math>2AR signaling</b>			
<b>Cardioprotective</b>	<b>Ref.</b>	<b>Cardiotoxic</b>	<b>Ref.</b>
Antiapoptotic →Gai-G $\beta$ $\gamma$ -PI3K-Akt (1)	(1) (Zhu <i>et al.</i> , 2001), (DeGeorge <i>et al.</i> , 2008)	Gai → GRK upregulation → $\beta$ AR desensitization and internalization →promotion of adrenal catecholamine production (1) →Apoptosis (2)	(1)(Lympopoulos, Rengo and Koch, 2012) (2) (Sato <i>et al.</i> , 2018)
→Gai-MAPKp38 (2)	(2) (Communal, Colucci, and Singh, 2000)		
Counteracts hypertrophy: →Internalisation of $\beta$ 2AR →Gai-G $\beta$ $\gamma$ activation at endosome →ERK activation →Inhibition of ATII, and Inhibition of $\beta$ 1AR mediated PIP hydrolysis at the Golgi apparatus	(Wei and Smrcka, 2023)	Hypertrophic: Gai- G $\beta$ $\gamma$ →ERK1/2	(Zou <i>et al.</i> , 1999)
		Fibrosis	(Brouri <i>et al.</i> , 2004)
$\beta$ 2AR Gas positive inotropic pathway does not activate the CAMKII apoptotic pathway	(Mangmool, Shukla and Rockman, 2010), (Woo <i>et al.</i> , 2015)	Neg. Inotropic: Gai inhibition of the Gas-PKA-cAMP pathway	(El-Armouche <i>et al.</i> , 2003), (Fajardo <i>et al.</i> , 2013).
Angiogenic: VEGF/PKB/eNOs pathway	(G. Rengo <i>et al.</i> , 2012)	Promotes inflammation: $\beta$ 2AR in Immune cells →	(Tanner, Maitz and Grisanti, 2021)
Positive correlation of $\beta$ 2AR and ErbB2	(Sysa-Shah <i>et al.</i> , 2016)	Macrophage infiltration	

### 1.2.2.6 Possible novel treatment strategies with $\beta$ 2AR as a target

The pursuit of novel treatment strategies in the realm of  $\beta$ 2AR signaling and downstream targets has yielded promising avenues for addressing heart failure.

One innovative approach involves a combination of the fully escalated heart failure medication which involves  $\beta$ -blockers, an ACE-I, an ARB, digoxin, and an aldosterone receptor combined with  $\beta$ 2-adrenoceptor-agonist clenbuterol, presenting a protective drug design strategy for mechanical left ventricular assistance in advanced heart failure stages (Hall *et al.*, 2007).

Exploring further combination therapies, the combination of a  $\beta$ 1ARs antagonist with  $\beta$ 2ARs agonists like fenoterol is proposed (Talan *et al.*, 2011). In their review, Woo and colleagues suggest a  $G_{\alpha s}$ -biased  $\beta$ 2AR agonist combined with a  $\beta$ 1AR antagonist, leveraging  $\beta$ 2AR-specific  $G_{\alpha s}$  signaling to achieve a positive inotropic effect without the cardiotoxicity associated with the  $\beta$ 1AR  $G_{\alpha s}$  pathway and mitigating the negative  $G_{\alpha i}$ -mediated effects (Woo *et al.*, 2015).

Normalizing  $\beta$ -adrenergic signaling encompasses multiple therapeutic targets, with GRK2 inhibition emerging as a proposed strategy for heart failure treatment (Lymperopoulos, Rengo, and Koch, 2012). This approach could potentially reduce  $G_{\alpha i}$  signaling, minimizing  $\beta$ ARs desensitization and internalization. Studies combining GRK2 inhibition with a  $\beta$ -blocker have demonstrated additive or synergistic effects in various heart failure models (Sato *et al.*, 2015). Another approach is to target the  $\beta$ -arrestin signaling (Patel, Tilley, and Rockman, 2008). Additionally, ErbB2 kinase emerges as a potential novel therapeutic target within the downstream  $\beta$ 2AR signaling cascade (Sysa-Shah *et al.*, 2016).

These innovative strategies provide valuable insights into the evolving landscape of therapeutic interventions centered around  $\beta$ 2AR signaling and downstream targets in the context of heart failure.

### 1.2.2.7 The unknown in $\beta$ 2AR signaling

In conclusion, the uncertainties surrounding  $\beta$ 2AR signaling contribute to ongoing debates within the scientific community. Questions persist regarding the delicate balance between the antiapoptotic and negative inotropic effects of Gai-mediated  $\beta$ 2AR signaling, as highlighted by W. Zhu et al. (W. Zhu *et al.*, 2005).

The functional existence of  $\beta$ 2-adrenoceptor-Gai signaling in the chronically failing human heart has been a matter of debate. Proponents such as Kilts and Gong argue for the presence of increased Gai proteins in human heart failure cells, suggesting a potential role in the pathophysiology of the condition (Kilts *et al.*, 2000), (Kilts *et al.*, 2003), (Gong *et al.*, 2002). Contrastingly, Molenaar challenges the idea of an important negative inotropic role of Gai coupling in human heart failure (Molenaar *et al.*, 2007). Another human study countering the idea of  $\beta$ 2AR receptors playing a role in heart failure found no evidence of  $\beta$ 2AR activity correlating with heart failure risk (Baudier *et al.*, 2023).

Navigating the intricate nature of  $\beta$ 2AR, a multifaceted receptor with both promoting and counteracting effects on cardiac remodeling and heart failure, underscores its complexity in engaging diverse pathways and manifesting distinct effects in various cardiac cells. The ongoing discourse raises fundamental questions about whether  $\beta$ 2AR signaling acts as a regulator, balancing between the promotion and counteraction of cardiac remodeling and heart failure.

Given these complexities, some suggest that targeting downstream molecules may offer a more intuitive approach to achieving specific therapeutic effects (Giuseppe Rengo, Femminella, *et al.*, 2012). While the scientific community generally agrees on the overarching goal of restoring  $\beta$ AR signaling to its former state, diverse opinions persist on the most effective strategies to attain this objective.

Despite extensive research, the precise role of  $\beta$ 2AR in human heart failure remains elusive, emphasizing the need for continued exploration. The complexities surrounding  $\beta$ 2AR signaling underscore the demand for further research to unravel its exact role in cardiac function and pathology.

### ***1.3 Objectives and description of the thesis project***

$\beta$ 2ARs play a pivotal role in regulating cardiac function and contribute to the development of heart failure. While regulatory pathways are being discovered, much remains unknown, leading to debates on how these pathways interact within cells and their roles in human heart cells. Therefore, it is crucial to gather more data on  $\beta$ 2ARs and their implications for humans to assess the translatability of insights from animal models to human cardiomyocyte function. Therefore, the main aims of this thesis are to investigate:

1. Alterations in  $\beta$ 2AR expression patterns in cardiomyocytes isolated from control and hypertensive Dahl salt-sensitive rats during early- and late-stage cardiac remodeling.
2. Alteration of  $\beta$ 2AR expression patterns during  $\beta$ AR stimulation from control and hypertensive Dahl salt-sensitive rats
3. Changes in  $\beta$ 2AR expression levels during heart failure in the human myocardium.
4. Comparative alterations of  $\beta$ 2ARs in relation to changes in  $\beta$ 1ARs expression in Dahl salt-sensitive rats

## 2. Material and Methods

### 2.1 Overview

In this experiment, we employed a hypertensive rat model, dividing it into two groups of healthy and hypertensive rats based on the salt concentration in their diet. Upon reaching a predetermined age, we euthanized the rats and isolated the cells using the Langendorff method. Furthermore, heart tissue samples were collected for Western Blot analysis and RNA microarray, with a focus on  $\beta$ 2-adrenergic receptors. The isolated cardiomyocytes were stained for  $\beta$ 2AR, and the cells were analyzed using fluorescence microscopy. This data was compared with the  $\beta$ 1AR data collected using Immunocytochemistry (ICC) (Figure 10).

For human samples, we utilized a bank of heart tissues obtained from transplant donors. Western Blot analyses were conducted to quantify  $\beta$ 2AR expression.

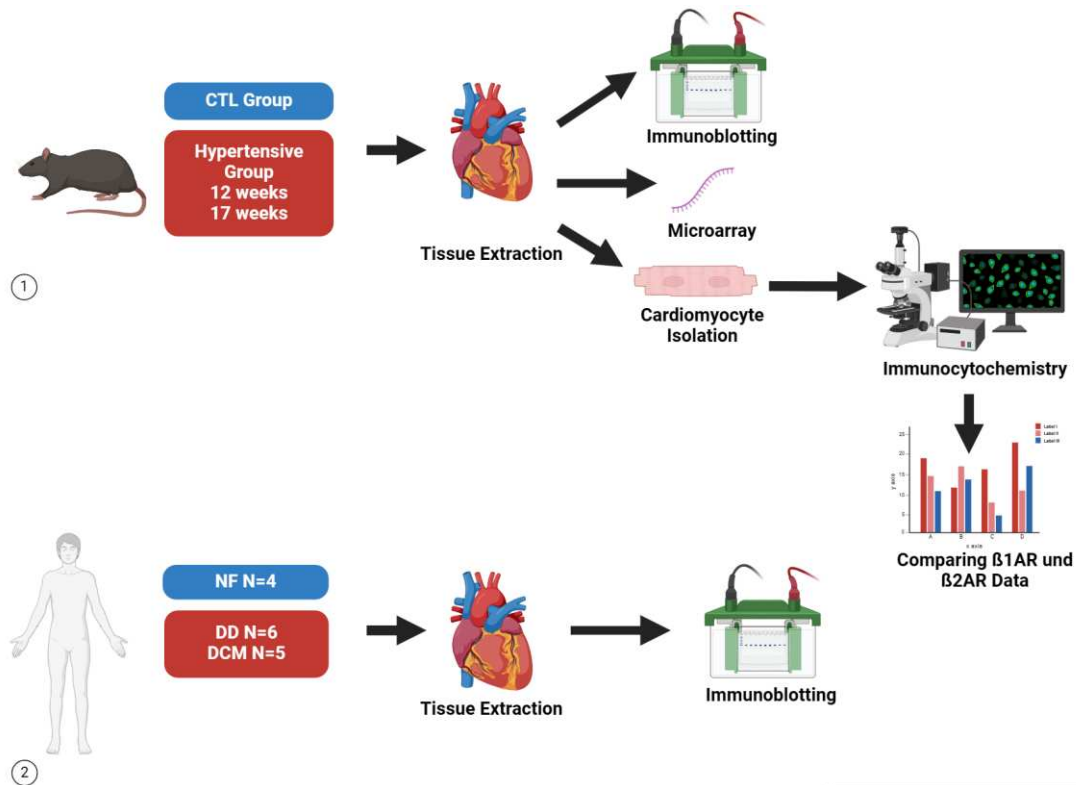


**Figure 10: Overview of the experiments**

The figure provides an overview of the methods employed in this thesis. Data collection included (1) Dahl-salt-sensitive rats, with a hypertensive group euthanized at 12, 17, and 19 weeks and a corresponding normotensive control group (CTL).  $\beta$ 2ARs were analyzed in rat hearts using immunoblotting, microarray, and Immunocytochemistry (ICC) of isolated cardiomyocytes. Isolated cardiomyocytes were also treated with a  $\beta$ -agonist to analyze the rapid desensitization behavior of

$\beta$ 2AR in both groups. The ICC data was then compared to  $\beta$ 1AR ICC data collected by Matzer, Ingrid Msc. (Matzer, 2021). Additionally, (2) human data was obtained from the Human Organ Donor Bank, consisting of 5 non-failing (NF) hearts, 6 hearts with diastolic dysfunction (DD), and 5 hearts with dilated cardiomyopathy (DCM). Immunoblotting of left ventricular tissue was utilized for quantifying  $\beta$ 2AR in the human hearts. Created with BioRender.com.

## **2.2 Dahl salt-sensitive rat model**

To replicate the human scenario of hypertension-induced cardiomyopathy, we utilized the male Dahl salt-sensitive rat model from Charles River Laboratories in the USA. These rats are selectively bred for their development of hypertension due to salt sensitivity, exhibiting low renin, a salt-sensitive form of hypertension, which is uncommon in salt-resistant wild-type rats (Charles River Laboratories, 2009). It is reported that these rats develop heart failure at 15-20 weeks due to induced hypertension (Schwarzer, 2016). This model was selected specifically for its close resemblance to the phenotype observed in humans with hypertension, including alterations in left ventricular geometry and heart function (Doi *et al.*, 2000). Ethical approval for the use of these rats was obtained from the Austrian Ministry (BMBWF: 2020-0.192.430) and the rats were treated according to European ethical regulations.

From weeks 0-7 both groups received a low-salt-diet (LSD, 0.3% NaCl; Research Diets; D10001R). The test group received a high-salt-diet (HSD, 8% NaCl; Research Diets; D05032408Y) starting at week seven, while the control group continued with the LSD.

Starting at week 7, live parameters including blood pressure and body weight were collected every two weeks. Systolic and diastolic blood pressure were measured, using the CODA® tail cuff system (Kent Scientific Corporation, Torrington, CT, USA). Recordings were performed in a steady state and were the average of three consecutive measurements. Transthoracic echocardiography measurements, including ejection fraction (EF) to assess systolic heart failure and E/e' to evaluate diastolic heart failure, were performed shortly before the experimental timepoints with Vevo 3100 (VisualSonics, Toronto, ON, Canada) under light anesthesia (Isoflurane, 1-1.5%, and 1.5–2 l/min oxygen flow). The EF was measured in the parasternal long axis. To obtain the E/e' ratio, the mitral annular velocity (e') was

obtained using the tissue doppler in a parasternal short axis, while the early mitral inflow velocity (E) was acquired using the flow doppler in a modified parasternal long axis.

Rats received deep anesthesia with Isoflurane before euthanization by guillotine. After euthanizing the rats, heart mass was obtained and normalized to body mass to indicate hypertrophic cardiac growth. Heart samples were collected at an early stage (12 weeks) and late stage (17 weeks) timepoints, either for subsequent microarray or utilized for the isolation of ventricular cardiomyocytes to assess differentiation in receptor expression and hypertrophy. Rats used for immunoblotting were used from an older cohort which was euthanized at 19 weeks (Figure 11).

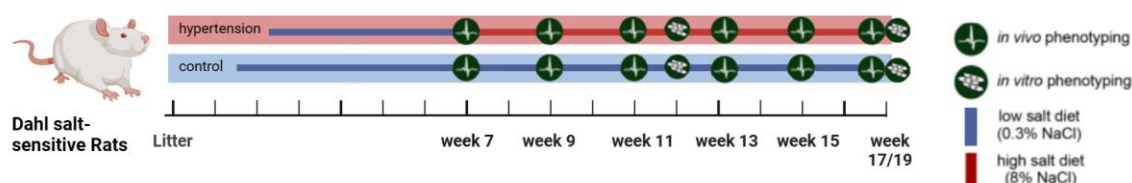


**Figure 11: Experimental timeline and parameters for the high-salt-diet induced hypertension study**

The male Dahl salt-sensitive rat cohorts were divided into two groups: a control group receiving a low-salt-diet and the hypertension group receiving a high-salt-diet from week seven. *In vivo* phenotyping, encompassing blood pressure and body weight, was conducted biweekly starting from week seven. Heart tissue collection was performed at both an early timepoint of 12 weeks and a late timepoint of 17 or 19 weeks. Adapted from the figure by Holzer, Senka (Holzer, Senka, 2019), created using Biorender.

The *in vivo* data and results presented in this thesis are integral to a broader project, involving Ms. Ingrid Matzer's Master's thesis "Role of  $\beta$ 1-adrenergic signaling in early- and late-stage hypertensive cardiac remodeling" (Matzer, 2021), Dr. Julia Voglhuber's Ph.D. thesis "the perinuclear region in cardiac remodeling" which is under revision and the paper " $\beta$ -Adrenergic Receptor Stimulation Maintains NCX-CaMKII Axis and Prevents Overactivation of IL6R-Signaling in Cardiomyocytes upon Increased Workload" (Matzer *et al.*, 2022). Dr. Julia Voglhuber and Ms Ingrid Matzer collected the *in vivo* data analyzed in this thesis. The *in vivo* data used for analysis pertain to the rats utilized in Microarray, immunoblotting, and ICC experiments, as well as the hypertrophy data that I contributed to collecting.

### **2.3 Human tissue collection**

All experiments with human heart probes were approved by the Ethical Committee of the Medical University of Graz (Nr. 28-508 ex 15/16), and they were performed in accordance with principles outlined in the *Declaration of Helsinki*. Informed consent was obtained from patients with terminal heart failure. However, it was not feasible to collect informed consent from all patients who did not have terminal heart failure. Therefore, the ethical committee waived the requirement for informed consent for these patients, considering that their underlying medical condition prevented them from providing it. Upon transport in ice-cold Custodiol cardioplegic solution supplemented with 2,3-butanedione monoxime (BDM 10mM), Sigma cat.no B0753, before transportation to the laboratory as a precaution against hypoxic damage.

Cardiomyocyte Isolation via the Langendorff perfusion method was attempted. Tissue samples were extracted from the left ventricle, anonymized, and stored in cooled nitrogen at -40°C. These samples were later utilized in immunoblotting for  $\beta$ 2AR. Patient data, including LVEF, weight, age, and gender, were anonymized and recorded in a file. The patients were then classified into three groups: not failing (NF), diastolic dysfunction (DD), and dilated cardiomyopathy (DCM). In our study, Diastolic Dysfunction is observed with HFpEF.

DCM is characterized by left ventricular dilation and contractile dysfunction, resulting in a reduced LVEF. Echocardiography reveals ventricular hypokinesis, and dilation can occur in both the left and right ventricles (Weintraub, Semsarian, and Macdonald, 2017).

## 2.4 Ventricular cardiomyocyte rat isolation via Langendorff perfusion

Langendorff Perfusion is an isolation method wherein various solutions are slowly infused through the coronary arteries of the heart. Our Langendorff perfusion setup maintained constant flow through a Peristaltic Pump, and pressure overload was counteracted with a bubble trap. (Figure 12).

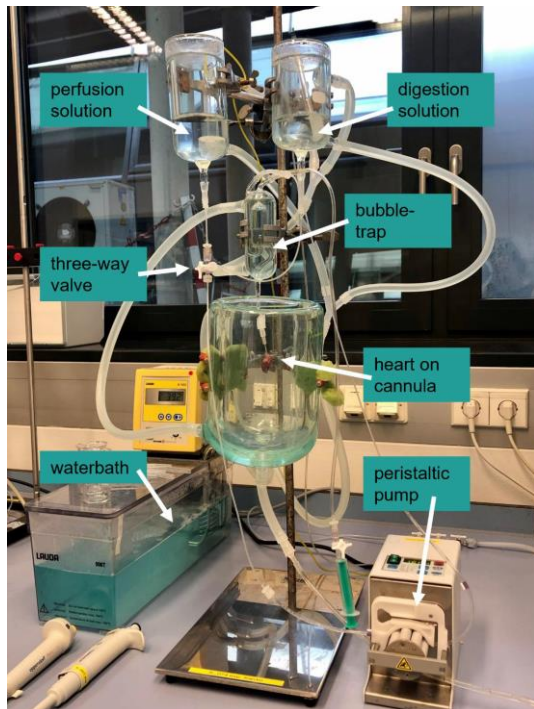


**Figure 12: Langendorff perfusion setup**

In the following figure, the Langendorff perfusion setup is depicted, consisting of a water bath regulating temperature, a peristaltic pump controlling solution velocity into the vessels, a three-way valve directing solution flow, and a bubble trap preventing pressure overload. The solutions then infiltrate the heart, attached to the cannula via the aorta. After the digestion process is complete, the heart is removed from the Langendorff perfusion setup for subsequent steps in the isolation protocol. Source: (Matzer, 2021) used with kind permission from Matzer Ingrid Msc.

The isolation of ventricular cardiomyocytes from rat hearts involved an adapted Langendorff-based perfusion protocol (Ljubojevic *et al.*, 2014). Dahl salt-sensitive HSD- and LSD-fed Rats at 12 and 17 weeks received an intraperitoneal injection of Heparin (500 IE; Gilvasan; ET34622) 15 minutes before anesthesia with isoflurane (Baxter; 1087151) and subsequent decapitation via guillotine. Following the opening of the thoracic cavity, the heart was excised, and the aorta was promptly cannulated.

The Langendorff setup was employed, and after retrograde perfusion with cannulation solution, the heart underwent perfusion with Ca<sup>2+</sup>-free solution (perfusion solution) for 1 minute and 30 seconds. The primary function of the isolation process involves the cannulation solution, designed to wash out toxic metabolites that accumulate during hypoxia and stress associated with euthanization. This solution aims to mimic an environment in which cardiomyocytes feel comfortable. Butanedione monoxime (BDM) is added to inhibit permanent contracture, thereby reducing ischemia-reperfusion injury (Li *et al.*, 1985).

The hearts were then digested with myocyte digestion solution for approximately 10 minutes until clear signs of digestion were observed. The digestion solution is intended to break down the tissue surrounding the cardiomyocytes, including fibroblasts, connective tissue, and vascular cells, using enzymes such as Liberase and Trypsin. The digestion process should be stopped to prevent the cardiomyocytes from being digested as well, and this is achieved with the rat myocyte stopping solution 1. Digested ventricles, excluding the atria, were cut from the cannula, immersed in myocyte stop solution 1, and sieved through a 300 µm mesh. The obtained myocytes settled through gravity and underwent exposure to a series of solutions with increasing Ca<sup>2+</sup> concentrations, to obtain functioning contracting cardiomyocytes. The last Ca<sup>2+</sup> solution is BDM-free to allow proper contraction.

Finally, the isolated ventricular cardiomyocytes were plated on Laminin-coated glass-bottom cell culture dishes (Greiner bio-one; 627861) and allowed to attach for 1 hour at room temperature. These cells were then used for hypertrophy measurements and ICC.

### 2.4.1 Solutions for rat ventricular cardiomyocyte isolation

All solutions were prepared using ddH<sub>2</sub>O (Millipore) unless stated otherwise.

**Table 2: Rat perfusion solution, pH =7.4**

<b>Reagent</b>	<b>Company</b>	<b>Cat. No.</b>	<b>Conc. [mM]</b>
NaCl	Roth	3957.1	135
KCl	Roth	P017.1	4.7
KH <sub>2</sub> PO <sub>4</sub>	Roth	P018.1	0.6
HNa <sub>2</sub> PO <sub>4</sub> dibasic	Sigma	S0876	0.6
MgSO <sub>4</sub> *7H <sub>2</sub> O	Roth	P037.1	1.2
HEPES	Roth	6763.1	10
Taurin	Sigma	T0625	30

**Table 3: Rat perfusion buffer**

<b>Reagent</b>	<b>Company</b>	<b>Cat. No.</b>	<b>Conc. [mM]</b>
Perfusion solution	See table 2	-	-
Butanedione monoxime	Sigma	B0753	10
Glucose	Merck	50-99-7	10

**Table 4: Rat cannulation solution**

<b>Reagent</b>	<b>Company</b>	<b>Cat. No.</b>	<b>Conc. [mM]</b>
Perfusion solution	See table 2	-	-
CaCl <sub>2</sub>	Sigma Aldrich	21115	1

**Table 5: Rat calcium solutions**

<b>Reagent</b>	<b>Company</b>	<b>Cat. No.</b>	<b>Conc. [mM]</b>
CaCl <sub>2</sub>	Sigma Aldrich	21115	100
CaCl <sub>2</sub>	Sigma Aldrich	21115	10

**Table 6: Rat myocyte digestion solution**

Reagent	Company	Cat. No.	Quantity
Perfusion solution	See table 2	-	40mL
Liberase TM Research Grade	Roche	0540 1127001	1200 – 1300µL
Trypsin	GIBCO	15090-046	222µL
10mM CaCl <sub>2</sub>	Sigma Aldrich	21115	150µL

**Table 7: Rat myocyte stopping solution 1**

Reagent	Company	Cat. No.	Quantity
Perfusion solution	See table 2	-	22.5mL
BCS	Sigma Aldrich	12133C	2.5mL
10mM CaCl <sub>2</sub>	Sigma Aldrich	21115	31.26µL

**Table 8: Rat myocyte stopping solution 2**

Reagent	Company	Cat. No.	Quantity
Perfusion solution	See table 2	-	48mL
BCS	Sigma Aldrich	12133C	2.5mL
10mM CaCl <sub>2</sub>	Sigma Aldrich	21115	63.16µL

**Table 9: Rat calcium series.**

Calcium solutions were diluted from the myocyte stopping solution 2.

No.	CaCl <sub>2</sub> [mM]
1	0.125
2	0.25
3	0.5
4	1
5	1.5

**Table 10: Rat normal tyrode solution (NT)**

<b>Reagent</b>	<b>Company</b>	<b>Cat. No.</b>	<b>Conc. [mM]</b>
NaCl	Roth	3957.1	140
KCl	Roth	P017.1	4
MgCl <sub>2</sub> *6H <sub>2</sub> O	Roth	HN03.2	1
HEPES	Roth	6763.1	10
CaCl <sub>2</sub>	Sigma Aldrich	21115	1.5
Glucose	Merck	50-99-7	5

One of my responsibilities was to optimize the human heart Langendorff isolation protocol. There were two timepoints during my laboratory work when the parameters were aligned, coinciding with the extraction of organs from deceased donors at the LKH Medical University Clinic in Graz, where the heart was not suitable for transplantation. Unfortunately, at the first timepoint, I could not yield enough viable cells. In the second timepoint, although I obtained some cells, their survival rate was not sufficient to proceed with ICC, and consequently, this aspect was excluded from my results and discussion.

## ***2.5 Hypertrophy measurements***

To assess cardiomyocyte specific hypertrophy, cellular dimensions of isolated cardiomyocytes from LSD- and HSD-fed Dahl salt-sensitive rats at 12 and 17 weeks were measured from Differential Interference Contrast images. All live cell imaging was performed at room temperature (22-24°C). Attached cardiomyocytes were captured at the largest sectional plane available and imaged using confocal fluorescence microscopes (Zeiss LSM 510 Meta or LSM 700 (Carl Zeiss, Germany), Nikon A1 (Nikon Europe B.V., The Netherlands) or Olympus Fluoview 1000 (Olympus, USA). Cell width and cell length measurements were conducted using ImageJ software (National Institutes of Health, USA).

## **2.6 Immunocytochemistry (ICC)**

The ICC protocol was obtained from the paper: “Early Remodeling of Perinuclear Ca<sup>2+</sup> Stores and Nucleoplasmic Ca<sup>2+</sup> Signaling During the Development of Hypertrophy and Heart Failure” (Ljubojevic *et al.*, 2014).

### **2.6.1 Drug treatments and fixing isolated Cardiomyocytes**

The cardiomyocytes collected at the late timepoint (17 weeks) were seeded onto cell culture dishes. Subsequently, they were incubated for one hour at 37°C in two groups: one with 3 mL containing 100 nM Isoprenaline hydrochloride (ISO), a beta-agonist, and another with 3 mL of Normal Tyrode (NT), devoid of any drug treatment.

After that cells were fixed for 10 minutes with 1 mL of 4% paraformaldehyde (Morphisto; 1176200500), yielding a 1% paraformaldehyde fixation solution. Cells were then rinsed three times with phosphate-buffered saline (PBS, Sigma Aldrich; P4417-100TAB) and stored at 4°C in the dark until further usage.

### **2.6.2 ICC staining**

Permeabilization was carried out using 0.6% Triton-X100 (Sigma Aldrich; T8787-100ML)/PBS for 10 minutes. Triton-X100 facilitates antibody penetration into intracellular structures, while PBS, a phosphate buffered saline solution, maintains physiological pH and environment. Following a single wash in PBS, cells underwent incubation with the primary antibody (ADRB2, Thermofisher BS-0947R polyclonal LOT: AG 10096795) at a concentration of 1:100 in 5% BSA (Sigma Aldrich; B6917)/3% goat serum (Abcam; ab7481)/0.01% Triton/PBS at room temperature for a minimum of 3 hours (or at 4°C overnight), with gentle shaking. Bovine Serum Albumin (BSA) was employed as a blocking agent to prevent nonspecific binding, stabilize antibodies, and serve as a diluent.

Following two washes in 0.01% Triton-X100/PBS, the cells were exposed to the secondary antibody (anti-rabbit Alexa647 (Cell signaling; 4414) 1:1000 in 5% BSA (Sigma Aldrich; B6917)/3% goat serum (Abcam; ab7481)/0.01% Triton/PBS for 2 hours at room temperature in the dark. Subsequently, cells underwent two washes with 0.01% TritonX-100/PBS and two additional washes with PBS before being stained with DAPI (Carl Roth; 6335.1; 1:200 in 5% BSA/PBS) for 10 minutes at room temperature in the dark. DAPI is a DNA fluorescent stain used to visualize cell

nuclei, emitting blue fluorescence. Following this, cells were washed twice with PBS and kept in PBS for imaging.

Images were recorded on a confocal fluorescence microscope (Zeiss LSM 510 Meta) with a Plan Neofluar 40x/1.3 oil-immersion objective. Image J software (National Institutes of Health, USA) was used to measure the intensity of the recorded fluorescence signal. Ventricular cardiomyocytes with ADRB2 staining were analyzed for their whole cell and fluorescence signal subtracting the nucleus (Figure 13). To ensure equal staining of all treatment groups, cardiomyocytes of each group were stained together. Background corrected data was used for statistical analysis.

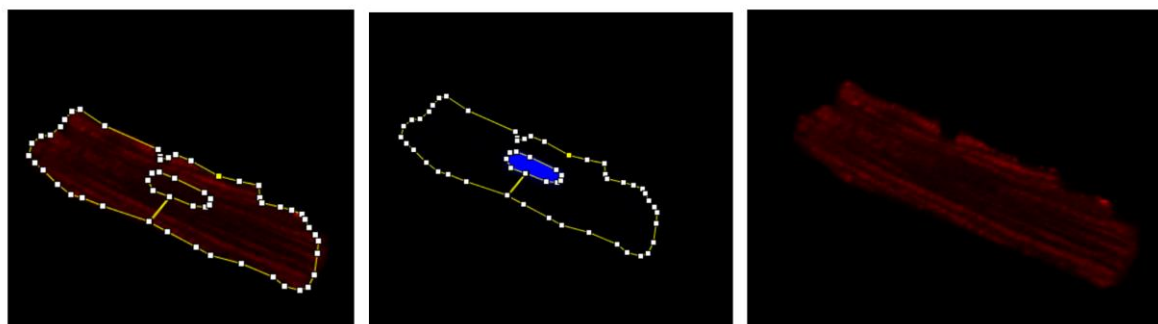


**Figure 13: Cardiomyocyte ADRB2 fluorescence analysis using Image J software**

This figure illustrates the fluorescence analysis conducted using ImageJ software. The cell image was captured on a confocal fluorescence microscope with two lasers, allowing differentiation between the blue DAPI staining representing the nucleus and the red staining representing the ADRB2 antibody. In the software, the entire cell area was selected, excluding the nucleus.

## ***2.7 Immunoblotting***

The Western Blot protocol was used in the master thesis “Role of  $\beta$ 1-adrenergic signalling in early- and late-stage hypertensive cardiac remodeling” (Matzer, 2021). Human left ventricular heart tissue was used for one Western Blot comprising of individuals with not failing hearts, diastolic dysfunction, and dilated cardiomyopathy. Dahl salt-sensitive LSD- and HSD-fed rats were used for the other immunoblot. These comprised rats from the first cohort which were euthanized at 12 weeks and 19 weeks.

### 2.7.1 Tissue homogenization

Homogenization of tissue is crucial for obtaining reliable results in subsequent protein quantification. Tissue samples were homogenized using a freshly prepared ice-cold homogenization buffer and an electric pestle (VWR). After obtaining the supernatant through two brief centrifugation steps at 8000 rpm at 4°C, the homogenate underwent final centrifugation at maximum speed for 10 minutes at 4°C to isolate the protein fraction in the supernatant. The samples were then either immediately utilized for a BCA assay or stored at -80°C for subsequent use.

**Table 11: Homogenisation buffer**

Reagent	Company	Cat. No.	Conc.
IGEPAL CA-630	Sigma Aldrich	I8896-50ML	1%
Glycerol	Carl Roth	3783.1	10%
NaCl	Carl Roth	3957.1	137 mM
Tris-HCl, pH=7.4	Carl Roth	8789.2	20 mM
NaF	Sigma Aldrich	S7920-100G	20 mM
Sodium orthovanadate	Sigma Aldrich	S6508	1 mM
Sodium pyrophosphate	Sigma Aldrich	S6422-100G	1 mM
$\beta$ -Glycerophosphate	Fluka BioChemika	50020	50 mM
EDTA (Ethylenediamin- etetraaceticacid), pH=8	Sigma Aldrich	EDS-500G	10 mM
EGTA (Ethylene glycol-bis- 2-aminoethyl-ether), pH=7	Sigma Aldrich	E4378-100G	1 mM
Aprotinin	Carl Roth	6367.1	4 $\mu$ g/mL
Leupeptin	Sigma Aldrich	L2023	4 $\mu$ g/mL
Pepstatin A	Sigma Aldrich	P4265-5MG	4 $\mu$ g/mL
PMSF (Phenylmethyl- sulfonylfluorid)	Carl Roth	6367.1	1 mM

### **2.7.2 Pierce BCA assay**

To determine the total protein concentration of the samples intended for Western Blot analysis, a BCA Assay (ThermoFisher Scientific; 23225) was conducted following the manufacturer's protocol. A standard curve was generated using nine dilutions of BSA (Pierce; 23209) ranging from 0.0 to 2.0 mg/mL. Subsequently, samples were diluted 1:15 in ddH<sub>2</sub>O, and 10 µL of each sample or standard was added in duplicate to a clear flat-bottom 96-well plate.

The BCA protein assay reagent A and BCA protein assay reagent B were mixed in a ratio of 50+1, and 200 µL of the mixture was added to each well. After incubation for 30 minutes at 26°C, absorbance was measured at 562 nm using a SpectraMax® Plus 374 photometer (Avantor by VWR). Individual protein concentrations were calculated by interpolating the absorption values of unknowns into the BSA standard curve.

### **2.7.3 Sodium dodecyl sulfate polyacrylamide gel electrophoresis (SDS-PAGE) and immunoblotting**

For Each sample, 30µg were prepared by combining them with 4XT sample buffer (Bio-Rad, 1610791), XT reducing agent (Bio-Rad; 161-0792), and homogenization buffer, resulting in a final volume of 25 µl per sample.

The Western Blot Apparatus was assembled, placing gels in the running chambers. The top chamber was filled with running buffer (XT Mops, Biorad 161-0788), while the lower chamber was filled 1/3 with diluted running buffer (100 ml MOPS + 1900 ml ddH<sub>2</sub>O). Subsequently, 24 µl of each sample was pipetted onto 4-12% Bis-Tris gradient gels (Bio-Rad: 345-0124). Standards, including Precision Plus Protein, All Blue, and Dual Color Standards (Bio-Rad: 161-0374), were loaded on the first and last wells. Electrophoresis started at 70 Volts for 10 minutes, followed by an increase to 120 Volts for approximately 2.5 hours.

For wet protein transfer a membrane, a transfer cassette with 2 sponges, 2 filter papers, and a transfer chamber were employed with a Transfer Buffer composed of 250 ml Transfer buffer, 500 ml Methanol, and 1750 ml ddH<sub>2</sub>O. The transfer took place at 400 mA and 4°C for 2 hours.

Following the transfer, membranes were incubated for 3-5 minutes in Ponceau S (Sigma Aldrich; P7170), washed with water until bands were visible without a strong background, and imaged using a ChemiDoc Touch Imaging System (BioRad) to assess protein transfer efficiency.

Subsequently, membranes underwent a 1-hour blocking step in 5% milk powder (MP; Carl Roth; T145.1)/TBST at room temperature. A primary antibody for detecting the  $\beta$ 2AR (ADRB2, Thermofisher BS-0947R polyclonal LOT: AG 10096795) at a 1:200 dilution was applied. After three washes in TBST, a secondary antibody (anti-rabbit HRP conjugated; Ge LifeScience; NA934V) at 1:5000 was incubated for 1 hour at room temperature. For detection, membranes were exposed to Clarity Western ECL substrate (Bio-Rad; 1705061) for 2-3 minutes and imaged in signal accumulation mode using the ChemiDoc Touch Imaging System.

Following membrane stripping, anti-GAPDH (Cell Signaling; 5174S) was applied at a 1:2000 dilution overnight at 4°C in 0.5% MP/TBST. Subsequently, the secondary antibody was applied, and proteins were detected using the ChemiDoc Touch Imaging system as described above.

#### **2.7.4 Membrane stripping**

Stripping refers to the chemical removal of bound protein from the membrane. Immunostaining for ADRB2 resulted in nonspecific bands near GAPDH (band at 37 kD). The membrane was washed with TBST. Consequently, the stripping buffer (Thermo Fisher; 21059) at room temperature for 7 minutes was applied after immunostaining for ADRB2 to eliminate bound antibodies from this region. The membrane was then washed again. Following the stripping process, the membrane was blocked for 20 minutes in 5% MP/TBST, underwent three washes with TBST, and was subsequently reincubated with the secondary antibody. Stripping efficiency was evaluated using the ChemiDoc touch. After successful stripping (indicating no detectable band), the membrane was further incubated with the primary antibody against GAPDH.

### **2.7.5 Analysis**

Densitometric quantification of bands was carried out using ImageLab software (Bio-Rad Laboratories Inc.) with the "lanes and bands" tool, including manual adjustments. ADRB2 quantification was normalized to GAPDH.

## **2.8 Microarray**

To study  $\beta$ 2AR gene expression behavior a microarray was utilized. RNA extraction from the left ventricular tissue of Dahl salt-sensitive LSD and HSD-fed rats at 12 weeks and 17 weeks was performed using the microRNeasy® Mini Kit (Qiagen, Hilden, Germany) following the manufacturer's guidelines. Subsequently, The RNA concentration was evaluated using NanoDrop™ 2000 (Thermo Fisher Scientific, Waltham, USA) before forwarding the samples to ATLAS Biolabs (Berlin, Germany) for transcriptomic profiling. Affymetrix WT Expression Profiling microarray Clariom D (Thermo Fisher Scientific, Waltham, USA) was utilized for this purpose. The obtained CEL files were imported into the Transcriptome Analysis Console, version 4.0 (Applied Biosystems, USA), where individual data points were extracted. The values presented in the results are the mean signal intensities transformed to log<sub>2</sub>.

The entire datasets were accessible to me and I conducted the statistical analysis of the genes of interest.

## **2.9 Statistical Analysis**

Data were presented as mean  $\pm$  standard error of the mean (SEM). Statistical analyses for *in vivo* and *in vitro* data were conducted using GraphPad Prism 8 (GraphPad Software, CA, USA). Normality testing was performed for all data groups using the Shapiro-Wilk and Kolmogorov-Smirnov tests, depending on the group size.

### **Phenotypication:**

Comparisons of repeated measurements (systolic and diastolic blood pressure and body weight) were conducted using two-way ANOVA with post-hoc Sidak's multiple comparisons test. Heart weight to body weight ratio, Left Ventricular mass, Echocardiography, and Hypertrophy data were analyzed, with normality tested beforehand. Unpaired t-tests were employed for data with Gaussian distribution,

while Mann-Whitney U tests were applied for not normally distributed data. Echocardiography data was analyzed using one-way ANOVA with post-hoc Holm-Sidak's multiple comparisons test or Kruskal-Wallis with Dunn's post-hoc test. A significance level of  $p \leq 0.05$  was considered significant.

**Microarray:**

Normality was tested using the Shapiro-Wilk test. As all groups passed the normality test, data were compared using one-way ANOVA with post-hoc Holm-Sidak's multiple comparisons test. A two-tailed  $p \leq 0.05$  was considered significant.

**ICC:**

Normality was tested. Unpaired t-tests were utilized for data with a Gaussian distribution, and Mann-Whitney U tests were applied for not normally distributed data. A two-tailed  $p \leq 0.05$  was considered significant.

**Western Blot:**

$\beta$ 2AR protein quantification was normalized to GAPDH. The normality of data groups was tested with the Shapiro-Wilk test. For rat immunoblotting, as all data passed the test, comparisons were made using one-way ANOVA with posthoc Holm-Sidak's multiple comparisons test. In the human experiment, Kruskal-Wallis with Dunn's post-hoc test was performed instead of ANOVA, as the non-failing heart group did not pass the normality test. A two-tailed  $p \leq 0.05$  was considered significant.

## 3. Results

### 3.1 Dahl salt-sensitive rats

#### 3.1.1 *In vivo* and *in vitro* phenotyping of hypertensive Dahl salt-sensitive rats

Baseline measurements for *in vivo* parameters, including blood pressure (BP) and body weight (BW), were conducted at seven weeks of age and continued at a biweekly plan. Subsequently, at seven weeks the regular chow diet was replaced either by a low-salt-diet (LSD, 0.3% NaCl) or a high-salt-diet (HSD, 8% NaCl) (Figure 14 A).

Upon the initiation of HSD feeding, both systolic and diastolic blood pressure exhibited significant increases within the first two weeks in HSD rats (Figure 14 B-C). Two-way ANOVA revealed significant differences in systolic and diastolic BP between HSD and LSD rats at each timepoint starting at week nine ( $p < 0.0001$  for each comparison, except for diastolic BP at week nine with  $p = 0.0004$ ). BW consistently increased with age in all groups (Figure 14 D), with the mean weight rising from  $228.7 \pm 20.14$  g at week seven to  $375.5 \pm 16.21$  g at week 17.

Upon euthanizing at 12 weeks of age, the heart-to-body-weight ratio, a determinant of cardiac hypertrophy, did not show a significant increase in HSD animals (Figure 14 E). However, during late-stage remodeling, the increase in the heart-to-body-weight ratio in HSD rats became statistically significant compared to LSD rats ( $p = 0.0004$ ). (Figure 14 F). Left ventricular mass was significantly higher in the HSD group at both early and late harvesting timepoints ( $p < 0.0001$ ) (Figure 14 G-H).

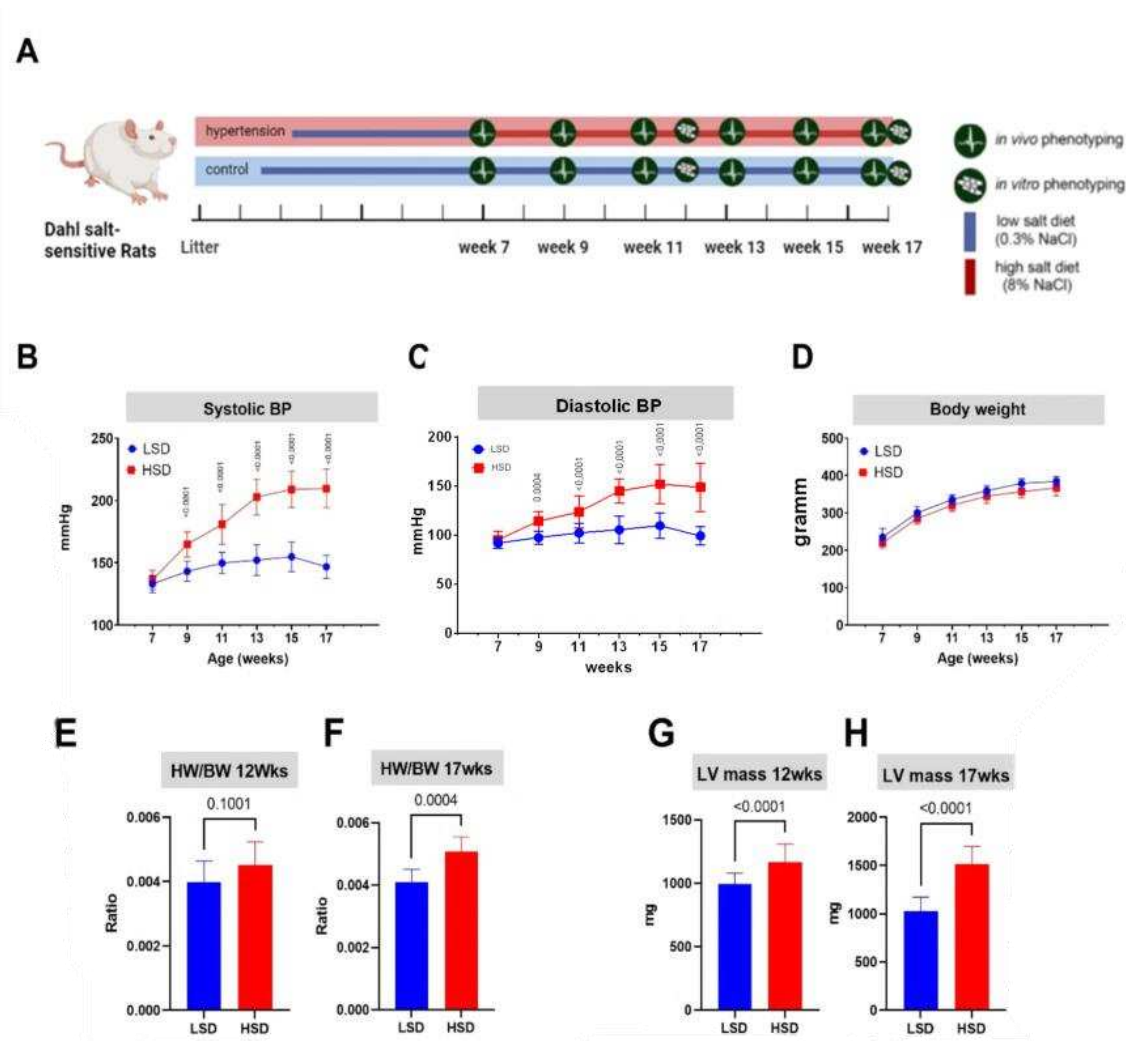


**Figure 14: Phenotypical characterization and *in vivo* measurements of Dahl salt-sensitive rats on low-salt-diet (LSD) and high-salt-diet (HSD).**

The Dahl salt-sensitive rat group with hypertension is depicted as red, control group is blue. (A) Overview of the rat treatment plan; (B) Systolic blood pressure; (C) Diastolic blood pressure; (D) Body weight; (E) Heart weight/bodyweight ratio at early timepoint 12 Weeks (F) Heart weight/bodyweight ratio at late timepoint 17 weeks; (G) Left ventricular mass at early timepoint 12 Weeks (H) Left ventricular mass at late timepoint 17 weeks; B-D: N=17 HSD rats and N=19 LSD rats at 12 weeks, N=7 HSD rats and N=9 LSD rats at 17 weeks. E; G, N=10 HSD, and LSD rats at 12 weeks. F; H, N=7 HSD and N=9 LSD rats at 17 weeks. (B-D) were calculated by two-way ANOVA with post-hoc Sidak's multiple comparisons test. (E-H) were calculated using an unpaired t-test or Mann-Whitney U test.

*In vitro*, rat cardiomyocytes were assessed for hypertrophy. At both early and late timepoints, HSD rats exhibited statistically significantly larger cells in terms of both length and width compared to the LSD counterparts ( $p < 0.0001$ , except for cell width at 12 weeks, where  $p = 0.0394$ ) (Figure 15).

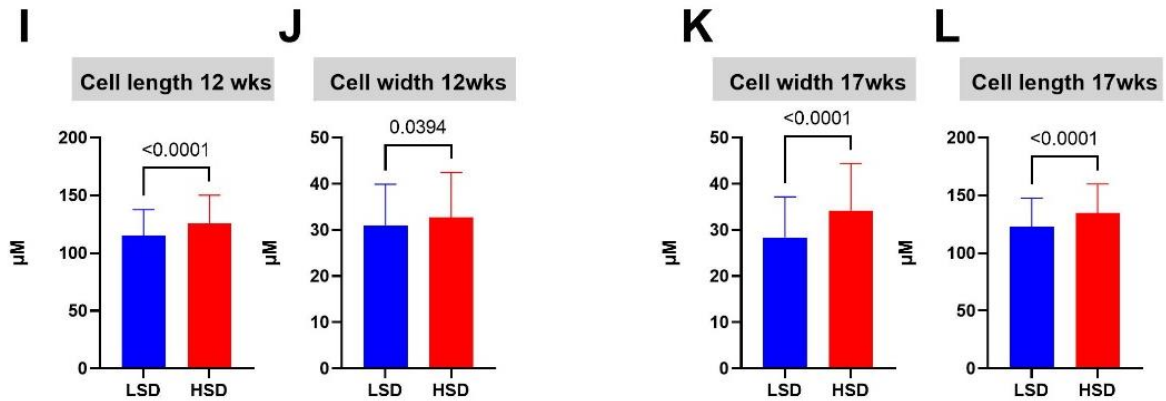


**Figure 15: *In vitro* cell hypertrophy of Dahl salt-sensitive rat cardiomyocytes divided into low-salt-diet (LSD) and high-salt-diet (HSD) groups**

The Dahl salt-sensitive rat group with HSD is depicted as red, control group with LSD is blue. Cell length in  $\mu\text{m}$  at early (I) and late (L) timepoint, Cell width in  $\mu\text{m}$  at early (J) and late (K) timepoint; I-J: N=6 HSD rats with N=243 cells, N=6 LSD rats with N=199 cells at 12 weeks; K-L: N=4 HSD rats N=121 cells, N=5 LSD rats N=159 cells at 17 weeks. P-values (I-L) were calculated using an unpaired t-test or Mann-Whitney U test.

Together, these results indicate that the Dahl salt-sensitive rat model was effective in inducing the development of hypertension and left ventricular cardiac hypertrophy.

### 3.1.2 Echocardiography development of diastolic dysfunction with preserved ejection fraction in Dahl salt-sensitive rats

Echocardiography was performed by Julia Voglhuber PhD, thesis not yet published, at 12 and 17 weeks before euthanizing. The Echocardiography showed no statistically significant difference in EF. It is noteworthy that both rat groups did not manifest systolic dysfunction, as evidenced by EF values around 80% (Figure 16 M-N), which is considered normal for the model (van Ham *et al.*, 2022). It was observed that the HSD group at 12 weeks had a statistically higher EF compared to the LSD group ( $p=0.005$ ).

Furthermore, a statistically significant difference in  $E/e'$ , was not noted between LSD and HSD rats at both timepoints. (Figure 16 O-P). Our rats at 12 weeks had a mean value of  $18.15 (\pm 3.38)$   $E/e'$  in the LSD group and  $21.37 (\pm 3.5)$  in the HSD group. At 17 weeks, the LSD group had a mean of  $17.50 (\pm 2.23)$ , and the HSD group had a mean of  $20.46 (\pm 4.06)$ . In the review from van Ham *et al* an  $E/e'$  ratio of a maximum of 20 was considered normal in the Dahl-salt-sensitive rat model (van Ham *et al.*, 2022), (Zhang *et al.*, 2020).

In summary, this echocardiography data cannot fully indicate that the HSD group developed diastolic dysfunction. However, the HSD group exhibits a preserved EF.

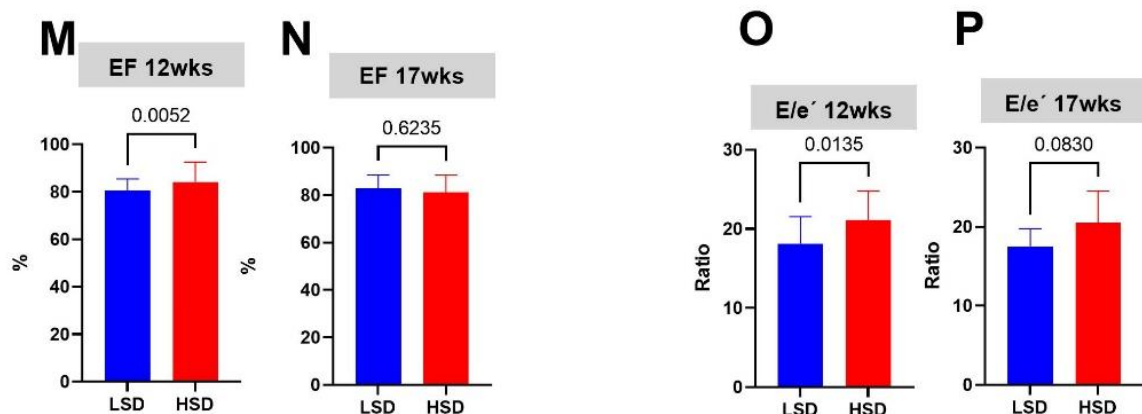


**Figure 16: Echocardiography measurements of Dahl salt-sensitive rats on low-salt-diet (LSD) and high-salt-diet (HSD):**

The Dahl salt-sensitive rat group with HSD is depicted as red, control group with LSD is blue. Ejection fraction (EF) at early 12 weeks (M) and late 17 weeks (N) timepoint;  $E/e'$  at early (O) and late (P) timepoint, M-P, N=18 HSD rats, and N=20 LSD rats at 12 weeks. P-values were calculated using an unpaired t-test or Mann-Whitney U test.

### 3.1.3 $\beta$ 2AR expression decreases in the whole cell in hypertensive Dahl salt-sensitive rats

The ICC data exclusively depicts cardiomyocytes from the late-stage cardiac remodeling timepoint (17 weeks). The whole cell  $\beta$ 2AR fluorescence signal exhibited significantly lower expression of  $\beta$ 2AR in cardiomyocytes from the HSD group compared to the LSD group ( $p < 0.001$ ). This observation held for both isoproterenol (ISO) treated and untreated cells (Figure 17, Figure 18)

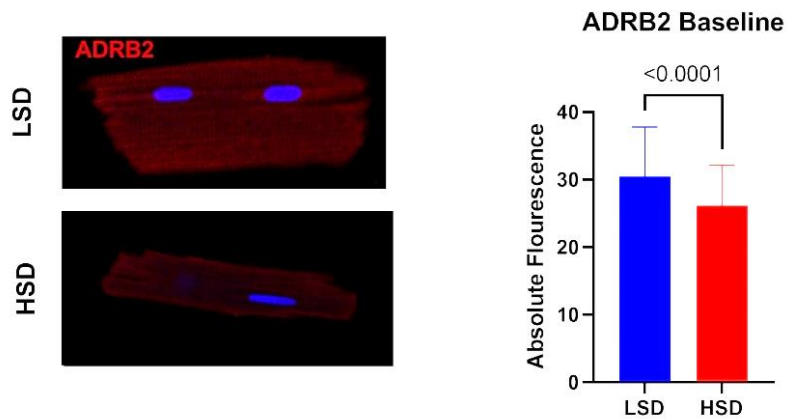


**Figure 17: Expression of  $\beta$ 2AR in isolated cardiomyocytes from the low-salt-diet (LSD) and high-salt-diet (HSD) Dahl salt-sensitive rats.**

The Dahl salt-sensitive rat group with HSD is depicted as red, control group with LSD is blue. On the left: Sample images of LSD and HSD rat cardiomyocytes stained with DAPI (blue) and ADRB2 (red) antibody from the confocal microscope; N=4 rats per group with N=123 cells of HSD rats, and N=160 cells of LSD rats. P-values were calculated using an unpaired t-test or Mann-Whitney U test.

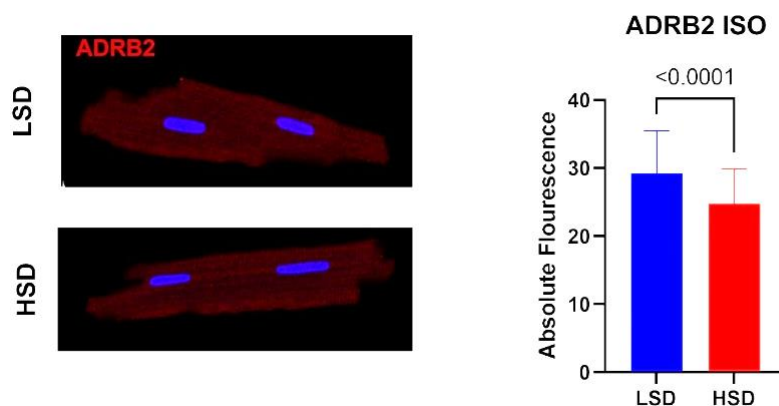


**Figure 18: Expression of  $\beta$ 2AR in isolated cardiomyocytes from the low-salt-diet (LSD) and high-salt-diet (HSD) Dahl salt-sensitive rats upon  $\beta$ -adrenergic stimulation with 100 nM isoprenaline (ISO) for 1h.**

The Dahl salt-sensitive rat group with HSD is depicted as red, control group with LSD is blue. On the left: Sample images of LSD and HSD rat cardiomyocytes stained with DAPI (blue) and ADRB2 (red) antibody from the confocal microscope; N=4 rats per group with N=119 cells of HSD rats, and N=165 cells of LSD rats. P-values were calculated using an unpaired t-test or Mann-Whitney U test.

### 3.1.4 $\beta$ AR stimulation decreases $\beta$ 2AR expression in ICC of the LSD Dahl salt-sensitive rat group

$\beta$ -adrenergic stimulation resulted in the reduction of  $\beta$ 2AR expression in cardiomyocytes. This effect was evident in the LSD group at 17 weeks ( $p=0.008$ ). A similar trend was observed in the HSD group at 17 weeks, although it did not reach statistical significance ( $p=0.0594$ ) (Figure 19).

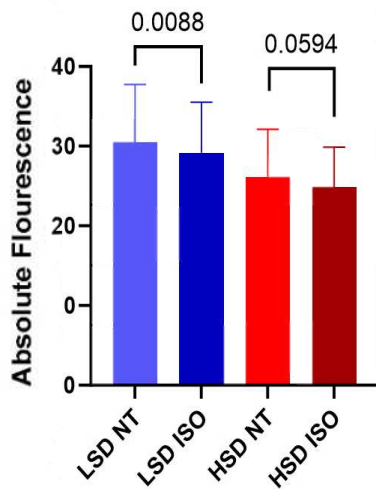


**Figure 19: Expression of  $\beta$ 2AR in isolated cardiomyocytes from the low-salt-diet (LSD) and high-salt-diet (HSD) Dahl salt-sensitive rats upon  $\beta$ -adrenergic stimulation with 100 nM isoprenaline (ISO) for 1h compared to normal tyrode (NT).**

The Dahl salt-sensitive rat group with HSD is depicted as red, control group with LSD is blue. ISO-treated cells are the darker shade of each color. ISO-treated cells encompassed N=4 rats per group with N=119 cells of HSD rats, and N=165 cells of LSD rats. Normal Tyrode (NT) not stimulated cells encompassed: N=4 rats per group with N=123 cells of HSD rats, N=160 cells of LSD rats. P-values were calculated using an unpaired t-test or Mann-Whitney U test.

### **3.1.5 $\beta$ 2AR expression in relation to $\beta$ 1AR expression in Dahl salt-sensitive rats**

$\beta$ 2AR behavior in relation to  $\beta$ 1AR was analyzed, as it is frequently cited in the literature. The mean fluorescence of  $\beta$ 2AR antibodies decreased from LSD 30.46 ( $\pm$ 7.28) to HSD 26.15 ( $\pm$ 5.95), signifying a reduction in fluorescence by 14.15% at 17 weeks. The study comprised 4 rats per group, with N=123 cells for HSD and N=160 cells for LSD.

Ingrid Matzer's raw data for comparison with  $\beta$ 1AR was used with kind permission, including 3 LSD rats with N=127 cells and 3 HSD rats with N=89 cells. Among the LSD rats, the mean fluorescence was 46.24 ( $\pm$ 16.96), which decreased to 41.41 ( $\pm$ 10.17), resulting in a 10.45% reduction in fluorescence at 17 weeks (Matzer, 2021). In our experiments on Dahl salt-sensitive rats with HFpEF, the extent of downregulation was similar for both  $\beta$ AR subtypes.

### 3.1.6 $\beta$ 2AR expression in the left ventricular tissue at early- and late-stage cardiac remodeling

The results discussed above revealed a diminished expression of  $\beta$ 2AR in cardiomyocytes from HSD compared to LSD rats during late-stage cardiac remodeling. To verify this observation, an immunoblot with an ADRB2 antibody to quantify  $\beta$ 2AR was done with left ventricular tissue, using samples from the first Dahl salt-sensitive rat cohort where the late timepoint of euthanization was set at 19 weeks instead of the 17 weeks of the other cohorts. Unexpectedly, the analysis showed no significant differences in  $\beta$ 2AR expression among any of the groups. However, upon closer examination of the data points, a trend of downregulation is discernible, suggesting that with a larger group size, these differences might attain statistical significance (Figure 20).

Consequently, the present study did not allow for the validation of ICC data through immunoblotting.

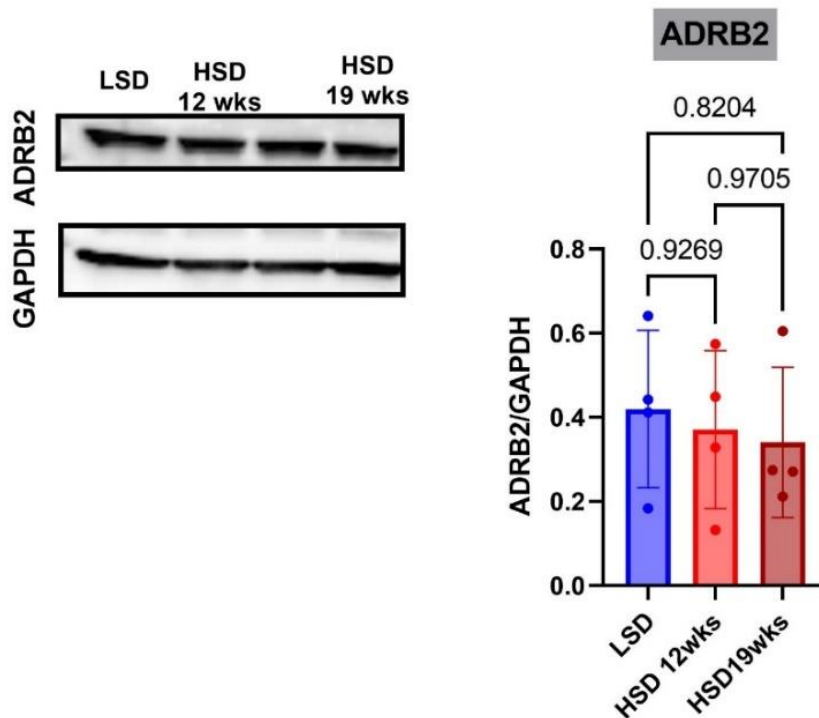


**Figure 20:  $\beta$ 2AR immunoassay of the left ventricle of Dahl salt-sensitive rats in early (12 weeks) and late (19 weeks)-stage remodeling.**

Immunoblot with ADRB2 antibody to detect  $\beta$ 2AR in left ventricular tissue lysates. GAPDH was used for normalization. Corresponding quantification of  $\beta$ 2AR in low-salt diet (LSD) rats (blue), high-salt-diet (HSD) 12 week old rats (red light), and HSD 19-week-old rats (red dark). Statistical analysis was performed using one-way ANOVA with Tukey's post hoc test. N=4 rats/group.

### 3.1.7 $\beta$ 2AR gene expression is downregulated in the late cardiac remodeling stage

The ICC results indicating the downregulation of  $\beta$ 2AR were corroborated by the microarray analysis of Dahl salt-sensitive rat heart tissue. The early timepoint refers to euthanasia at 12 weeks, while the late timepoint corresponds to euthanasia at 17 weeks.

The analysis revealed a significant reduction in  $\beta$ 2AR gene expression from the LSD group to the HSD group at the late timepoint ( $p=0.002$ ) and a significant reduction in  $\beta$ 2AR gene expression when comparing the early and late timepoint HSD groups ( $p=0.002$ ). However, no significant differences in expression were observed between the LSD and early timepoint HSD group (Figure 21).

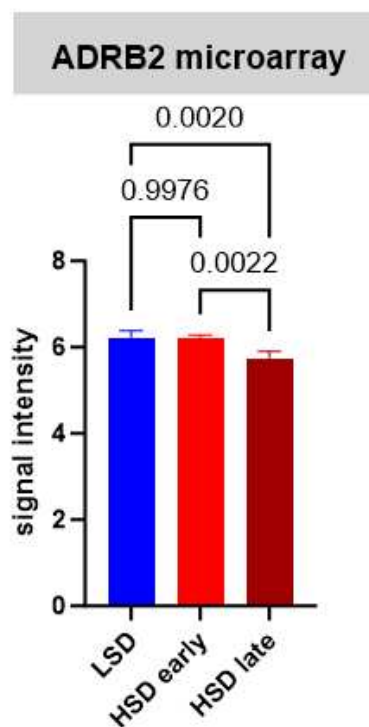


**Figure 21: Expression of  $\beta$ 2AR mRNA in left ventricular tissue from low-salt-diet (LSD) and high-salt diet (HSD) Dahl salt-sensitive rats in early (12 weeks) and late (17 weeks) timepoints.** The Dahl salt-sensitive rat group with HSD is depicted as light red (12 weeks) and dark red (17 weeks), control group with LSD is blue. N=6 rats HSD 17 weeks, N=4 rats HSD 12 weeks, N=4 rats LSD. Differences between groups were calculated using one-way ANOVA with Tukey's post hoc test.

## 3.2 Human data

### 3.2.1 Human cohort characteristics

For the human data, a Western Blot analysis was conducted using tissue obtained from organ donors. Among these donors, 4 had NF hearts, 6 exhibited DD, and 5 were diagnosed with DCM.

The non-failing group had a mean age of 53 years ( $\pm 14.9$ ), with 40% being female. The mean EF was 61.2% ( $\pm 6.1$ ). The Diastolic dysfunction group had a mean age of 60 years ( $\pm 7.9$ ), 33.3% were female, with an EF mean of 62.2% ( $\pm 5.4$ ), thereby belonging to the HFpEF group. According to the ESC guidelines, any EF over 50% is generally regarded as normal (McDonagh *et al.*, 2021).

The group with dilated cardiomyopathy had a mean age of 46.6 ( $\pm 10.6$ ), with 40% being female. This group exhibited a reduced EF with a mean of 26% ( $\pm 10.6$ ), thereby classifying them as HFrEF. Body Mass Index (BMI) was comparable across all groups, averaging around 27 kg/m<sup>2</sup> which is classified as overweight (Table 12).

---

Human Cohort Characteristics			
Group	NF	DD	DCM
Age	53,6 ( $\pm 14,9$ )	60 ( $\pm 7,9$ )	46,6 ( $\pm 10,6$ )
Gender (% female)	40%	33,3%	40%
BMI	27,6 ( $\pm 5,2$ )	27,8 ( $\pm 5$ )	27,1 ( $\pm 6$ )
EF (%)	61,2% ( $\pm 6,1$ )	62,2% ( $\pm 5,4$ )	26% ( $\pm 10,6$ )

**Table 12: Human cohort characteristics for the immunoblot experiment**

Parameters from human donors, with N=4 not failing (NF), N=6 diastolic dysfunction (DD), N=5 dilated cardiomyopathy (DCM). Mean value with standard deviations.

### 3.2.2 $\beta$ 2AR is decreased in humans during diastolic dysfunction

The expression of  $\beta$ 2AR in humans showed a significant decrease during DD ( $p=0.0255$ ) and a trend towards significance in DCM ( $p=0.0534$ ) compared to the non-failing group. The comparison between the DD and DCM groups revealed no statistical significance (Figure 22).

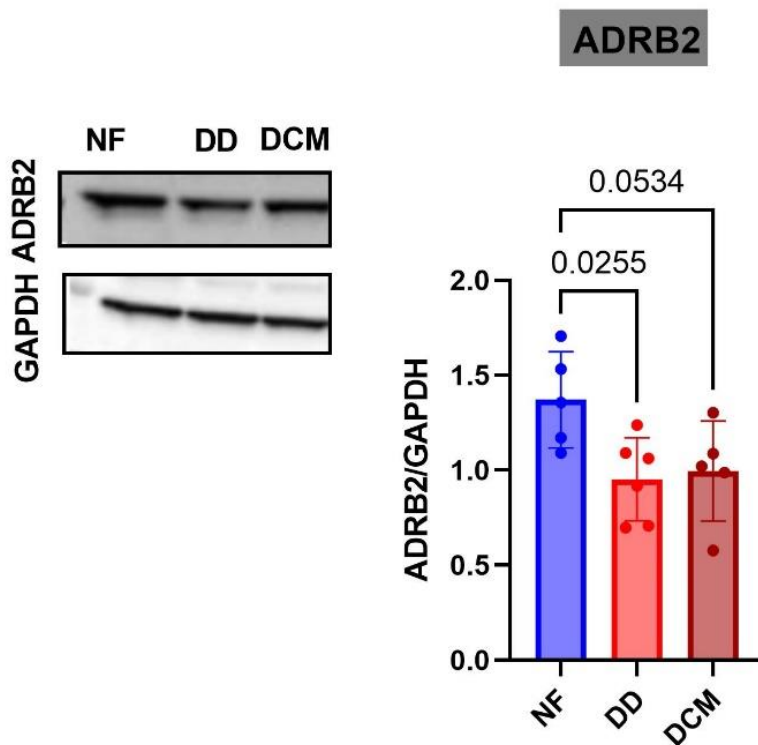


**Figure 22:  $\beta$ 2AR immunoblot of the left ventricle in humans with not failing (NF) hearts, hearts with diastolic dysfunction (DD), or dilated cardiomyopathy (DCM).**

Immunoblot with ADRB2 antibody to detect  $\beta$ 2AR in left ventricular tissue lysates. GAPDH was used for normalization. Corresponding quantification of  $\beta$ 2AR in NF (not failing) blue N=5, DD (diastolic dysfunction) light red, N=6, DCM (dilated cardiomyopathy) dark red N=5 human hearts. Statistical analysis was performed using Kruskal-Wallis with Dunn's post-hoc test.

## 4. Discussion

### ***4.1 HSD-fed Dahl salt-sensitive rats develop a hypertensive phenotype with hypertrophy, preserved ejection fraction, and diastolic dysfunction***

Research indicates that Dahl salt-sensitive rats serve as a valid animal model for investigating the onset of hypertension-induced cardiac remodeling. These rats demonstrate hypertrophy and diastolic dysfunction comparable to human cardiovascular disease (van Ham *et al.*, 2022).

In our investigation, Dahl salt-sensitive rats fed a high-salt-diet exhibited a hypertensive phenotype, showing relevant systolic and diastolic hypertension within two weeks and left ventricular hypertrophy. Gravimetric and cellular analyses confirmed hypertrophy, with cellular myocyte hypertrophy apparent at an early stage and gravimetric changes becoming evident later. A similar study by Hasan *et al.* with Dahl salt-sensitive rats at 15 weeks also observed cellular myocyte hypertrophy (Hasan *et al.*, 2018). Notably, significant heart weight to body weight differences were found at nine weeks (Kimura *et al.*, 2019), and studies reported gravimetric differences at weeks 12-13 (Klotz *et al.*, 2006), (Gallet *et al.*, 2016).

The delay in finding relevant heart weight-to-body weight differences in our study compared to others raises discussion points. Matzer *et al.* suggested differences in gravimetric methods as a potential factor, with two techniques employed: one for organ collection only, directly measuring wet weight after removal of excess blood, and another for Langendorff perfusion, measuring the weight of the heart in a beaker with perfusion solution, wherein the weight of beaker and solution were later subtracted (Matzer, 2021).

Previous studies using this animal model linked it to HFpEF when exposed to a HSD (Abdellatif *et al.*, 2021), (Nakajima *et al.*, 2019), (van Ham *et al.*, 2022). The study from Doi *et al.* also developed a Dahl-salt-sensitive model with different heart failure phenotypes depending on the HSD starting timepoint. Rat groups starting at seven weeks developed isolated diastolic heart failure while groups starting at eight weeks developed both systolic and diastolic dysfunction (Doi *et al.*, 2000).

In the data provided in this thesis, definitive conclusions regarding the development of HFpEF in our model are not possible. Echocardiographic measurements revealed a preserved EF in the Dahl salt-sensitive rat model. However, assessing E/e' proved to be more challenging. Van Ham et al. suggest that in the Dahl salt-sensitive rat model, an E/e' value exceeding 20 indicates elevated filling pressures, a criterion met by our HSD group. Despite this, Van Ham et al. acknowledge the limited data on E/e' parameters in Dahl salt-sensitive rats, suggesting that normal parameters might not be firmly established (van Ham *et al.*, 2022).

Echocardiography inherently introduces significant subjective bias, particularly dependent on the analyzer. Absolute values should only be used when plentiful data is provided such as in measurements in humans. In humans, an E/e' ratio higher than 15 is a sign of diastolic dysfunction (Hagendorff *et al.*, 2015). The ESC describes an E/e' ratio >9 to have a higher risk of cardiovascular mortality (McDonagh *et al.*, 2021). Our study minimized this bias by conducting all measurements through a single analyzer, Dr. Julia Voglhuber-Höller. However, in animal models where data points are limited, references from the control group are more appropriate to provide valid results compared to absolute values.

This thesis only utilized a subset of the data, primarily from cohorts used for the  $\beta$ 2AR experiments, and failed to demonstrate significant changes in E/e' parameters compared to the control group, precluding a definitive HFpEF diagnosis. However, Dr. Julia Voglhuber-Höller's thesis (unpublished), which encompasses a larger sample size and multiple rat cohorts, observed a significant increase in E/e' compared to the control group, allowing for a more reliable diagnosis of HFpEF. Thus, with this additional data, we can conclude that the Dahl salt-sensitive rat model indeed developed HFpEF.

The observed hypertrophy may be the reason why the high-salt-diet group showed a higher ejection fraction at the early 12 week timepoint, possibly adapting to the pressure overload from hypertension. Both groups had EF around 80% which is considered normal (van Ham *et al.*, 2022).

Another important feature to diagnose heart failure in humans is the clinical symptoms, such as shortness of breath, peripheral edema, and weakness. These symptoms could be translated to the rat model as decreased activity levels and weakness compared to the control group (Zhang *et al.*, 2020). These parameters may have given more insight if our rat model developed heart failure with preserved ejection fraction.

With the additional data from Dr. Julia Voglhuber-Höller's thesis, we can conclusively state that our Dahl salt-sensitive rat model has effectively developed hypertension accompanied by left ventricular hypertrophy and diastolic dysfunction, thus characterizing the model as representing HFpEF.

#### ***4.2 $\beta$ 2AR expression decreases in rats that develop hypertension in late-stage remodeling***

The work of Bristow *et al.* with human failing and non-failing heart tissue analyzed  $\beta$ -adrenergic subpopulations using radioligand binding techniques. In their study, they observed that the  $\beta$ 1: $\beta$ 2 adrenergic receptor profiles change in the failing heart predominately due to  $\beta$ 1AR downregulation. (Bristow *et al.*, 1986). However, this finding contrasts with the study using radioligand bindings indicating  $\beta$ 2AR receptor downregulation plays a significant role during heart failure in humans (Takahashi *et al.*, 1992).

In a study on rats, Zhao *et al.* demonstrated a more pronounced downregulation of  $\beta$ 2AR compared to  $\beta$ 1AR upon norepinephrine stimulation (Zhao, Hagler, and Muntz, 1996). In the case of Dahl salt-sensitive rats, Puleo *et al.* found elevated plasma norepinephrine levels, likely applicable to animals in our study, and would thus favor  $\beta$ 2AR downregulation (Puleo *et al.*, 2020).

We observed a significant downregulation of  $\beta$ 2AR in HSD-fed Dahl salt-sensitive rat cardiomyocytes at the 17 week late timepoint, in both ICC experiments: baseline and stimulated with ISO. This finding was replicated in our microarray experiments with HSD-fed Dahl-salt-sensitive rat heart tissue. Considering that hypertension is characterized by higher levels of norepinephrine and epinephrine, it is plausible to expect a certain amount of  $\beta$ 2AR downregulation. The pathophysiology may be

explained by an increase in GRK during cardiac remodeling, leading to greater GPCR desensitization and internalization, as  $\beta$ 2AR is a GPCR (see section: Molecular mechanisms of GPCR; page: 16).

The observed downregulation was not recapitulated in the immunoblot analysis, as previously discussed. Possible contributing factors include the limited sample size and the nature of immunoblotting, which detects protein fractions from denatured proteins. Furthermore, heart tissue from one of the first Dahl salt-sensitive rat cohorts was used, which were euthanized at 19 weeks, so two weeks later than the other cohorts. This may lead to another factor that should be put into consideration when analyzing the results. Notably, immunoblotting encompasses the entire ventricular tissue, comprising a variety of cell types expressing  $\beta$ 2AR, such as vasculature, fibroblasts, or immune cells. This cellular diversity may introduce variations when compared to ICC, where only cardiomyocytes were examined. The microarray analysis also utilized the whole ventricular tissue and demonstrated a downregulation exclusively in the late stage of remodeling, thereby adding complexity to the previous argument. Additional experiments to quantify  $\beta$ 2AR in immunoblotting should be repeated with a higher sample size, and ideally, in isolated ventricular cardiomyocytes.

Combining the results, our experiments indicate that hypertensive cardiac remodeling coincides with  $\beta$ 2AR receptor downregulation at a late timepoint both in genetic expression as well as receptor concentration in the cell membrane.

### ***4.3 $\beta$ 2AR receptor is downregulated when stimulated with ISO in LSD rats***

The capacity for acute adjustments in cardiac output during heightened cardiac demand is a well-established effect of  $\beta$ -adrenergic stimulation. In instances of diminished responsiveness to  $\beta$ -adrenergic signaling, as noted in heart failure (Bristow *et al.*, 1982), individuals experience a decline in contractile function during physiological stress or exercise.

In experimental settings, the conventional approach to emulate  $\beta$ -adrenergic tone involves administering the synthetic catecholamine ISO (Matzer, 2021).

Consequently, our study focused on investigating the impact of acute ISO treatment on the expression of  $\beta$ 2AR in cardiomyocytes undergoing cardiac remodeling.

Treatment with ISO leads to rapid desensitization of  $\beta$ 2AR (Moffett *et al.*, 2001). This downregulation in healthy cells is probably a compensatory mechanism to prevent cellular exhaustion. Rapid agonist-promoted desensitization is achieved through phosphorylation of the  $\beta$ 2AR by a specific GRK, also known as  $\beta$ ARK and PKA (Moffett *et al.*, 2001). The study suggests that long-term stimulation, as seen in a hypertensive state, may lead to persistent phosphorylation of the receptor and contribute to long-term desensitization. Here, the enzyme PKA seems to play a more significant role in desensitization when cells are treated long-term with a  $\beta$ -agonist, as it exhibits significantly lower activity in this state (McGraw *et al.*, 1998). Receptor internalization also appears to play a role but at a much slower rate compared to beta ARK and PKA (Roth *et al.*, 1991).

In our experiments, we observed rapid fluorescence signal downregulation in the LSD group when treated with ISO, which may be explained by phosphorylation of the receptor through PKA and GRK. The downregulation was not significant in the HSD group, indicating a potential change or dysfunction in rapid receptor desensitization and internalization. As discussed earlier, the hypertensive state with higher catecholamine levels may already lead to  $\beta$ 2ARs being downregulated making them less responsive to rapid changes in catecholamine levels (see section: 4.2  $\beta$ 2AR expression decreases in rats that develop hypertension in late-stage remodeling, page: 62).

Conclusively, ventricular cardiomyocytes lose their responsiveness to fast changes of ISO in the late stage of cardiac remodeling regarding  $\beta$ 2AR regulation.

#### **4.4 $\beta$ 2AR is downregulated in humans with diastolic dysfunction**

The identification of  $\beta$ 2AR downregulation in the human samples with diastolic dysfunction classifying as a HFpEF is a noteworthy discovery, facilitating the translation of insights derived from animal models to clinically relevant human scenarios. A statistically significant  $\beta$ 2AR downregulation was not evident in dilated cardiomyopathy, though a trend towards downregulation was observed.

It is worth noting that this human experiment with immunoblotting, with a total sample size of N=16, might show a significant difference compared to the rat immunoblotting results, which had a smaller group size of N=12. The increased sample size in the human study could potentially contribute to the observed differences and variations in statistical significance.

While ICC experiments offer the advantage of detecting both acute and long-term effects, immunoblotting is primarily suited for analyzing long-term effects. Important to say is that human heart tissue was used during the immunoblots, not specific cells. Given the inherent limitations associated with the immunoblotting experiments, the next step would be replicating the findings through ICC experiments of cardiomyocytes and microarray analyses in human heart cells and tissue. Immunoblots with bigger sample sizes could additionally give more statistical strength to our findings. Additional investigation would validate the observed patterns and strengthen the translational relevance of the research with rat models, bridging the gap between preclinical models and clinical implications.

#### **4.5 Comparing $\beta$ 2AR with $\beta$ 1AR expression behavior**

In our experiments on isolated Dahl salt-sensitive rat cardiomyocytes with HFpEF at a late timepoint of 17 weeks, the downregulation pattern was similar for both receptors, with  $\beta$ 2AR having a downregulation of 14.15% and  $\beta$ 1AR being 10.45% downregulated, contradicting Bristow's results in human heart failure which state that  $\beta$ 2AR concentration does not change significantly during heart failure. The method used in this study involved radioligand bindings from tissue samples obtained from organ donors with dilated cardiomyopathy exhibiting a HFrEF and pulmonary hypertension (Bristow *et al.*, 1986). These differences in results may be attributed to challenges in translating animal models to the human context, variations in heart failure types (HFrEF vs. HFpEF), as well as differences in samples (heart tissue vs. cardiomyocytes).

The argument that different etiologies might have different receptor profiles is underlined through the study of Brodde's *et al.* It found that ischemic cardiomyopathy and mitral valve disease in humans led to a decrease of both  $\beta$ 1AR

as well as  $\beta$ 2AR while idiopathic dilated cardiomyopathy led to isolated  $\beta$ 1AR downregulation (Brodde *et al.*, 1989), (Michel, Maisel, and Brodde, 1990).

In literature, the stage of remodeling also plays a role. Takahashi *et al.* observed a higher downregulation of  $\beta$ 2AR in later stages of heart failure (NYHA II-IV) in their *in vivo* study with humans, while  $\beta$ 1 downregulation started occurring in mild heart failure. They studied this through the evaluation of adrenoceptor-mediated contractility measured by echocardiography, adrenergic receptor assays, and radioligand bindings. In the essays, the relations were  $\beta$ 1: $\beta$ 2 NYHA I 62:37 proportion, while at NYHA IV, it was 56:44, with both receptors being significantly downregulated. The groups were very diverse with NYHA IV patients having dilated cardiomyopathy, amyloidosis, sarcoidosis, or ischemic cardiomyopathy. NYHA I patients had a preserved EF while the severer cases had a mean EF of 48% (Takahashi *et al.*, 1992).

The timepoint of downregulation is also an intriguing parameter and can coincide with NYHA stages. In the Dahl salt-sensitive rat heart tissue microarray and immunoblots, we differentiated between an early timepoint of 12 weeks and a late timepoint of 17 weeks for the microarray and 19 weeks for the immunoblot. We observed that there was a tendency for downregulation in the immunoblots especially at a late timepoint, though this was not statistically relevant. The microarray on the other hand could show a statistically relevant downregulation on a late timepoint of 17 weeks. At the early timepoint, there were no relevant findings on the  $\beta$ 2AR downregulation.  $\beta$ 1AR downregulation on the other hand is already found at early timepoint (Matzer, 2021). It would be intriguing to collect ICC data during the early stages of cardiac remodeling, specifically at the 12 week timepoint. This would aim to reproduce the microarray results indicating that  $\beta$ 2AR downregulation predominantly occurs in the later stages of cardiac remodeling.

Additionally, my results from human immunoblotting coincide with the fact that patients with HFpEF exhibit  $\beta$ 2AR downregulation. This was not reproduced in patients with dilated cardiomyopathy, which were characterized by an HFrEF, indicating that different heart failure subtypes may have a different  $\beta$ -adrenergic profile.

Unlike  $\beta$ 1AR, which exhibits staining in distinct regions like perinuclear areas (Matzer, 2021),  $\beta$ 2AR showed an overall fluorescence, suggesting their presence on the cell membrane. This finding aligns with existing literature asserting that  $\beta$ 2ARs are predominantly expressed on the cell membrane in t-tubules and caveolae (Gorelik *et al.*, 2013), (MacDougall *et al.*, 2012). We did not observe a distinct change in expression behavior in terms of localization on the cell surface during cardiac remodeling, only a reduction in overall fluorescence. This limitation arises from our methods, which cannot differentiate where the  $\beta$ 2AR is being expressed on the cell surface. As mentioned above, the literature suggests that in heart failure  $\beta$ 2AR ceases to be confined to the structural indentations of the cell membrane and is expressed throughout the cell surface (see section: 1.2.2.5  $\beta$ 2AR pathophysiology in heart failure, page: 25). This phenomenon was identified through the observation of  $\beta$ 2AR-mediated cAMP signals (Nikolaev *et al.*, 2010). Another drawback of ICC is that the quality of the quantitative analysis depends on the subjective assessment of the analyzer, which we addressed in this work by strictly predefined analysis criteria (read: 2.6.2 ICC staining; page: 42).

Given the diversity of heart failure types, it is crucial to continue studying  $\beta$ 1: $\beta$ 2 downregulation with different types of heart failure and diverse animal models. This will lead to more differentiated data and results, providing a better understanding of the mechanisms behind  $\beta$ AR signaling during heart failure.

## 5. Conclusion

In the present study, we describe changes and alterations occurring in early (12 weeks) - and late-stage (17 and 19 weeks) cardiac remodeling focusing on  $\beta$ 2AR expression and emphasizing the late-stage timepoint. These observations were conducted utilizing a Dahl salt-sensitive rat model and experiments involving human cardiac tissue.

1. A significant downregulation of  $\beta$ 2AR was observed especially at late timepoints in the microarray of heart tissue and ICC analyses of cardiomyocytes of the Dahl salt-sensitive rat model. Conversely, rat heart tissue immunoblots failed to reproduce this observation.
2. Impaired rapid-ISO induced  $\beta$ 2AR downregulation was observed in HSD Dahl-salt-sensitive rat cardiomyocytes.
3.  $\beta$ 2AR downregulation was observed in human heart tissue immunoblot for diastolic dysfunction, but not for dilated cardiomyopathy.
4. Rates of  $\beta$ 1AR and  $\beta$ 2AR downregulation in Dahl salt-sensitive rat cardiomyocytes in the ICC at late timepoints were found to be comparable.

## 6. Future perspectives

The complexity of adrenergic receptor profiles seems greater than previously conceived, displaying variations due to heart failure cause, stage, and classification (HFpEF, HFrEF).

To further solidify and expand our results, a more extensive investigation of the early timepoint and a replication of the Immunoblot experiments with an increased sample size is needed. Another experiment of great value would be to redo the immunoblots only with isolated cardiomyocytes, endothelial cells, lymphoid cells, and myeloid cells. This would help to understand the receptors' role in the specific cell. Reproducing the remaining experiments, microarray, and ICC on human tissue would guarantee the translational value of our results. Microarray analysis on healthy human heart tissue has already been done by "the human heart atlas" and brings novel insight into this topic, such as the distribution of  $\beta$ 2AR in different cell types of the heart (*cellxgene*, 2023).

Given the ongoing debate surrounding Gai signaling of the  $\beta$ 2AR in human heart failure, a compelling avenue for investigation involves conducting a microarray analysis on Gai and Gas proteins. This analysis would shed light on potential differences in early- and late-stage remodeling. Examining downstream molecules, such as cAMP, ERK1/2, PI3K, Akt, and MAPKp38, while blocking the  $\beta$ 1AR would provide further insights into the role of  $\beta$ 2AR in the heart and during heart failure. This approach may unveil additional information regarding the predominant downstream signaling pathways in various scenarios.

## 7. References

Abdellatif, M. et al. (2021) 'Nicotinamide for the treatment of heart failure with preserved ejection fraction', *Science Translational Medicine*, 13(580), p. eabd7064. Available at: <https://doi.org/10.1126/scitranslmed.abd7064>

Agüero, J. et al. (2012) 'Myocardial G protein receptor-coupled kinase expression correlates with functional parameters and clinical severity in advanced heart failure', *Journal of Cardiac Failure*, 18(1), pp. 53–61. Available at: <https://doi.org/10.1016/j.cardfail.2011.10.008>.

Ahmed, S.H. et al. (2006) 'Matrix metalloproteinases/tissue inhibitors of metalloproteinases: relationship between changes in proteolytic determinants of matrix composition and structural, functional, and clinical manifestations of hypertensive heart disease', *Circulation*, 113(17), pp. 2089–2096. Available at: <https://doi.org/10.1161/CIRCULATIONAHA.105.573865>.

Anguita Sánchez, M. et al. (2008) 'Prevalence of heart failure in the Spanish general population aged over 45 years. The PRICE Study', *Revista Espanola De Cardiologia*, 61(10), pp. 1041–1049. Available at: [https://doi.org/10.1016/s1885-5857\(09\)60007-4](https://doi.org/10.1016/s1885-5857(09)60007-4).

Arzneimittelkommission Der Deutschen Apotheker et al. (2023) NVL Chronische Herzinsuffizienz – Langfassung. Bundesärztekammer (BÄK); Kassenärztliche Bundesvereinigung (KBV); Arbeitsgemeinschaft der Wissenschaftlichen Medizinischen Fachgesellschaften (AWMF). Available at: <https://doi.org/10.6101/AZQ/000510>.

Avolio, E. and Madeddu, P. (2016) 'Discovering cardiac pericyte biology: From physiopathological mechanisms to potential therapeutic applications in ischemic heart disease', *Vascular Pharmacology*, 86, pp. 53–63. Available at: <https://doi.org/10.1016/j.vph.2016.05.009>.

Bathe-Peters, M. et al. (2021) 'Visualization of  $\beta$ -adrenergic receptor dynamics and differential localization in cardiomyocytes', *Proceedings of the National Academy of*

Sciences of the United States of America, 118(23), p. e2101119118. Available at: <https://doi.org/10.1073/pnas.2101119118>.

Baudier, C. et al. (2023) 'Unraveling the relationships between alpha- and beta-adrenergic modulation and the risk of heart failure', *Frontiers in Cardiovascular Medicine*, 10, p. 1148931. Available at: <https://doi.org/10.3389/fcvm.2023.1148931>.

Bengel, P. et al. (2021) 'Detrimental proarrhythmogenic interaction of Ca<sup>2+</sup>/calmodulin-dependent protein kinase II and NaV1.8 in heart failure', *Nature Communications*, 12(1), p. 6586. Available at: <https://doi.org/10.1038/s41467-021-26690-1>.

Berk, B.C., Fujiwara, K. and Lehoux, S. (2007) 'ECM remodeling in hypertensive heart disease', *The Journal of Clinical Investigation*, 117(3), pp. 568–575. Available at: <https://doi.org/10.1172/JCI31044>.

Blumenfeld, J.D. et al. (1999) ' $\beta$ -adrenergic receptor blockade as a therapeutic approach for suppressing the renin-angiotensin-aldosterone system in normotensive and hypertensive subjects\*', *American Journal of Hypertension*, 12(5), pp. 451–459. Available at: [https://doi.org/10.1016/S0895-7061\(99\)00005-9](https://doi.org/10.1016/S0895-7061(99)00005-9).

Böhm, M., Castellano, M., et al. (1994) 'Cardiac norepinephrine, beta-adrenoceptors, and Gi alpha-proteins in prehypertensive and hypertensive spontaneously hypertensive rats', *Journal of Cardiovascular Pharmacology*, 23(6), pp. 980–987. Available at: <https://doi.org/10.1097/00005344-199406000-00017>.

Böhm, M., Eschenhagen, T., et al. (1994) 'Radioimmunochemical quantification of Gi alpha in right and left ventricles from patients with ischaemic and dilated cardiomyopathy and predominant left ventricular failure', *Journal of Molecular and Cellular Cardiology*, 26(2), pp. 133–149. Available at: <https://doi.org/10.1006/jmcc.1994.1017>.

Boivin, B. et al. (2006) 'Functional beta-adrenergic receptor signalling on nuclear membranes in adult rat and mouse ventricular cardiomyocytes', *Cardiovascular*

Research, 71(1), pp. 69–78. Available at:  
<https://doi.org/10.1016/j.cardiores.2006.03.015>.

Borlaug, B.A. and Redfield, M.M. (2011) 'Diastolic and Systolic Heart Failure are Distinct Phenotypes of the Heart Failure Syndrome', *Circulation*, 123(18), pp. 2006–2014. Available at: <https://doi.org/10.1161/CIRCULATIONAHA.110.954388>.

Bristow, M.R. et al. (1982) 'Decreased catecholamine sensitivity and beta-adrenergic-receptor density in failing human hearts', *The New England Journal of Medicine*, 307(4), pp. 205–211. Available at:  
<https://doi.org/10.1056/NEJM198207223070401>.

Bristow, M.R. et al. (1986) 'Beta 1- and beta 2-adrenergic-receptor subpopulations in nonfailing and failing human ventricular myocardium: coupling of both receptor subtypes to muscle contraction and selective beta 1-receptor down-regulation in heart failure', *Circulation Research*, 59(3), pp. 297–309. Available at:  
<https://doi.org/10.1161/01.res.59.3.297>.

Bristow, M.R. et al. (1989) 'Beta 1- and beta 2-adrenergic receptor-mediated adenylate cyclase stimulation in nonfailing and failing human ventricular myocardium', *Molecular Pharmacology*, 35(3), pp. 295–303. Available at:  
<https://pubmed.ncbi.nlm.nih.gov/2564629/>

Brodde, O.E. et al. (1986) 'Regional distribution of beta-adrenoceptors in the human heart: coexistence of functional beta 1- and beta 2-adrenoceptors in both atria and ventricles in severe congestive cardiomyopathy', *Journal of Cardiovascular Pharmacology*, 8(6), pp. 1235–1242. Available at:  
<https://doi.org/10.1097/00005344-198611000-00021>.

Brodde, O.-E. et al. (1989) 'Drug- and disease-induced changes of human cardiac 1- and 2-adrenoceptors', *European Heart Journal*, 10(suppl B), pp. 38–44. Available at: [https://doi.org/10.1093/eurheartj/10.suppl\\_B.38](https://doi.org/10.1093/eurheartj/10.suppl_B.38).

Brouri, F. et al. (2004) 'Blockade of beta 1- and desensitization of beta 2-adrenoceptors reduce isoprenaline-induced cardiac fibrosis', *European Journal of Pharmacology*, 485(1–3), pp. 227–234. Available at: <https://doi.org/10.1016/j.ejphar.2003.11.063>.

Brower, G.L. et al. (2006) 'The relationship between myocardial extracellular matrix remodeling and ventricular function', *European Journal of Cardio-Thoracic Surgery: Official Journal of the European Association for Cardio-Thoracic Surgery*, 30(4), pp. 604–610. Available at: <https://doi.org/10.1016/j.ejcts.2006.07.006>.

Milano, Ca. et al. (1994) 'Enhanced myocardial function in transgenic mice overexpressing the beta 2-adrenergic receptor', *Science (New York, N.Y.)*, 264(5158). Available at: <https://doi.org/10.1126/science.8160017>.

cellxgene (2024) Heart Cell Atlas v2. Available at: <https://www.heartcellatlas.org/v2/global/> (Accessed: 9 March 2024).

Ceolotto, G. et al. (2008) 'An abnormal gene expression of the beta-adrenergic system contributes to the pathogenesis of cardiomyopathy in cirrhotic rats', *Hepatology (Baltimore, Md.)*, 48(6), pp. 1913–1923. Available at: <https://doi.org/10.1002/hep.22533>.

Charles River Laboratories (2023) 'Technical Sheet: Dahl\_SS\_SS\_JrHsdMcwiCrl\_Rat & SS-13BN\_SS-Chr 13BN\_McwiCrl\_ Consomic Control'. Available at: [https://www.criver.com/sites/default/files/Technical%20Resources/Dahl\\_SS%20S\\_S\\_JrHsdMcwiCrl\\_%20Rat%20%26%20SS-13BN%20SS-Chr%2013BN\\_McwiCrl\\_%20Consomic%20Control.pdf](https://www.criver.com/sites/default/files/Technical%20Resources/Dahl_SS%20S_S_JrHsdMcwiCrl_%20Rat%20%26%20SS-13BN%20SS-Chr%2013BN_McwiCrl_%20Consomic%20Control.pdf)

Choi, D.J. et al. (1997) 'Mechanism of beta-adrenergic receptor desensitization in cardiac hypertrophy is increased beta-adrenergic receptor kinase', *The Journal of Biological Chemistry*, 272(27), pp. 17223–17229. Available at: <https://doi.org/10.1074/jbc.272.27.17223>.

Communal, C., Colucci, W.S. and Singh, K. (2000) 'p38 Mitogen-activated Protein Kinase Pathway Protects Adult Rat Ventricular Myocytes against  $\beta$ -Adrenergic Receptor-stimulated Apoptosis', *Journal of Biological Chemistry*, 275(25), pp. 19395–19400. Available at: <https://doi.org/10.1074/jbc.M910471199>.

Cros, C. and Brette, F. (2013) 'Functional subcellular distribution of  $\beta$ 1- and  $\beta$ 2-adrenergic receptors in rat ventricular cardiac myocytes', *Physiological Reports*, 1(3), p. e00038. Available at: <https://doi.org/10.1002/phy2.38>.

Cushman, W.C. et al. (2016) 'SPRINT Trial Results: Latest News in Hypertension Management', *Hypertension (Dallas, Tex.: 1979)*, 67(2), pp. 263–265. Available at: <https://doi.org/10.1161/HYPERTENSIONAHA.115.06722>.

Dai, Z. et al. (2012) 'Coronary perivascular fibrosis is associated with impairment of coronary blood flow in patients with non-ischemic heart failure', *Journal of Cardiology*, 60(5), pp. 416–421. Available at: <https://doi.org/10.1016/j.jicc.2012.06.009>.

DeGeorge, B.R. et al. (2008) 'Targeted inhibition of cardiomyocyte Gi signaling enhances susceptibility to apoptotic cell death in response to ischemic stress', *Circulation*, 117(11), pp. 1378–1387. Available at: <https://doi.org/10.1161/CIRCULATIONAHA.107.752618>.

Devereux, R.B. et al. (1987) 'Left ventricular hypertrophy in hypertension. Prevalence and relationship to pathophysiologic variables', *Hypertension (Dallas, Tex.: 1979)*, 9(2 Pt 2), pp. 1153-60. Available at: [https://doi.org/10.1161/01.hyp.9.2\\_pt\\_2.ii53](https://doi.org/10.1161/01.hyp.9.2_pt_2.ii53).

Dewenter, M. et al. (2017) 'Calcium/Calmodulin-Dependent Protein Kinase II Activity Persists During Chronic  $\beta$ -Adrenoceptor Blockade in Experimental and Human Heart Failure', *Circulation. Heart Failure*, 10(5), p. e003840. Available at: <https://doi.org/10.1161/CIRCHEARTFAILURE.117.003840>.

Dickhout, J.G., Carlisle, R.E. and Austin, R.C. (2011) 'Interrelationship between cardiac hypertrophy, heart failure, and chronic kidney disease: endoplasmic reticulum stress as a mediator of pathogenesis', *Circulation Research*, 108(5), pp. 629–642. Available at: <https://doi.org/10.1161/CIRCRESAHA.110.226803>.

Dixon, R.A. et al. (1986) 'Cloning of the gene and cDNA for mammalian beta-adrenergic receptor and homology with rhodopsin', *Nature*, 321(6065), pp. 75–79. Available at: <https://doi.org/10.1038/321075a0>.

Doi, R. et al. (2000) 'Development of different phenotypes of hypertensive heart failure: systolic versus diastolic failure in Dahl salt-sensitive rats', *Journal of Hypertension*, 18(1), pp. 111–120. Available at: <https://doi.org/10.1097/00004872-200018010-00016>.

Dorn, G.W. et al. (1999) 'Low- and high-level transgenic expression of beta2-adrenergic receptors differentially affect cardiac hypertrophy and function in Galphaq-overexpressing mice', *Proceedings of the National Academy of Sciences of the United States of America*, 96(11), pp. 6400–6405. Available at: <https://doi.org/10.1073/pnas.96.11.6400>.

Dzimiri, N. et al. (2004) 'Differential functional expression of human myocardial G protein receptor kinases in left ventricular cardiac diseases', *European Journal of Pharmacology*, 489(3), pp. 167–177. Available at: <https://doi.org/10.1016/j.ejphar.2004.03.015>.

El-Armouche, A. et al. (2003) 'Inhibitory G-proteins and their role in desensitization of the adenylyl cyclase pathway in heart failure', *Cardiovascular Research*, 60(3), pp. 478–487. Available at: <https://doi.org/10.1016/j.cardiores.2003.09.014>.

Elliott, W.J. (2007) 'Systemic Hypertension', *Current Problems in Cardiology*, 32(4), pp. 201–259. Available at: <https://doi.org/10.1016/j.cpcardiol.2007.01.002>.

Escobar, E. (2002) 'Hypertension and coronary heart disease', *Journal of Human Hypertension*, 16 Suppl 1, pp. S61-63. Available at: <https://doi.org/10.1038/sj.jhh.1001345>.

François, F., Liaudet, L. and Bernard, W. (2009) 'The macrocirculation and microcirculation of hypertension', *Current hypertension reports*, 11(3). Available at: <https://doi.org/10.1007/s11906-009-0033-6>.

Facundo, H. di T.F. et al. (2017) 'Mitochondria and Cardiac Hypertrophy', *Advances in Experimental Medicine and Biology*, 982, pp. 203–226. Available at: [https://doi.org/10.1007/978-3-319-55330-6\\_11](https://doi.org/10.1007/978-3-319-55330-6_11).

Fajardo, G. et al. (2013) 'Deletion of the  $\beta$ 2-adrenergic receptor prevents the development of cardiomyopathy in mice', *Journal of Molecular and Cellular Cardiology*, 63, pp. 155–164. Available at: <https://doi.org/10.1016/j.yjmcc.2013.07.016>.

Feihl, F. et al. (2008) 'Hypertension and microvascular remodelling', *Cardiovascular Research*, 78(2), pp. 274–285. Available at: <https://doi.org/10.1093/cvr/cvn022>.

Franssen, C. et al. (2016) 'Myocardial Microvascular Inflammatory Endothelial Activation in Heart Failure With Preserved Ejection Fraction', *JACC. Heart failure*, 4(4), pp. 312–324. Available at: <https://doi.org/10.1016/j.jchf.2015.10.007>.

Frazier, C.G. et al. (2007) 'Associations of Gender and Etiology With Outcomes in Heart Failure With Systolic Dysfunction: A Pooled Analysis of 5 Randomized Control Trials', *Journal of the American College of Cardiology*, 49(13), pp. 1450–1458. Available at: <https://doi.org/10.1016/j.jacc.2006.11.041>.

Frohlich, E.D. (2001) 'Fibrosis and ischemia: the real risks in hypertensive heart disease', *American Journal of Hypertension*, 14(6 Pt 2), pp. 194S-199S. Available at: [https://doi.org/10.1016/s0895-7061\(01\)02088-x](https://doi.org/10.1016/s0895-7061(01)02088-x).

Galderisi, M. et al. (2002) 'Coronary flow reserve and myocardial diastolic dysfunction in arterial hypertension', *The American Journal of Cardiology*, 90(8), pp. 860–864. Available at: [https://doi.org/10.1016/s0002-9149\(02\)02708-x](https://doi.org/10.1016/s0002-9149(02)02708-x).

Gallet, R. et al. (2016) 'Cardiosphere-derived cells reverse heart failure with preserved ejection fraction (HFpEF) in rats by decreasing fibrosis and inflammation', *JACC. Basic to translational science*, 1(1–2), pp. 14–28. Available at: <https://doi.org/10.1016/j.jacbts.2016.01.003>.

Ghigo, A. et al. (2014) 'Myocyte signalling in leucocyte recruitment to the heart', *Cardiovascular Research*, 102(2), pp. 270–280. Available at: <https://doi.org/10.1093/cvr/cvu030>.

Gong, H. et al. (2002) 'Specific beta(2)AR blocker ICI 118,551 actively decreases contraction through a G(i)-coupled form of the beta(2)AR in myocytes from failing human heart', *Circulation*, 105(21), pp. 2497–2503. Available at: <https://doi.org/10.1161/01.cir.0000017187.61348.95>.

Gong, H. et al. (2017) 'The effects and possible mechanism of  $\beta$ 2AR gene expression in cardiocytes of canines with heart failure', *Experimental and Therapeutic Medicine*, 14(1), pp. 539–546. Available at: <https://doi.org/10.3892/etm.2017.4521>.

González, A., Schelbert, E.B., et al. (2018) 'Myocardial Interstitial Fibrosis in Heart Failure: Biological and Translational Perspectives', *Journal of the American College of Cardiology*, 71(15), pp. 1696–1706. Available at: <https://doi.org/10.1016/j.jacc.2018.02.021>.

González, A., Ravassa, S., et al. (2018) 'Myocardial Remodeling in Hypertension', *Hypertension (Dallas, Tex.: 1979)*, 72(3), pp. 549–558. Available at: <https://doi.org/10.1161/HYPERTENSIONAHA.118.11125>.

Gorelik, J. et al. (2013) 'Spatial control of the  $\beta$ AR system in heart failure: the transverse tubule and beyond', *Cardiovascular Research*, 98(2), pp. 216–224. Available at: <https://doi.org/10.1093/cvr/cvt005>.

Gros, R. et al. (1997) 'G-protein-coupled receptor kinase activity is increased in hypertension', *The Journal of Clinical Investigation*, 99(9), pp. 2087–2093. Available at: <https://doi.org/10.1172/JCI119381>.

Hage, F.G. (2014) 'C-reactive protein and hypertension', *Journal of Human Hypertension*, 28(7), pp. 410–415. Available at: <https://doi.org/10.1038/jhh.2013.111>.

Hagendorff, A. et al. (2015) 'Echokardiografische Parameter bei der diastolischen Herzinsuffizienz', *Kardiologie up2date*, 11(03), pp. 133–138. Available at: <https://doi.org/10.1055/s-0034-1393032>.

Hall, J.L. et al. (2007) 'Molecular signature of recovery following combination left ventricular assist device (LVAD) support and pharmacologic therapy', *European Heart Journal*, 28(5), pp. 613–627. Available at: <https://doi.org/10.1093/eurheartj/ehl365>.

Hall, R.A. et al. (1998) 'The  $\beta$ 2-adrenergic receptor interacts with the Na<sup>+</sup>/H<sup>+</sup>-exchanger regulatory factor to control Na<sup>+</sup>/H<sup>+</sup> exchange', *Nature*, 392(6676), pp. 626–630. Available at: <https://doi.org/10.1038/33458>.

van Ham, W.B. et al. (2022) 'Clinical Phenotypes of Heart Failure With Preserved Ejection Fraction to Select Preclinical Animal Models', *JACC: Basic to Translational Science*, 7(8), pp. 844–857. Available at: <https://doi.org/10.1016/j.jacbts.2021.12.009>.

Hartupee, J. and Mann, D.L. (2017) 'Neurohormonal activation in heart failure with reduced ejection fraction', *Nature Reviews. Cardiology*, 14(1), pp. 30–38. Available at: <https://doi.org/10.1038/nrcardio.2016.163>.

Hasan, P. et al. (2018) 'Mitochondrial fission protein, dynamin-related protein 1, contributes to the promotion of hypertensive cardiac hypertrophy and fibrosis in Dahl-salt sensitive rats', *Journal of Molecular and Cellular Cardiology*, 121, pp. 103–106. Available at: <https://doi.org/10.1016/j.yjmcc.2018.07.004>.

Holzer, Senka (2019) 'Proposal Targeting Excitation-Transcription Coupling for Managing Hypertensive Cardiomyopathy'.

Hussain, R.I. et al. (2013) 'The functional activity of inhibitory G protein (G(i)) is not increased in failing heart ventricle', *Journal of Molecular and Cellular Cardiology*, 56, pp. 129–138. Available at: <https://doi.org/10.1016/j.yjmcc.2012.11.015>.

Idris-Khodja, N. et al. (2014) 'Dual opposing roles of adaptive immunity in hypertension', *European Heart Journal*, 35(19), pp. 1238–1244. Available at: <https://doi.org/10.1093/eurheartj/ehu119>.

Kamo, T., Akazawa, H. and Komuro, I. (2015) 'Cardiac nonmyocytes in the hub of cardiac hypertrophy', *Circulation Research*, 117(1), pp. 89–98. Available at: <https://doi.org/10.1161/CIRCRESAHA.117.305349>.

Kanemaru, K. et al. (2023) 'Spatially resolved multiomics of human cardiac niches', *Nature*, 619(7971), pp. 801–810. Available at: <https://doi.org/10.1038/s41586-023-06311-1>.

Kearney, P.M. et al. (2005) 'Global burden of hypertension: analysis of worldwide data', *Lancet* (London, England), 365(9455), pp. 217–223. Available at: [https://doi.org/10.1016/S0140-6736\(05\)17741-1](https://doi.org/10.1016/S0140-6736(05)17741-1).

Khan, M.G. (2006) 'Beta-Blockers', in M.G. Khan (ed.) *Encyclopedia of Heart Diseases*. Burlington: Academic Press, pp. 159–167. Available at: <https://doi.org/10.1016/B978-012406061-6/50028-X>.

Kilts, J.D. et al. (2000) 'Beta(2)-adrenergic and several other G protein-coupled receptors in human atrial membranes activate both G(s) and G(i)', *Circulation Research*, 87(8), pp. 705–709. Available at: <https://doi.org/10.1161/01.res.87.8.705>.

Kilts, J.D. et al. (2003) 'Age increases expression and receptor-mediated activation of G alpha i in human atria', *Journal of Cardiovascular Pharmacology*, 42(5), pp. 662–670. Available at: <https://doi.org/10.1097/00005344-200311000-00013>.

Kim, I.-M. et al. (2008) 'Beta-blockers alprenolol and carvedilol stimulate beta-arrestin-mediated EGFR transactivation', *Proceedings of the National Academy of Sciences of the United States of America*, 105(38), pp. 14555–14560. Available at: <https://doi.org/10.1073/pnas.0804745105>.

Kimura, T. et al. (2019) 'Inhibitory Effects of Tofogliflozin on Cardiac Hypertrophy in Dahl Salt-Sensitive and Salt-Resistant Rats Fed a High-Fat Diet', *International Heart Journal*, 60(3), pp. 728–735. Available at: <https://doi.org/10.1536/ihj.18-392>.

Klauber, J. et al. (2014) 'Versorgungs-Report 2013/2014 Schwerpunkt: Depression', Schattauer, Redaktion Versorgungs-Report Wissenschaftliches Institut der AOK, pp. 209-225 Available at: [https://www.wido.de/fileadmin/Dateien/Dokumente/Publikationen\\_Produkte/Buchreihen/Versorgungsreport/2013-2014/Kapitel%20mit%20Deckblatt/wido\\_vsr20132014\\_kap04.pdf](https://www.wido.de/fileadmin/Dateien/Dokumente/Publikationen_Produkte/Buchreihen/Versorgungsreport/2013-2014/Kapitel%20mit%20Deckblatt/wido_vsr20132014_kap04.pdf)

Klotz, S. et al. (2006) 'Development of heart failure in chronic hypertensive Dahl rats: focus on heart failure with preserved ejection fraction', *Hypertension (Dallas, Tex.: 1979)*, 47(5), pp. 901–911. Available at: <https://doi.org/10.1161/01.HYP.0000215579.81408.8e>.

Konukoglu, D. and Uzun, H. (2017) 'Endothelial Dysfunction and Hypertension', *Advances in Experimental Medicine and Biology*, 956, pp. 511–540. Available at: [https://doi.org/10.1007/5584\\_2016\\_90](https://doi.org/10.1007/5584_2016_90).

Kuschel, M. et al. (1999) 'G(i) protein-mediated functional compartmentalization of cardiac beta(2)-adrenergic signaling', *The Journal of Biological Chemistry*, 274(31), pp. 22048–22052. Available at: <https://doi.org/10.1074/jbc.274.31.22048>.

Kvakan, H., Luft, F.C. and Muller, D.N. (2009) 'Role of the immune system in hypertensive target organ damage', *Trends in Cardiovascular Medicine*, 19(7), pp. 242–246. Available at: <https://doi.org/10.1016/j.tcm.2010.02.004>.

Lavoie, C. et al. (2002) ' $\beta$ 1/ $\beta$ 2-Adrenergic Receptor Heterodimerization Regulates  $\beta$ 2-Adrenergic Receptor Internalization and ERK Signaling Efficacy \*', *Journal of Biological Chemistry*, 277(38), pp. 35402–35410. Available at: <https://doi.org/10.1074/jbc.M204163200>.

Leineweber, K. et al. (2005) 'G-protein-coupled receptor kinase activity in human heart failure: effects of beta-adrenoceptor blockade', *Cardiovascular Research*, 66(3), pp. 512–519. Available at: <https://doi.org/10.1016/j.cardiores.2005.01.025>.

Levick, S.P. et al. (2010) 'Sympathetic nervous system modulation of inflammation and remodeling in the hypertensive heart', *Hypertension (Dallas, Tex.: 1979)*, 55(2), pp. 270–276. Available at: <https://doi.org/10.1161/HYPERTENSIONAHA.109.142042>.

Levy, D. et al. (1996) 'The Progression From Hypertension to Congestive Heart Failure', *JAMA*, 275(20), pp. 1557–1562. Available at: <https://doi.org/10.1001/jama.1996.03530440037034>.

Li, T. et al. (1985) 'Effects of diacetyl monoxime on cardiac excitation-contraction coupling', *The Journal of Pharmacology and Experimental Therapeutics*, 232(3), pp. 688–695. Available at: <https://pubmed.ncbi.nlm.nih.gov/3156242/>

Liggett, S.B. et al. (2000) 'Early and delayed consequences of beta(2)-adrenergic receptor overexpression in mouse hearts: critical role for expression level', *Circulation*, 101(14), pp. 1707–1714. Available at: <https://doi.org/10.1161/01.cir.101.14.1707>.

Lijnen, P. and Petrov, V. (1999) 'Renin-angiotensin system, hypertrophy and gene expression in cardiac myocytes', *Journal of Molecular and Cellular Cardiology*, 31(5), pp. 949–970. Available at: <https://doi.org/10.1006/jmcc.1999.0934>.

Ling, H. et al. (2009) 'Requirement for Ca<sup>2+</sup>/calmodulin-dependent kinase II in the transition from pressure overload-induced cardiac hypertrophy to heart failure in mice', *The Journal of Clinical Investigation*, 119(5), pp. 1230–1240. Available at: <https://doi.org/10.1172/JCI38022>.

Ljubojevic, S. et al. (2014) 'Early remodeling of perinuclear Ca<sup>2+</sup> stores and nucleoplasmic Ca<sup>2+</sup> signaling during the development of hypertrophy and heart failure', *Circulation*, 130(3), pp. 244–255. Available at: <https://doi.org/10.1161/CIRCULATIONAHA.114.008927>.

Ljubojevic-Holzer, S. et al. (2020) 'CaMKII $\delta$ C Drives Early Adaptive Ca<sup>2+</sup> Change and Late Eccentric Cardiac Hypertrophy', *Circulation Research*, 127(9), pp. 1159–1178. Available at: <https://doi.org/10.1161/CIRCRESAHA.120.316947>.

López, B. et al. (2006) 'Alterations in the Pattern of Collagen Deposition May Contribute to the Deterioration of Systolic Function in Hypertensive Patients With Heart Failure', *Journal of the American College of Cardiology*, 48(1), pp. 89–96. Available at: <https://doi.org/10.1016/j.jacc.2006.01.077>.

de Lucia, C. et al. (2014) 'Adrenal adrenoceptors in heart failure', *Frontiers in Physiology*, 5, p. 246. Available at: <https://doi.org/10.3389/fphys.2014.00246>.

de Lucia, C., Eguchi, A. and Koch, W.J. (2018) 'New Insights in Cardiac  $\beta$ -Adrenergic Signaling During Heart Failure and Aging', *Frontiers in Pharmacology*, 9, p. 904. Available at: <https://doi.org/10.3389/fphar.2018.00904>.

Lymperopoulos, A., Rengo, G. and Koch, W.J. (2012) 'GRK2 inhibition in heart failure: something old, something new', *Current Pharmaceutical Design*, 18(2), pp. 186–191. Available at: <https://doi.org/10.2174/138161212799040510>.

MacDougall, D.A. et al. (2012) 'Caveolae compartmentalise  $\beta$ 2-adrenoceptor signals by curtailing cAMP production and maintaining phosphatase activity in the sarcoplasmic reticulum of the adult ventricular myocyte', *Journal of Molecular and Cellular Cardiology*, 52(2), pp. 388–400. Available at: <https://doi.org/10.1016/j.yjmcc.2011.06.014>.

Mangmool, S., Shukla, A.K. and Rockman, H.A. (2010) 'beta-Arrestin-dependent activation of Ca(2+)/calmodulin kinase II after beta(1)-adrenergic receptor stimulation', *The Journal of Cell Biology*, 189(3), pp. 573–587. Available at: <https://doi.org/10.1083/jcb.200911047>.

Martin, M.L. et al. (2012) 'G-Protein-Coupled Receptors in the Heart', in *Muscle: fundamental biology and mechanisms of disease*. Elsevier, pp. 87–112. Available at: <https://doi.org/10.1016/B978-0-12-381510-1.00008-9>.

Matzer, I. (2021) 'Role of  $\beta$ 1-adrenergic signalling in early- and late-stage hypertensive cardiac remodelling, Master thesis submitted at the Master Degree Course Mass Spectrometry and Molecular Analytics for the degree Master of Science in Engineering (MSc)'.

Matzer, I. et al. (2022) 'beta-Adrenergic Receptor Stimulation Maintains NCX-CaMKII Axis and Prevents Overactivation of IL6R-Signaling in Cardiomyocytes upon Increased Workload', *Biomedicines*, 10(7), p. 1648. Available at: <https://doi.org/10.3390/biomedicines10071648>.

McCain, M.L. and Parker, K.K. (2011) 'Mechanotransduction: the role of mechanical stress, myocyte shape, and cytoskeletal architecture on cardiac function', *Pflugers Archiv: European Journal of Physiology*, 462(1), pp. 89–104. Available at: <https://doi.org/10.1007/s00424-011-0951-4>.

McDonagh, T.A. et al. (2021) '2021 ESC Guidelines for the diagnosis and treatment of acute and chronic heart failure', *European Heart Journal*, 42(36), pp. 3599–3726. Available at: <https://doi.org/10.1093/eurheartj/ehab368>.

McGraw, D.W. et al. (1998) 'Role of beta ARK in long-term agonist-promoted desensitisation of the beta 2-adrenergic receptor', *Cellular Signalling*, 10(3), pp. 197–204. Available at: [https://doi.org/10.1016/s0898-6568\(97\)00112-5](https://doi.org/10.1016/s0898-6568(97)00112-5).

McLenachan, J.M. and Dargie, H.J. (1990) 'Ventricular arrhythmias in hypertensive left ventricular hypertrophy. Relationship to coronary artery disease, left ventricular dysfunction, and myocardial fibrosis', *American Journal of Hypertension*, 3(10), pp. 735–740. Available at: <https://doi.org/10.1093/ajh/3.10.735>.

McMaster, W.G. et al. (2015) 'Inflammation, immunity, and hypertensive end-organ damage', *Circulation Research*, 116(6), pp. 1022–1033. Available at: <https://doi.org/10.1161/CIRCRESAHA.116.303697>.

Michel, M.C., Maisel, A.S. and Brodde, O.E. (1990) 'Mitigation of beta 1- and/or beta 2-adrenoceptor function in human heart failure', *British Journal of Clinical Pharmacology*, 30 Suppl 1(Suppl 1), pp. 37S-42S. Available at: <https://doi.org/10.1111/j.1365-2125.1990.tb05466.x>.

Moffett, S. et al. (2001) 'The palmitoylation state of the beta(2)-adrenergic receptor regulates the synergistic action of cyclic AMP-dependent protein kinase and beta-adrenergic receptor kinase involved in its phosphorylation and desensitization', *Journal of Neurochemistry*, 76(1), pp. 269–279. Available at: <https://doi.org/10.1046/j.1471-4159.2001.00005.x>.

Molenaar, P. et al. (2007) '(-)-Adrenaline elicits positive inotropic, lusitropic, and biochemical effects through beta2 -adrenoceptors in human atrial myocardium from nonfailing and failing hearts, consistent with Gs coupling but not with Gi coupling', *Naunyn-Schmiedeberg's Archives of Pharmacology*, 375(1), pp. 11–28. Available at: <https://doi.org/10.1007/s00210-007-0138-x>.

Montó, F. et al. (2012) 'Different expression of adrenoceptors and GRKs in the human myocardium depends on heart failure etiology and correlates to clinical variables', *American Journal of Physiology. Heart and Circulatory Physiology*, 303(3), pp. H368-376. Available at: <https://doi.org/10.1152/ajpheart.01061.2011>.

Motiejunaite, J., Amar, L. and Vidal-Petiot, E. (2021) 'Adrenergic receptors and cardiovascular effects of catecholamines', *Annales D'endocrinologie*, 82(3–4), pp. 193–197. Available at: <https://doi.org/10.1016/j.ando.2020.03.012>.

Myagmar, B.-E. et al. (2017) 'Adrenergic Receptors in Individual Ventricular Myocytes: The Beta-1 and Alpha-1B Are in All Cells, the Alpha-1A Is in a Subpopulation, and the Beta-2 and Beta-3 Are Mostly Absent', *Circulation research*, 120(7), pp. 1103–1115. Available at: <https://doi.org/10.1161/CIRCRESAHA.117.310520>.

Nadruz, W. (2015) 'Myocardial remodeling in hypertension', *Journal of Human Hypertension*, 29(1), pp. 1–6. Available at: <https://doi.org/10.1038/jhh.2014.36>.

Nakajima, Y. et al. (2019) 'A dipeptidyl peptidase-IV inhibitor improves diastolic dysfunction in Dahl salt-sensitive rats', *Journal of Molecular and Cellular Cardiology*, 129, pp. 257–265. Available at: <https://doi.org/10.1016/j.yjmcc.2019.03.009>.

Narula, J. et al. (2001) 'Apoptosis and the systolic dysfunction in congestive heart failure. Story of apoptosis interruptus and zombie myocytes', *Cardiology Clinics*, 19(1), pp. 113–126. Available at: [https://doi.org/10.1016/s0733-8651\(05\)70198-3](https://doi.org/10.1016/s0733-8651(05)70198-3).

Nash, C.A. et al. (2019) 'Golgi localized  $\beta$ 1-adrenergic receptors stimulate Golgi PI4P hydrolysis by PLC $\epsilon$  to regulate cardiac hypertrophy', *eLife*, 8, p. e48167. Available at: <https://doi.org/10.7554/eLife.48167>.

Neubauer, S. (2007) 'The failing heart--an engine out of fuel', *The New England Journal of Medicine*, 356(11), pp. 1140–1151. Available at: <https://doi.org/10.1056/NEJMra063052>.

Nikolaev, V.O. et al. (2006) 'Cyclic AMP imaging in adult cardiac myocytes reveals far-reaching beta1-adrenergic but locally confined beta2-adrenergic receptor-mediated signaling', *Circulation Research*, 99(10), pp. 1084–1091. Available at: <https://doi.org/10.1161/01.RES.0000250046.69918.d5>.

Nikolaev, V.O. et al. (2010) 'β<sub>2</sub>-Adrenergic Receptor Redistribution in Heart Failure Changes cAMP Compartmentation', *Science*, 327(5973), pp. 1653–1657. Available at: <https://doi.org/10.1126/science.1185988>.

Noma, T. et al. (2007) 'Beta-arrestin-mediated beta<sub>1</sub>-adrenergic receptor transactivation of the EGFR confers cardioprotection', *The Journal of Clinical Investigation*, 117(9), pp. 2445–2458. Available at: <https://doi.org/10.1172/JCI31901>.

O'Callaghan, C.J. and Williams, B. (2002) 'The regulation of human vascular smooth muscle extracellular matrix protein production by alpha- and beta-adrenoceptor stimulation', *Journal of hypertension*, 20(2). Available at: <https://doi.org/10.1097/00004872-200202000-00019>.

Ogata, T. et al. (2004) 'Myocardial fibrosis and diastolic dysfunction in deoxycorticosterone acetate-salt hypertensive rats is ameliorated by the peroxisome proliferator-activated receptor-alpha activator fenofibrate, partly by suppressing inflammatory responses associated with the nuclear factor-kappa-B pathway', *Journal of the American College of Cardiology*, 43(8), pp. 1481–1488. Available at: <https://doi.org/10.1016/j.jacc.2003.11.043>.

van Oort, R.J. et al. (2010) 'Ryanodine receptor phosphorylation by calcium/calmodulin-dependent protein kinase II promotes life-threatening ventricular arrhythmias in mice with heart failure', *Circulation*, 122(25), pp. 2669–2679. Available at: <https://doi.org/10.1161/CIRCULATIONAHA.110.982298>.

Palmiero, P. et al. (2014) 'Hypertensive Cardiomyopathy in asymptomatic patients: a neglected diagnosis', *Current Hypertension Reviews*, 10(4), pp. 239–245. Available at: <https://doi.org/10.2174/157340211004150319123635>.

Patel, P.A., Tilley, D.G. and Rockman, H.A. (2008) 'Beta-arrestin-mediated signaling in the heart', *Circulation Journal: Official Journal of the Japanese*

Circulation Society, 72(11), pp. 1725–1729. Available at: <https://doi.org/10.1253/circj.cj-08-0734>.

Penela, P. et al. (2006) 'Mechanisms of regulation of G protein-coupled receptor kinases (GRKs) and cardiovascular disease', *Cardiovascular Research*, 69(1), pp. 46–56. Available at: <https://doi.org/10.1016/j.cardiores.2005.09.011>.

Phillips, R.A. and Diamond, J.A. (2001) 'Diastolic function in hypertension', *Current Cardiology Reports*, 3(6), pp. 485–497. Available at: <https://doi.org/10.1007/s11886-001-0071-4>.

Pieske, B. et al. (2019) 'How to diagnose heart failure with preserved ejection fraction: the HFA–PEFF diagnostic algorithm: a consensus recommendation from the Heart Failure Association (HFA) of the European Society of Cardiology (ESC)', *European Heart Journal*, 40(40), pp. 3297–3317. Available at: <https://doi.org/10.1093/eurheartj/ehz641>.

Puleo, F. et al. (2020) 'Sympathetic Regulation of the NCC (Sodium Chloride Cotransporter) in Dahl Salt-Sensitive Hypertension', *Hypertension (Dallas, Tex.: 1979)*, 76(5), pp. 1461–1469. Available at: <https://doi.org/10.1161/HYPERTENSIONAHA.120.15928>.

Raake, P.W. et al. (2008) 'G protein-coupled receptor kinase 2 ablation in cardiac myocytes before or after myocardial infarction prevents heart failure', *Circulation Research*, 103(4), pp. 413–422. Available at: <https://doi.org/10.1161/CIRCRESAHA.107.168336>.

Rain, C. and Rada, G. (2015) 'Is carvedilol better than other beta-blockers for heart failure?', *Medwave*, 15 Suppl 1, p. e6168. Available at: <https://doi.org/10.5867/medwave.2015.6168>.

Rengo, G. et al. (2009) 'Myocardial Adeno-Associated Virus Serotype 6– $\beta$ ARKct Gene Therapy Improves Cardiac Function and Normalizes the Neurohormonal Axis

in Chronic Heart Failure', *Circulation*, 119(1), pp. 89–98. Available at: <https://doi.org/10.1161/CIRCULATIONAHA.108.803999>.

Rengo, Giuseppe, Femminella, G.D., et al. (2012) 'Dalla ricerca di base alla pratica clinica: nuove prospettive terapeutiche nello scompenso cardiaco', *Giornale Italiano di Cardiologia*, 13(4), pp. 254–262. Available at: <https://www.giornaledicardiologia.it/archivio/1056/articoli/11557/>

Rengo, G. et al. (2012) 'Myocardial  $\beta(2)$  -adrenoceptor gene delivery promotes coordinated cardiac adaptive remodelling and angiogenesis in heart failure', *British Journal of Pharmacology*, 166(8), pp. 2348–2361. Available at: <https://doi.org/10.1111/j.1476-5381.2012.01954.x>.

Rengo, Giuseppe, Perrone-Filardi, P., et al. (2012) 'Targeting the  $\beta$ -Adrenergic Receptor System Through G-Protein–Coupled Receptor Kinase 2: A New Paradigm for Therapy and Prognostic Evaluation in Heart Failure', *Circulation: Heart Failure*, 5(3), pp. 385–391. Available at: <https://doi.org/10.1161/CIRCHEARTFAILURE.112.966895>.

Ribas, C. et al. (2007) 'The G protein-coupled receptor kinase (GRK) interactome: role of GRKs in GPCR regulation and signaling', *Biochimica Et Biophysica Acta*, 1768(4), pp. 913–922. Available at: <https://doi.org/10.1016/j.bbamem.2006.09.019>.

Rodefeld, M.D. et al. (1996) 'Beta-adrenergic and muscarinic cholinergic receptor densities in the human sinoatrial node: identification of a high beta 2-adrenergic receptor density', *Journal of Cardiovascular Electrophysiology*, 7(11), pp. 1039–1049. Available at: <https://doi.org/10.1111/j.1540-8167.1996.tb00479.x>.

Rohr, S. (2012) 'Arrhythmogenic Implications of Fibroblast-Myocyte Interactions', *Circulation: Arrhythmia and Electrophysiology*, 5(2), pp. 442–452. Available at: <https://doi.org/10.1161/CIRCEP.110.957647>.

Romero, L.M. (2010) 'Fight or Flight Responses', in M.D. Breed and J. Moore (eds) *Encyclopedia of Animal Behavior*. Oxford: Academic Press, pp. 710–714. Available at: <https://doi.org/10.1016/B978-0-08-045337-8.00261-8>.

Roth, N.S. et al. (1991) 'Comparative rates of desensitization of beta-adrenergic receptors by the beta-adrenergic receptor kinase and the cyclic AMP-dependent protein kinase', *Proceedings of the National Academy of Sciences of the United States of America*, 88(14), pp. 6201–6204. Available at: <https://doi.org/10.1073/pnas.88.14.6201>.

Ruilope, L.M. and Schmieder, R.E. (2008) 'Left ventricular hypertrophy and clinical outcomes in hypertensive patients', *American Journal of Hypertension*, 21(5), pp. 500–508. Available at: <https://doi.org/10.1038/ajh.2008.16>.

Rybin, V.O. et al. (2000) 'Differential targeting of beta -adrenergic receptor subtypes and adenylyl cyclase to cardiomyocyte caveolae. A mechanism to functionally regulate the cAMP signaling pathway', *The Journal of Biological Chemistry*, 275(52), pp. 41447–41457. Available at: <https://doi.org/10.1074/jbc.M006951200>.

Salas-Pacheco, J.L. et al. (2022) 'Longitudinal systolic dysfunction in hypertensive cardiomyopathy with normal ejection fraction', *Echocardiography (Mount Kisco, N.Y.)*, 39(1), pp. 46–53. Available at: <https://doi.org/10.1111/echo.15267>.

Sato, P.Y. et al. (2015) 'The evolving impact of g protein-coupled receptor kinases in cardiac health and disease', *Physiological Reviews*, 95(2), pp. 377–404. Available at: <https://doi.org/10.1152/physrev.00015.2014>.

Sato, P.Y. et al. (2018) 'Restricting mitochondrial GRK2 post-ischemia confers cardioprotection by reducing myocyte death and maintaining glucose oxidation', *Science Signaling*, 11(560), p. eaau0144. Available at: <https://doi.org/10.1126/scisignal.aau0144>.

Savarese, G. et al. (2023) 'Global burden of heart failure: a comprehensive and updated review of epidemiology', *Cardiovascular Research*, 118(17), pp. 3272–3287. Available at: <https://doi.org/10.1093/cvr/cvac013>.

Schwartzkopff, B. et al. (1993) 'Structural and functional alterations of the intramyocardial coronary arterioles in patients with arterial hypertension', *Circulation*, 88(3), pp. 993–1003. Available at: <https://doi.org/10.1161/01.cir.88.3.993>.

Schwarzer, M. (2016) 'Chapter 8 - Models to Investigate Cardiac Metabolism', in M. Schwarzer and T. Doenst (eds) *The Scientist's Guide to Cardiac Metabolism*. Boston: Academic Press, pp. 103–122. Available at: <https://doi.org/10.1016/B978-0-12-802394-5.00008-X>.

Severino, P. et al. (2020) 'Ischemic Heart Disease and Heart Failure: Role of Coronary Ion Channels', *International Journal of Molecular Sciences*, 21(9), p. 3167. Available at: <https://doi.org/10.3390/ijms21093167>.

Shah, A.S. et al. (2001) 'In Vivo Ventricular Gene Delivery of a  $\beta$ -Adrenergic Receptor Kinase Inhibitor to the Failing Heart Reverses Cardiac Dysfunction', *Circulation*, 103(9), pp. 1311–1316. Available at: <https://doi.org/10.1161/01.CIR.103.9.1311>.

Shah, S.J. et al. (2014) 'Ultrastructural and cellular basis for the development of abnormal myocardial mechanics during the transition from hypertension to heart failure', *American Journal of Physiology-Heart and Circulatory Physiology*, 306(1), pp. H88–H100. Available at: <https://doi.org/10.1152/ajpheart.00642.2013>.

Shenoy, S.K. and Lefkowitz, R.J. (2011) ' $\beta$ -Arrestin-mediated receptor trafficking and signal transduction', *Trends in Pharmacological Sciences*, 32(9), pp. 521–533. Available at: <https://doi.org/10.1016/j.tips.2011.05.002>.

Shinde, A.V. and Frangogiannis, N.G. (2017) 'Mechanisms of Fibroblast Activation in the Remodeling Myocardium', *Current Pathobiology Reports*, 5(2), pp. 145–152. Available at: <https://doi.org/10.1007/s40139-017-0132-z>.

Silbernagl, S. et al. (2020) 'Herzinsuffizienz', in *Taschenatlas Pathophysiologie*. 6., vollständig überarbeitete Auflage. Stuttgart New York: Georg Thieme Verlag, pp. 250–256.

Singh, M.V. and Anderson, M.E. (2011) 'Is CaMKII a link between inflammation and hypertrophy in heart?', *Journal of Molecular Medicine (Berlin, Germany)*, 89(6), pp. 537–543. Available at: <https://doi.org/10.1007/s00109-011-0727-5>.

Slivnick, J. and Lampert, B.C. (2019) 'Hypertension and Heart Failure', *Heart Failure Clinics*, 15(4), pp. 531–541. Available at: <https://doi.org/10.1016/j.hfc.2019.06.007>.

Solomon, S.D. et al. (2021) 'Dapagliflozin in heart failure with preserved and mildly reduced ejection fraction: rationale and design of the DELIVER trial', *European Journal of Heart Failure*, 23(7), pp. 1217–1225. Available at: <https://doi.org/10.1002/ejhf.2249>.

Sugden, P.H. and Clerk, A. (1998) 'Cellular mechanisms of cardiac hypertrophy', *Journal of Molecular Medicine*, 76(11), pp. 725–746. Available at: <https://doi.org/10.1007/s001090050275>.

Sun, Y. et al. (2008) 'Upregulation of GRP78 and caspase-12 in diastolic failing heart', *Acta Biochimica Polonica*, 55(3), pp. 511–516. Available at: <https://pubmed.ncbi.nlm.nih.gov/18787714/>

Sysa-Shah, P. et al. (2016) 'Bidirectional cross-regulation between ErbB2 and  $\beta$ -adrenergic signalling pathways', *Cardiovascular Research*, 109(3), pp. 358–373. Available at: <https://doi.org/10.1093/cvr/cvv274>.

Tackling, G. and Borhade, M.B. (2023) 'Hypertensive Heart Disease', in StatPearls. Treasure Island (FL): StatPearls Publishing. Available at: <http://www.ncbi.nlm.nih.gov/books/NBK539800/> (Accessed: 20 December 2023).

Tagawa, H. et al. (1996) 'Basis for increased microtubules in pressure-hypertrophied cardiocytes', *Circulation*, 93(6), pp. 1230–1243. Available at: <https://doi.org/10.1161/01.cir.93.6.1230>.

Takahashi, M. et al. (1992) 'Increased uncoupling of beta-, beta 1- and beta 2-adrenoceptor to myocardial contraction in failing human myocardium', *Japanese Circulation Journal*, 56(7), pp. 701–709. Available at: <https://doi.org/10.1253/jcj.56.701>.

Talan, M.I. et al. (2011) ' $\beta_2$  AR Agonists in Treatment of Chronic Heart Failure: Long Path to Translation', *Journal of molecular and cellular cardiology*, 51(4), pp. 529–533. Available at: <https://doi.org/10.1016/j.yjmcc.2010.09.019>.

Tanner, M.A., Maitz, C.A. and Grisanti, L.A. (2021) 'Immune cell  $\beta_2$ -adrenergic receptors contribute to the development of heart failure', *American Journal of Physiology. Heart and Circulatory Physiology*, 321(4), pp. H633–H649. Available at: <https://doi.org/10.1152/ajpheart.00243.2021>.

Tevaearai, H.T. et al. (2001) 'Ventricular Dysfunction After Cardioplegic Arrest Is Improved After Myocardial Gene Transfer of a  $\beta$ -Adrenergic Receptor Kinase Inhibitor', *Circulation*, 104(17), pp. 2069–2074. Available at: <https://doi.org/10.1161/hc4201.097188>.

Tilley, D.G. (2011) 'G protein-dependent and G protein-independent signaling pathways and their impact on cardiac function', *Circulation Research*, 109(2), pp. 217–230. Available at: <https://doi.org/10.1161/CIRCRESAHA.110.231225>.

Tuomainen, T. and Tavi, P. (2017) 'The role of cardiac energy metabolism in cardiac hypertrophy and failure', *Experimental Cell Research*, 360(1), pp. 12–18. Available at: <https://doi.org/10.1016/j.yexcr.2017.03.052>.

Ungerer, M. et al. (1994) 'Expression of beta-arrestins and beta-adrenergic receptor kinases in the failing human heart', *Circulation Research*, 74(2), pp. 206–213. Available at: <https://doi.org/10.1161/01.res.74.2.206>.

Velagaleti, R.S. et al. (2014) 'Left Ventricular Hypertrophy Patterns and Incidence of Heart Failure With Preserved Versus Reduced Ejection Fraction', *The American Journal of Cardiology*, 113(1), pp. 117–122. Available at: <https://doi.org/10.1016/j.amjcard.2013.09.028>.

Vidal, M. et al. (2012) ' $\beta$ -Adrenergic receptor stimulation causes cardiac hypertrophy via a G $\beta\gamma$ /Erk-dependent pathway', *Cardiovascular Research*, 96(2), pp. 255–264. Available at: <https://doi.org/10.1093/cvr/cvs249>.

Wang, Y. et al. (2021) 'Intracellular  $\beta$ 1-Adrenergic Receptors and Organic Cation Transporter 3 Mediate Phospholamban Phosphorylation to Enhance Cardiac Contractility', *Circulation Research*, 128(2), pp. 246–261. Available at: <https://doi.org/10.1161/CIRCRESAHA.120.317452>.

Wang, Z.V., Rothermel, B.A. and Hill, J.A. (2010) 'Autophagy in hypertensive heart disease', *The Journal of Biological Chemistry*, 285(12), pp. 8509–8514. Available at: <https://doi.org/10.1074/jbc.R109.025023>.

Wei, W. and Smrcka, A.V. (2023) 'Internalized  $\beta$ 2-Adrenergic Receptors Inhibit Subcellular Phospholipase C-Dependent Cardiac Hypertrophic Signaling', *bioRxiv: The Preprint Server for Biology*, p. 2023.06.07.544153. Available at: <https://doi.org/10.1101/2023.06.07.544153>.

Weintraub, R.G., Semsarian, C. and Macdonald, P. (2017) 'Dilated cardiomyopathy', *Lancet (London, England)*, 390(10092), pp. 400–414. Available at: [https://doi.org/10.1016/S0140-6736\(16\)31713-5](https://doi.org/10.1016/S0140-6736(16)31713-5).

Whelan, R.S., Kaplinskiy, V. and Kitsis, R.N. (2010) 'Cell death in the pathogenesis of heart disease: mechanisms and significance', *Annual Review of Physiology*, 72, pp. 19–44. Available at: <https://doi.org/10.1146/annurev.physiol.010908.163111>.

Whelton, P.K. and Carey, R.M. (2017) 'The 2017 Clinical Practice Guideline for High Blood Pressure', *JAMA*, 318(21), pp. 2073–2074. Available at: <https://doi.org/10.1001/jama.2017.18209>.

Wisler, J.W. et al. (2007) 'A unique mechanism of beta-blocker action: carvedilol stimulates beta-arrestin signaling', *Proceedings of the National Academy of Sciences of the United States of America*, 104(42), pp. 16657–16662. Available at: <https://doi.org/10.1073/pnas.0707936104>.

Woo, A.Y.-H. et al. (2015) 'Biased  $\beta_2$ -adrenoceptor signalling in heart failure: pathophysiology and drug discovery', *British Journal of Pharmacology*, 172(23), pp. 5444–5456. Available at: <https://doi.org/10.1111/bph.12965>.

Woo, A.Y.H. and Xiao, R. (2012) ' $\beta$ -Adrenergic receptor subtype signaling in heart: from bench to bedside', *Acta Pharmacologica Sinica*, 33(3), pp. 335–341. Available at: <https://doi.org/10.1038/aps.2011.201>.

Woodcock, E.A. et al. (2008) 'Cardiac alpha 1-adrenergic drive in pathological remodelling', *Cardiovascular Research*, 77(3), pp. 452–462. Available at: <https://doi.org/10.1093/cvr/cvm078>.

Xiao, R.-P. et al. (2003) 'Enhanced Gi Signaling Selectively Negates  $\beta_2$ -Adrenergic Receptor (AR)– but Not  $\beta_1$ -AR–Mediated Positive Inotropic Effect in Myocytes From Failing Rat Hearts', *Circulation*, 108(13), pp. 1633–1639. Available at: <https://doi.org/10.1161/01.CIR.0000087595.17277.73>.

Xiao, R.P., Ji, X. and Lakatta, E.G. (1995) 'Functional coupling of the beta 2-adrenoceptor to a pertussis toxin-sensitive G protein in cardiac myocytes', *Molecular Pharmacology*, 47(2), pp. 322–329. Available at: <https://pubmed.ncbi.nlm.nih.gov/7870040/>

Xu, X. et al. (2021) 'Binding pathway determines norepinephrine selectivity for the human  $\beta$ 1AR over  $\beta$ 2AR', *Cell Research*, 31(5), pp. 569–579. Available at: <https://doi.org/10.1038/s41422-020-00424-2>.

Xydas, S. et al. (2006) 'beta(2)-Adrenergic stimulation attenuates left ventricular remodeling, decreases apoptosis, and improves calcium homeostasis in a rodent model of ischemic cardiomyopathy', *The Journal of Pharmacology and Experimental Therapeutics*, 317(2), pp. 553–561. Available at: <https://doi.org/10.1124/jpet.105.099432>.

Yang, H.-Q. et al. (2020) 'Compartmentalized  $\beta$ 1-adrenergic signalling synchronizes excitation–contraction coupling without modulating individual  $\text{Ca}^{2+}$  sparks in healthy and hypertrophied cardiomyocytes', *Cardiovascular Research*, 116(13), pp. 2069–2080. Available at: <https://doi.org/10.1093/cvr/cvaa013>.

Yoshida, K. et al. (2005) 'Excess aldosterone under normal salt diet induces cardiac hypertrophy and infiltration via oxidative stress', *Hypertension Research: Official Journal of the Japanese Society of Hypertension*, 28(5), pp. 447–455. Available at: <https://doi.org/10.1291/hypres.28.447>.

Youn, J.-C. et al. (2013) 'Immunosenescent CD8+ T cells and C-X-C chemokine receptor type 3 chemokines are increased in human hypertension', *Hypertension (Dallas, Tex.: 1979)*, 62(1), pp. 126–133. Available at: <https://doi.org/10.1161/HYPERTENSIONAHA.113.00689>.

Zhai, R. et al. (2022) 'Double life: How GRK2 and  $\beta$ -arrestin signaling participate in diseases', *Cellular signalling*, 94, p. 110333. Available at: <https://doi.org/10.1016/j.cellsig.2022.110333>.

Zhang, L. et al. (2013) 'Phospholipase  $\text{C}\epsilon$  hydrolyzes perinuclear phosphatidylinositol 4-phosphate to regulate cardiac hypertrophy', *Cell*, 153(1), pp. 216–227. Available at: <https://doi.org/10.1016/j.cell.2013.02.047>.

Zhang, W. et al. (2020) 'Morphometric, Hemodynamic, and Multi-Omics Analyses in Heart Failure Rats with Preserved Ejection Fraction', *International Journal of Molecular Sciences*, 21(9), p. 3362. Available at: <https://doi.org/10.3390/ijms21093362>.

Zhao, M. et al. (2011) 'Cardiac pressure overload hypertrophy is differentially regulated by  $\beta$ -adrenergic receptor subtypes', *American Journal of Physiology. Heart and Circulatory Physiology*, 301(4), pp. H1461-1470. Available at: <https://doi.org/10.1152/ajpheart.00453.2010>.

Zhao, M., Hagler, H.K. and Muntz, K.H. (1996) 'Regulation of alpha 1-, beta 1-, and beta 2-adrenergic receptors in rat heart by norepinephrine', *The American Journal of Physiology*, 271(5 Pt 2), pp. H1762-1768. Available at: <https://doi.org/10.1152/ajpheart.1996.271.5.H1762>.

Zheng, M. et al. (2000) 'beta 2-adrenergic receptor-induced p38 MAPK activation is mediated by protein kinase A rather than by Gi or gbeta gamma in adult mouse cardiomyocytes', *The Journal of Biological Chemistry*, 275(51), pp. 40635–40640. Available at: <https://doi.org/10.1074/jbc.M006325200>.

Zhu, W. et al. (2005) 'The Enigma of  $\beta$ 2-Adrenergic Receptor Gi Signaling in the Heart', *Circulation Research*, 97(6), pp. 507–509. Available at: <https://doi.org/10.1161/01.RES.0000184615.56822.bd>.

Zhu, W. et al. (2007) 'Activation of CaMKII $\delta$  is a common intermediate of diverse death stimuli-induced heart muscle cell apoptosis', *The Journal of Biological Chemistry*, 282(14), pp. 10833–10839. Available at: <https://doi.org/10.1074/jbc.M611507200>.

Zhu, W. et al. (2012) 'Gi-biased  $\beta$ 2AR signaling links GRK2 upregulation to heart failure', *Circulation Research*, 110(2), pp. 265–274. Available at: <https://doi.org/10.1161/CIRCRESAHA.111.253260>.

Zhu, W.Z. et al. (2001) 'Dual modulation of cell survival and cell death by beta(2)-adrenergic signaling in adult mouse cardiac myocytes', *Proceedings of the National Academy of Sciences of the United States of America*, 98(4), pp. 1607–1612. Available at: <https://doi.org/10.1073/pnas.98.4.1607>.

Zhu, W.-Z. et al. (2003) 'Linkage of beta1-adrenergic stimulation to apoptotic heart cell death through protein kinase A-independent activation of Ca<sup>2+</sup>/calmodulin kinase II', *The Journal of Clinical Investigation*, 111(5), pp. 617–625. Available at: <https://doi.org/10.1172/JCI16326>.

Zhu, W.-Z. et al. (2005) 'Heterodimerization of  $\beta$ 1- and  $\beta$ 2-Adrenergic Receptor Subtypes Optimizes  $\beta$ -Adrenergic Modulation of Cardiac Contractility', *Circulation Research*, 97(3), pp. 244–251. Available at: <https://doi.org/10.1161/01.RES.0000176764.38934.86>.

Zile, M.R. et al. (2015) 'Myocardial Stiffness in Patients With Heart Failure and a Preserved Ejection Fraction', *Circulation*, 131(14), pp. 1247–1259. Available at: <https://doi.org/10.1161/CIRCULATIONAHA.114.013215>.

Zile, M.R. and Brutsaert, D.L. (2002) 'New Concepts in Diastolic Dysfunction and Diastolic Heart Failure: Part I', *Circulation*, 105(11), pp. 1387–1393. Available at: <https://doi.org/10.1161/hc1102.105289>.

Zimmer, H.G. (1997) 'Catecholamine-induced cardiac hypertrophy: significance of proto-oncogene expression', *Journal of Molecular Medicine (Berlin, Germany)*, 75(11–12), pp. 849–859. Available at: <https://doi.org/10.1007/s001090050176>.

Zinman, B. et al. (2015) 'Empagliflozin, Cardiovascular Outcomes, and Mortality in Type 2 Diabetes', *The New England Journal of Medicine*, 373(22), pp. 2117–2128. Available at: <https://doi.org/10.1056/NEJMoa1504720>.

Zou, Y. et al. (1999) 'Both Gs and Gi Proteins Are Critically Involved in Isoproterenol-induced Cardiomyocyte Hypertrophy \*', *Journal of Biological Chemistry*, 274(14), pp. 9760–9770. Available at: <https://doi.org/10.1074/jbc.274.14.9760>.

van Zwieten, P.A. and de Jonge, A. (1986) 'Interaction between the adrenergic and renin-angiotensin-aldosterone-systems', *Postgraduate Medical Journal*, 62 Suppl 1, pp. 23–27. Available at: <https://pubmed.ncbi.nlm.nih.gov/3534860/>